AN INVESTIGATION OF MULTIPLE GAMMA SCATTERING IN GERMANIUM AS APPLIED TO Ge(Li) GAMMA SPECTROMETERS

A THESIS

Presented to

The Faculty of the Graduate Division

by

David Marshall Walker

In Partial Fulfillment

of the Requirements for the Degree

Doctor of Philosophy

in the School of Nuclear Engineering

Georgia Institute of Technology

May, 1970

In presenting the dissertation as a partial fulfillment of the requirements for an advanced degree from the Georgia Institute of Technology, I agree that the Library of the Institute shall make it available for inspection and circulation in accordance with its regulations governing materials of this type. I agree that permission to copy from, or to publish from, this dissertation may be granted by the professor under whose direction it was written, or, in his absence, by the Dean of the Graduate Division when such copying or publication is solely for scholarly purposes and does not involve potential financial gain. It is understood that any copying from, or publication of, this dissertation which involves potential financial gain will not be allowed without written permission.

7/25/68

AN INVESTIGATION OF MULTIPLE GAMMA SCATTERING IN GERMANIUM

AS APPLIED TO Ge(Li) GAMMA SPECTROMETERS

Approved:

Date approved by Chairman: May 27, 19;

ACKNOWLEDGMENTS

I am indebted to many individuals whose willing contributions have made this thesis work possible and, indeed, enjoyable.

I was fortunate to have as my thesis advisor and reading committee members three professors who are expert in separate technical areas related to the thesis research. Dr. J. D. Clement, my advisor, initially introduced me to Monte Carlo methods and suggested many valuable techniques used in the computer programs. Dr. J. M. Palms of the Department of Physics at Emory University helped to formulate a meaningful approach to this research problem, which was an outgrowth of experimental detector studies at Emory. Dr. D. C. Ray provided support in the semiconductor physics area and in the mechanics of meeting the degree requirements. The enthusiasm and interest of each of the three helped to motivate and enliven the investigation.

Mr. H. E. Carr and Mr. M. E. McLain, Jr. provided many hours of constructive discussion and direct technical assistance for which I am most grateful.

I would like to thank five individuals in particular for their contributions to the experimental effort. They are Mr. O. H. Puckett for fabrication of the Ge(Li) detector and cryostat, Mr. D. Smith for preparing the special radioisotope sources, Mr. B. D. Statham for assistance with the instrumentation, Mr. J. M. Burke for devising the rectangular-hole collimators, and Mr. C. T. Brown and Advanced Research Corporation of Atlanta for the loan of the two-parameter instrumentation.

Dr. G. G. Eichholz kindly provided a detailed and very helpful critique of both the technical content and the style of the thesis manuscript. It was also a pleasure to work with a demanding professional such as Mrs. Lydia Geeslin, who edited and typed the manuscript.

Dr. C. J. Roberts has made more contributions to my efforts as a student and a co-worker than I can possibly acknowledge. The confidence one tends to develop in Dr. Roberts has an influence which extends beyond the task at hand.

I would be errant if I did not express my deep appreciation for the assistance and encouragement of my good friends and co-workers at the Nuclear Research Center. The assistance of the Engineering Experiment Station in many aspects of this work is also appreciated.

Finally, I am happy to acknowledge that this entire graduate education business has been a family affair. Our sons, Terry, Donald, and Michael have each contributed curiosity, humor, and understanding far beyond their years. But it is to my wife, Aline, that I owe the greatest thanks for patiently and good-humoredly prevailing over every conceivable unsung task of the graduate student's wife. The tasks ahead become adventures with her help.

TABLE OF CONTENTS

TABLE OF CONTENTS (Concluded)

LIST OF TABLES

LIST OF TABLES (Concluded)

LIST OF ILLUSTRATIONS

LIST OF ILLUSTRATIONS (Continued)

LIST OF ILLUSTRATIONS (Continued)

LIST OF ILLUSTRATIONS (Concluded)

SUMMARY

In spite of the improved gamma spectrometer performance afforded by the development of high resolution lithium-drifted germanium Ge(Li) detectors, the problem of interference counts from Compton scattering remains. Since 1967 several investigators have reported suppression of Compton interference by the use of spectrometer systems in which simultaneous gamma interactions must be observed in two or more electrically independent germanium volumes. The research described in this thesis is an investigation of multiple gamma scattering in finite germanium volumes as it pertains to the understanding, optimization, and evaluation of gamma spectroscopy concepts based on multiple scattering in Ge(Li) detectors.

A Monte Carlo computer model was developed to provide the specific information needed for the evaluation of multiple scattering Ge(Li) spectrometers, and the computed results were shown to correspond closely to the measured performance of an experimental sum-coincidence Ge(Li) spectrometer. Calculations with the model show that a major fraction of all events in which the entire energy of the incident gamma is captured involve more than one interaction, with three or more interactions being common.

For the gamma energy range of 320 keV to 2754 keV, the variation of full energy peak efficiency and peak-to-Compton ratio is given for selected hypothetical detectors as a function of external and internal detector geometry and of energy discrimination conditions. Below about

300 keV, sum-coincidence spectrometers are not competitive with regular Ge(Li) spectrometers of the same volume. Calculated and measured two-parameter energy spectra for coincident events show that events representing the entire energy of the incident gamma are highly localized on the energy surface. Two-dimensional discrimination techniques on the energy surface appear to offer additional Compton interference reduction for specific spectroscopy applications.

A figure-of-merit for Compton interference reduction is defined and used as a basis for comparing the performance of conventional Ge(Li) detectors to that of optimized sum-coincidence detectors and to the theoretical maximum performance of Ge(Li) detectors which require multiple gamma scattering. For cylindrical Ge(Li) detectors of up to 2 cm in length and about 25 cm^3 in volume, sum-coincidence operation was calculated to give an equivalent Compton suppression factor of about two. Only in random cases do spectrometers based on sum-coincidence operation of two-region Ge(Li) detectors appear to offer superior gamma spectroscopy capabilities over those offered by Ge(Li) spectrometers of 60 cm^3 or greater which accept all detected events. Poor relative efficiency is shown to be the major limitation to Compton interference reduction for sum-coincidence systems.

The full energy peak efficiencies of all sum-coincidence systems of this analysis are shown to be only minor fractions of the theoretical upper efficiency limits imposed by the requirement of multiple gamma scattering. Although selective efficiency improvements can be realized by special detector configurations, it appears that alternate methods of sensing the occurrence of multiple interactions within a single Ge(Li)

volume have the potential for a more general and significant reduction of Compton interference for gamma spectroscopy.

CHAPTER I

INTRODUCTION

The measurement of the energy and intensity of gammas by the use of semiconductor gamma spectrometers is obscured in many instances by the interference components from scattering events associated with incident gammas of higher energy. This report concerns the use of multiple gamma scattering phenomena in germanium as a means of minimizing this interference component.

A primary motivation for the development of high resolution detectors has been the need for improved measurements of intensity of each gamma component of complex multiple component spectra.[1,2,3] In the basic research area, improvements in the capabilities for resolving involved spectra are directly related to advancements in the study of nuclear decay schemes,[4] internal conversion coefficients,[5] spin moments by angular correlation techniques,[6,7] Mössbauer transitions,[8] and the structure of mesonic atoms.[9] For example, very complex decay schemes such as that of germanium-77 (67 gamma components in the energy range of 215 keV to 2514 keV) have recently been resolved using semiconductor spectrometer systems.[10]

In the applied area, a significant increase in the utility of activation analysis as a trace element measurement technique has been afforded by developments in high resolution gamma spectroscopy.[11,12] An important related problem is the study by direct instrumentation methods

of the buildup of fission products in nuclear fuels.[13] Extensive chemical separation techniques have been developed to separate out elements with large interference components in cases where direct instrumental analysis is not adequate.[14]

The persistent demand for improved gamma spectrometer performance has prompted the development and use of several new gamma measurement concepts since about 1950. Before 1950 the most widely used tool for gamma measurements was the lead absorber which, according to Hollander,[2] was distinguished by two characteristics: simplicity and poor results.

In the early 1950's, the crystal diffraction spectrometer[15] and the external conversion magnetic spectrometer[16] came into use for gamma spectroscopy. The Mark I curved crystal spectrometer of DuMond had FWHM* energy resolutions of approximately 0.3 keV and 20 keV at 100 keV and 1000 keV, respectively.[2] In the external-conversion magnetic spectrometer the incident gamma beam produces photoelectrons as it interacts in a heavy element radiator-window into a magnetic beta spectrometer. The electron spectrum is then measured to give a precise indication of the photon energy. A FWHM resolution of 3 keV at 1 MeV has been recorded for a double-focusing instrument.[2] In spite of the precision in absolute energy measurements and the good resolution offered by the two instruments, both found limited use because of their complexity, low efficiency and single-channel response.

Low efficiency is also a major limitation of the gas proportional

---

*Full Width at Half Maximum ≡ the energy interval at the half-maximum value of a peak in an energy spectrum. For Gaussian statistics, σ, the standard deviation, is related to FWHM by: FWHM = 2.354 σ.

counter for gamma-ray energy measurements above about 100 keV.[17] However, the low noise capabilities of proportional counters still present unique measurement capabilities in the keV and lower (below 100 eV) energy region.[18,19]

Scintillation gamma spectrometers[20,21] came into wide usage following the belated publication in 1948 by Curran and Baker of previously classified work done in 1944 on the coupling of photomultiplier tubes and scintillators.[22] Practical counting efficiencies for photons in the MeV range were made possible by the development of large volume organic scintillators and high atomic number materials such as NaI(Tℓ). The high efficiency, fast response, and general ease of use moved the scintillation detector into a position of prominence in gamma spectroscopy that only recently has been challenged by higher resolution, large volume lithium-drifted germanium detectors.

According to Price,[23] the direct collection of radiation-produced charge in a single crystal (silver chloride) was first reported in a thesis by Van Heerden in 1945.[24] These earlier bulk-conductivity types of detectors suffered from trapped space charge problems, which prompted McKay to investigate the detection of radiation with germanium junction devices shortly after their development in the late 1940's.[25] The first extensive use of junction detectors in nuclear research was reported by a group at Oak Ridge National Laboratories in 1958.[26] In 1962, Freck and Wakefield published an account of the first germanium gamma spectrometer,[27] which had an active volume of 0.22 cm^3. Improved efficiency and energy resolution have been realized through advances in detector volume (to 95 cm^3 and greater[28]), detector construction techniques, and in low-

noise preamplifiers and associated electronics equipment. A FWHM energy resolution for Ge(Li) systems of about 2 keV is typical as compared to 60 keV to 100 keV for a scintillation system.[28] Ge(Li) detector efficiencies frequently are quoted with respect to that of a 3 inch long by 3 inch diameter sodium iodide scintillation crystal; relative efficiencies of 10 percent to 15 percent are common for commercially available Ge(Li) detectors.[28] Pulse rise times of less than 100 nanoseconds are observed for Ge(Li) detectors operated with electric field strengths of 100 volts per mm or greater.[29]

In spite of the significant advancements in gamma energy measurements afforded by semiconductor detectors, a common problem is still present: how to distinguish between desired events in which the total photon energy is absorbed and Compton scattering events which leave only a portion of the incident photon energy within the detector. The Compton events produce a "background" spectrum of false events of energy from zero to a maximum energy approaching that of the incident photon.

Several instrumental methods have been investigated to minimize the Compton background contribution. The most common is the anticoincidence method in which a high resolution semiconductor detector is surrounded by a large volume, low resolution scintillation detector. Compton events in the high resolution detector produce reduced energy photons which have a significant probability of further interactions in the large "shield" detector. By operating the two in an anticoincidence mode, the ratio of the number of total energy events to the number of Compton-escape events can be enhanced. The performance of selected anticoincidence systems will be discussed in the next section. Techniques such as

pulse shape discrimination between partial and total energy events also show Compton supression capabilities, but of less effectiveness than the anticoincidence approach.[30]

The research described in this thesis is an investigation of yet another approach to discriminating against detected gamma events which do not represent the entire energy of the incident gamma. Specifically, Compton interference reduction based on the requirement that an incident gamma scatter more than once in the Ge(Li) detector will be investigated. In the following section, the theoretical basis for Compton interference reduction based on multiple gamma scattering will be discussed, and the reported performance of Ge(Li) detectors which require multiple interactions will be reviewed. The specific objectives for this study are then given.

CHAPTER II

DISCUSSION OF COMPTON SUPPRESSION CONCEPTS

Gamma Interaction Mechanisms in Germanium Detectors

It is a purpose of this research to investigate concepts and to develop practical procedures for suppressing the Compton component of the gamma spectrum as recorded by lithium-drifted germanium spectrometers. As a background to the analysis, it will be instructive first to consider the basis for semiconductor detector operation, and to relate each important gamma interaction mechanism to the resulting component of the recorded gamma spectrum. Previous methods for suppressing the Compton background component of the spectra can then be discussed, and an approach to the analysis of multiple scattering detectors can be defined.

To facilitate the discussion, several definitions are made which will be used throughout this thesis. A gamma "event" is considered to be the consequence of all interactions or scatterings of a single incident gamma. For example, an output signal from a Ge(Li) detector represents an "event" which is the result of a scattering "sequence" composed of one or more gamma interactions. A Ge(Li) detector operated in the "conventional" or "sum-only" mode records events consisting of any number of interactions in the active detector volume, including single interactions. A Ge(Li) detector system operated in the "multiple scattering" or "sum-coincidence" mode accepts only events in which more than one gamma interaction is detected in the active germanium volume. "Full

energy" events are gamma events in which the entire energy of the incident gamma is captured within the active volume of the Ge(Li) detector system. Full energy or "good" events make up the counts in the "full energy peak" of the recorded gamma energy spectrum. If only a portion of the energy of the incident gamma is captured by the gamma scattering sequence in the active detector volume, then a "partial energy" event or "bad" event is said to have occurred.

The semiconductor detector is often referred to as a solid state ionization chamber because of the similarity in the basic detection mechanisms of the two concepts. Detector action in both depends on the existence of a region of low free-charge carrier density in which an electric field may be maintained to sweep out and collect charge produced by radiation interactions.[31,32,33] The gas contained between charged electrodes in the ionization chamber has as its analogous component in semiconductor detectors the charge depleted volume between the n-type and p-type regions of a semiconductor junction. The n-type and p-type regions act as electrodes for collecting the charge produced in the intrinsic or charge depleted volume.

A junction region for semiconductor detectors may be formed by conventional diffused junction techniques in which a diode of large junction area is fabricated, or by using the junction-like behavior at a metal-to-semiconductor oxide interface.[34] In the latter technique, a metal film is deposited over a semiconductor oxide layer to produce the "surface barrier" detector. The thickness of the charge depleted region in junction semiconductors is found to vary approximately as the square root of the reverse bias on the junction, corresponding to the abrupt

junction approximation in semiconductor theory.[35] As a result, detector thickness is restricted to several millimeters by the upper electric field strength limits which can be used in actual detectors.

In an attempt to attain larger active or charge depleted volumes, techniques for producing large intrinsic regions were developed.[36,37] An intrinsic region is one in which the number of ionized charge acceptors and charge donors is nearly balanced, resulting in a greatly reduced net free charge. In practice the charge balancing (compensation) is accomplished by drifting donor lithium ions under the influence of an electric field through a region of excess acceptor concentration. The resulting p-i-n diode may have an intrinsic volume of up to 95 cm^3 or more which can be swept free of excess carriers by applying reverse bias at the p- and n-type regions.

The gamma detection mechanism in the Ge(Li) detector consists of three steps. First, the gamma interacts with an electron, transferring a portion of the incident gamma energy into kinetic energy of the electron. Secondly, the kinetic energy of the primary electron is then dissipated within the semiconductor material, primarily by the creation of free electron-hole pairs in the lattice. Finally, the excess charge represented by the electron-hole pairs introduced into the charge depleted region of the Ge(Li) detector is collected at the n-type and p-type regions. For detector applications, the mean number of electron-hole pairs created by the slowing of a charged particle in silicon and germanium can be assumed to depend only on the initial energy of the charged particle.[38,39] Thus the output pulse signal from the detector resulting from the collection of the excess charge is very nearly proportional to

the energy transferred to the primary electron in the photon-electron interaction. Even in an ideal detector, the output signal represents the total energy of the incident gamma only if all of the incident gamma energy is transferred to electrons within the active detector volume.

In the 0.3 to 3.0 MeV incident gamma energy region where the multiple scattering concept will be shown to offer competitive performance, three photon interaction mechanisms are responsible for the observed components of the recorded gamma spectrum. The three interactions, photoelectric absorption, Compton scattering, and pair-production in the field of the nucleus, produce energetic electrons or electron-positron pairs.[40,41]

The response of an ideal detector in terms of these three interaction mechanisms can be shown with the aid of Figures 1a through 1d. The monoenergetic incident gamma energy, $h\nu$, is assumed to be greater than $2\ m_o c^2$, where $m_o c^2$ is the electron rest mass energy. Counts in the full energy peak have as their terminal interaction a photoelectric absorption, the complete absorption of the energy of a photon by a bound electron. The electron ejected into the semiconductor lattice is of energy ($h\nu$-BE), where BE is the binding energy for the particular atomic shell initially occupied by the electron. The resulting spectrum contribution is shown in Figure 1a for photoelectric absorption as the only interaction, or as the final interaction when earlier scattering interactions also occurred in the active volume of the detector. If previous scattering of the photon has occurred outside the active volume, then the recorded energy may have any value between zero and $h\nu$.

The Compton interaction is the inelastic scattering of a photon by an essentially free electron, with the electron receiving any energy

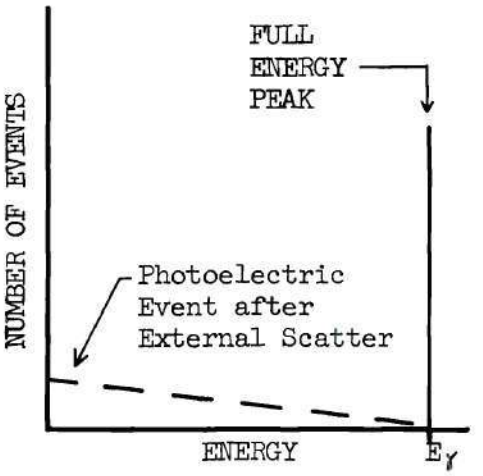

1a) Photoelectric Event as Final Interaction

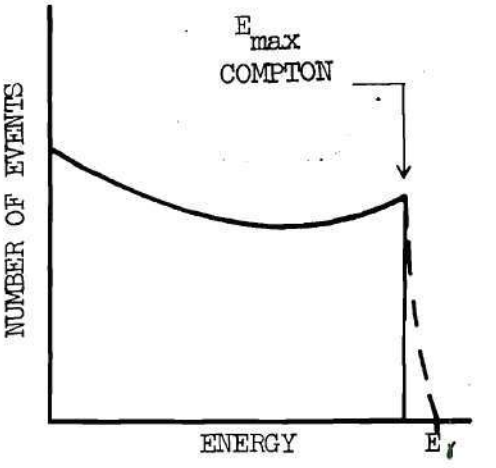

1b) Compton Event as Final Interaction

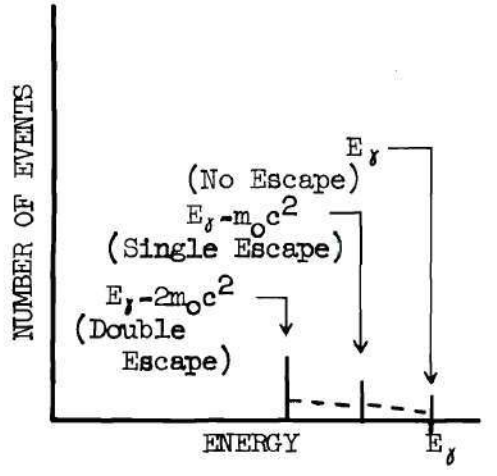

1c) Pair Production Events

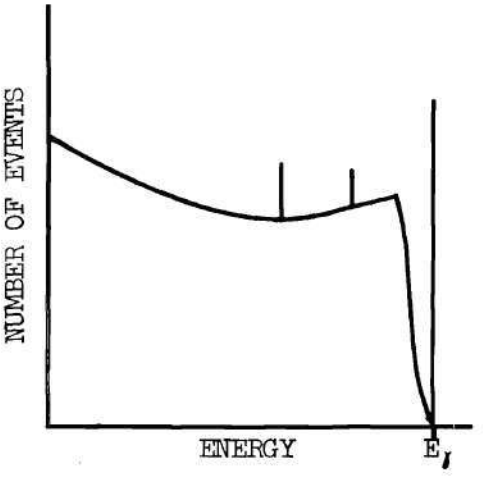

1d) Composite Spectrum for Monoenergetic Source

Figure 1. Gamma Spectrum as Recorded by an Ideal Semiconductor Detector for a Monoenergetic Gamma Source

between zero and a maximum imposed by the requirement of simultaneous energy and momentum conservation. The maximum electron energy, E_{max}, occurring for a backscattered photon ($\theta = 180°$), is[40]:

$$E_{max} = \frac{h\nu}{1 + \frac{m_o c^2}{2\ h\nu}} \qquad (1)$$

where $m_o c^2$ = electron rest energy

$h\nu$ = incident photon energy.

In the high energy limit for incident photon energy, E_{max} approaches $(h\nu - (m_o c^2/2))$, or within about 250 keV of the incident photon energy.

The solid line of Figure 1b shows the spectrum from Compton scattering for which the scattered electron energy is captured, and the scattered gamma escapes from the detector. The dashed line represents the occurrence of further Compton interactions before escape; a photoelectric absorption after any number of Compton scatterings would, of course, produce a count in the full energy peak. Because escape after a single Compton scatter is the most probable case for typical detector volumes, the Compton peak at energy E_{max} is usually in evidence in the spectrum.

Pair production in the field of the nucleus contributes the spectrum components shown in Figure 1c. Pair production is the interaction of the electromagnetic photon wave with the coulomb field of the nucleus, where $2\ m_o c^2$ of the photon energy goes into the creation of an electron-positron pair, and the remaining energy appears as kinetic energy of the electron, positron, and nucleus.[41] The relatively massive nucleus receives a negligible portion of the energy; therefore, if the kinetic

between zero and a maximum imposed by the requirement of simultaneous energy and momentum conservation. The maximum electron energy, E_{max}, occurring for a backscattered photon ($\theta = 180°$), is[40]:

$$E_{max} = \frac{h\nu}{1 + \frac{m_o c^2}{2\ h\nu}} \qquad (1)$$

where $m_o c^2$ = electron rest energy

$h\nu$ = incident photon energy.

In the high energy limit for incident photon energy, E_{max} approaches $(h\nu - (m_o c^2/2))$, or within about 250 keV of the incident photon energy.

The solid line of Figure 1b shows the spectrum from Compton scattering for which the scattered electron energy is captured, and the scattered gamma escapes from the detector. The dashed line represents the occurrence of further Compton interactions before escape; a photoelectric absorption after any number of Compton scatterings would, of course, produce a count in the full energy peak. Because escape after a single Compton scatter is the most probable case for typical detector volumes, the Compton peak at energy E_{max} is usually in evidence in the spectrum.

Pair production in the field of the nucleus contributes the spectrum components shown in Figure 1c. Pair production is the interaction of the electromagnetic photon wave with the coulomb field of the nucleus, where $2\ m_o c^2$ of the photon energy goes into the creation of an electron-positron pair, and the remaining energy appears as kinetic energy of the electron, positron, and nucleus.[41] The relatively massive nucleus receives a negligible portion of the energy; therefore, if the kinetic

energies of the electron and positron are expended entirely in ion pair production, the minimum charge signal in a detector will correspond to an energy of $(h\nu - 2\ m_o c^2)$. As the positron is slowed to thermal energy, it undergoes an annihilation event with a free electron,[40] releasing their combined rest mass energy, $2\ m_o c^2$, as oppositely directed photons of energy $m_o c^2$.

The low energy peak of Figure 1c corresponds to the case where both annihilation photons escape from the detector, the second peak to the case where one photon escapes and the other is absorbed, and the third full energy peak to the case were both photons are absorbed. The dashed line joining the peaks represents Compton scattering by either or both annihilation gammas.

Thus, even for the ideal detector discussed here, a source of monoenergetic incident gammas produces not a single peak, but the complex spectrum indicated in Figure 1d. If several monoenergetic gamma components are present, it can be seen that the spectrum indeed becomes complex, and that low intensity, full energy peaks superimposed on the Compton component from a higher energy gamma could be lost in the normal statistical variation in the number of events from the Compton contribution. If the incident gamma flux is continuously distributed in energy, the recorded spectrum is the result of a complex mixture of components from the various interaction mechanisms. It is the desire to eliminate these uninformative components of the recorded spectrum caused by Compton events which motivates studies of Compton suppression.

Other interactions occur in addition to the three types noted; Davisson discusses 13 possible interactions of photons with electrons,

the nucleus, and the coulomb fields of both.[42] However, the only further process with cross sections within an order of magnitude of the three interaction types discussed earlier is Rayleigh scattering. In Rayleigh scattering, the photon energy is absorbed by a tightly bound atomic electron, raising it to a higher energy state.[41] A second photon having nearly the same energy and direction of the incident photon is then emitted, since very little energy or momentum would be transferred to the massive recoiling nucleus. It has been shown experimentally[43] that 75 percent of the Rayleigh scattered photons are deflected in direction by an angle of less than

$$\Phi_c = 2 \sin^{-1} \left(0.026 \, Z^{\frac{1}{3}} \frac{m_o c^2}{h\nu}\right) \qquad (2)$$

where Z = atomic number

$m_o c^2$ = electron rest energy

$h\nu$ = photon energy.

The angle Φ_c is less than one degree for a one MeV photon in germanium, which has an atomic number of 32. Thus, so far as a radiation detector is concerned, no charge producing event has occurred, and the photon is altered only very slightly in energy and direction. Based on these considerations, Rayleigh scattering is expected to have a negligible effect on the detector performance to be calculated in this research.

An analysis of Compton suppression concepts to be discussed here will require considering in more detail the three major photon-electron interaction mechanisms previously noted. One important parameter is the interaction cross section as a function of gamma energy as displayed for

germanium in Figure 2.[42,44,45] Note the predominance of the probability for Compton interactions over the incident photon energy range from about 0.150 MeV to 8.0 MeV. A 1.5 MeV gamma, for example, is about 100 times more likely to be Compton scattered than to undergo a photoelectric absorption. Below 0.150 MeV, the rapid increase of the photoelectric cross section with decreasing incident photon energy causes the total interaction cross section to become orders of magnitude larger than for the mid-energy regions.

The characteristics of the cross sections with energy are of importance to both anticoincidence and sum-coincidence Compton suppression concepts. Although the Compton scattering interaction is the most likely process in the mid-energy region, each succeeding Compton scatter produces a lower energy gamma with increased probability for interaction and for that interaction to be a complete absorption in a photoelectric interaction. Because the photoelectric cross section is dependent on atomic number, Z, approximately as Z^5, the probability of photoelectric absorption is enhanced even more in high-Z materials.

A polar graph of the cross section for the number of gammas scattered into unit solid angle at a particular mean scattering angle is given in Figure 3. These curves show a greater probability of Compton interaction at lower energies, and also that larger scattering angles are increasingly favored as the gamma energy decreases. For a gamma of energy $h\nu$ scattered through angle θ, the scattered gamma energy $h\nu'$ is:

$$h\nu' = h\nu \frac{1}{1 + \alpha(1-\cos\theta)} \qquad (3)$$

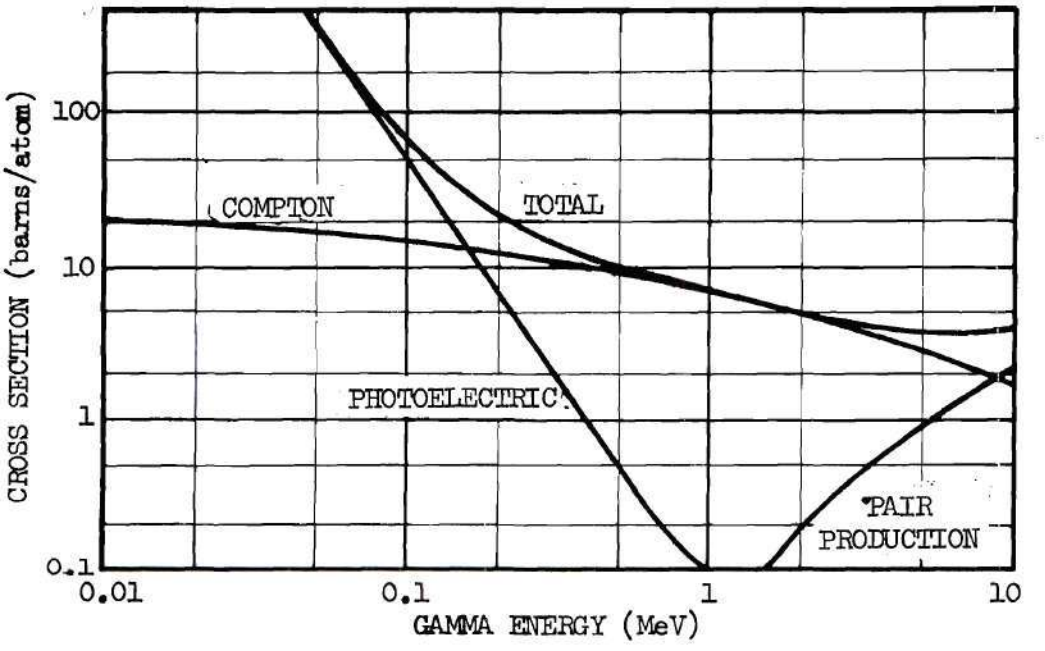

Figure 2. Gamma Interaction Cross Section versus Energy for Germanium (data from references 42,44, and 45)

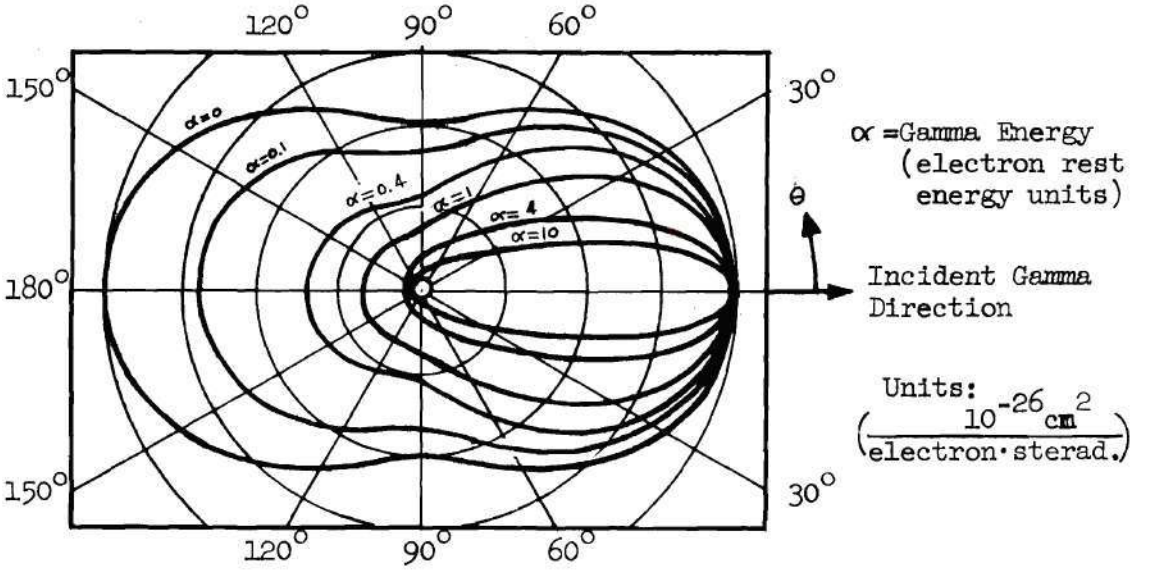

Figure 3. Cross Section for Number of Photons Scattered into Unit Solid Angle at a Mean Scattering Angle of θ (from reference 40)

where $\alpha = \frac{h\nu}{m_0 c^2}$

= incident gamma energy in electron rest energy units.

From the equation it can be seen that the energy retained by the scattered gamma decreases monotonically as the scattering angle increases. Thus, after each succeeding Compton collision, the cross section for a subsequent scatter, the probability for a larger angle scatter, and the probable fractional energy loss for the scattering gamma are greater. As the gamma energy is sufficiently reduced, termination of the collision sequence by a photoelectric interaction becomes highly favored.

Anticoincidence and Sum-Coincidence Spectrometers

The anticoincidence approach to Compton suppression as discussed in the introduction makes use of several characteristics of the photon interaction behavior. The object of the shield detector is to detect the escaping reduced-energy gamma resulting from a Compton scatter in the primary detector, thus providing a signal used to reject the partial energy event. From the previous discussion of interaction phenomena, desired properties of the shield detector are large volume, high atomic number, and placement in a preferred scattering direction from the primary detector.

Large volume shield detectors are commonly fabricated from plastic scintillation phosphors. R. Cooper and Brownell[46] report Compton suppression factors* of two for cesium-137 gammas using a 35 cm^3 Ge(Li) detector

*The Compton suppression factor for an anti-Compton system is defined as the ratio of the peak-to-Compton ratio for the system operated in the anti-Compton mode to that of operation as a single detector. Peak-to-Compton ratio (counts) is the number of counts in the full energy

surrounded by an 18 inch diameter by 18 inch long plastic scintillator. J. Cooper et al.,[47] used a 26 inch diameter by 24 inch long plastic scintillator around a 20 cm^3 Ge(Li) detector to obtain a Compton suppression factor of 7.5.

Nearly the same performance can be obtained with much smaller NaI(Tℓ) shields because of the higher effective atomic number of NaI(Tℓ). Adjacent cylindrical NaI(Tℓ) detectors[48,49] and split annular detectors[50,51] around the Ge(Li) detector show Compton suppression factors of two to seven. Camp,[48] for example, reports a Compton suppression factor of about seven for cobalt-60 gammas using two 9 inch diameter by 4.5 inch long scintillation crystals shaped about a 7 cm^3 Ge(Li) detector.

Michaelis and Kupfer[52] have combined the advantages of large volume and high-Z by taking advantage of the small scattering angle for photons which lose only a minor fraction of their energy in Compton scattering. The incident gamma beam, collimated through a hole in a lead cylinder, strikes a 4.9 cm^3 Ge(Li) planar detector in the center of a 20 inch diameter by 16 inch long plastic scintillator. On the beam axis behind the Ge(Li) detector is a 4 inch diameter by 6 inch long NaI(Tℓ) detector presenting an appreciable path length of high-Z detector for the photons scattered through a small angle. The Compton suppression ratio for cesium-137 gammas is approximately ten for this system.

As large volume, high resolution semiconductor detectors became

---

(Continued)
peak divided by the number in the distributed Compton spectrum. Peak-to-Compton ratio (height) is the ratio of the height on the energy spectrum of the full energy peak to the maximum height of the Compton distribution.

available, a coincidence-summing approach to Compton suppression using only semiconductor detectors was considered. The first reported applications of the sum-coincidence concept for Compton suppression were based on the use of NaI(Tℓ) scintillation detectors.[53,54] This approach basically consists of locating two independent detector volumes in a geometry which enhances the probability of total absorption of the incident gamma energy if an event is recorded in both detectors. For coincident events the summed signal from all detectors is recorded, but a signal from one detector only is rejected based on the large probability of escape of the scattered gamma after a single Compton scatter.

Neither of the previously defined peak-to-Compton ratios gives a truly uniform basis for comparison of the Compton interference observed with sum-coincidence and sum-only detector systems. As will be shown later, the Compton component of the sum-coincidence spectrum is distributed in a different manner than that for the sum-only or anticoincidence systems. Cooper[55] has suggested that a figure-of-merit (FOM) related to the ability of a detector to produce a usable signal peak at energy E_1 in the presence of distributed Compton counts from a gamma of higher energy E_2 is of the form

$$\text{FOM} \propto \frac{(\text{Number of counts in full energy peak at } E_1)}{(\text{Average number of counts per channel at } E_1 \text{ from Compton scatter of gamma of energy } E_2)^{\frac{1}{2}}} \qquad (4)$$

This ratio reflects the statistical consideration that the full energy counts must be distinguished from the normal fluctuation in the Compton plateau as represented by the standard deviation, or square root, of the

average Compton counts per channel for a Gaussian distribution. Cooper's equation also contained an energy resolution term which is assumed to be constant for all cases of this study. The FOM may be expressed in terms of the full energy peak efficiency and a peak-to-Compton ratio (height) which will be calculated and measured for this investigation:

$$\text{FOM} = \text{Constant} \left[\frac{(n_1 \, A_1 t)}{(n_2 \, A_2 \, t/R_{21})^{\frac{1}{2}}} \right] \tag{5}$$

where n_1 = peak efficiency at energy E_1

n_2 = peak efficiency at energy E_2

A_1 = gamma rate for component at E_1

A_2 = gamma rate for component at E_2

t = counting time

R_{21} = peak-to-Compton ratio (height, for Compton component at E_1 from gammas at E_2).

For fixed gamma rates A_1 and A_2 and counting time t, a relative FOM for comparing systems under the same conditions becomes

$$\text{FOM} = n_1 \left(\frac{R_{21}}{n_2} \right)^{\frac{1}{2}} \tag{6}$$

The figure-of-merit comparison will be used later in this analysis. Insufficient experimental data are presented in the literature on Compton suppression spectrometers to allow the conversion of the reported performance to one basis of comparison.

Figure 4a shows the detector geometry for one of the earliest Ge(Li) sum-coincidence spectrometer (SCS) experiments.[56] Gruhn et al.

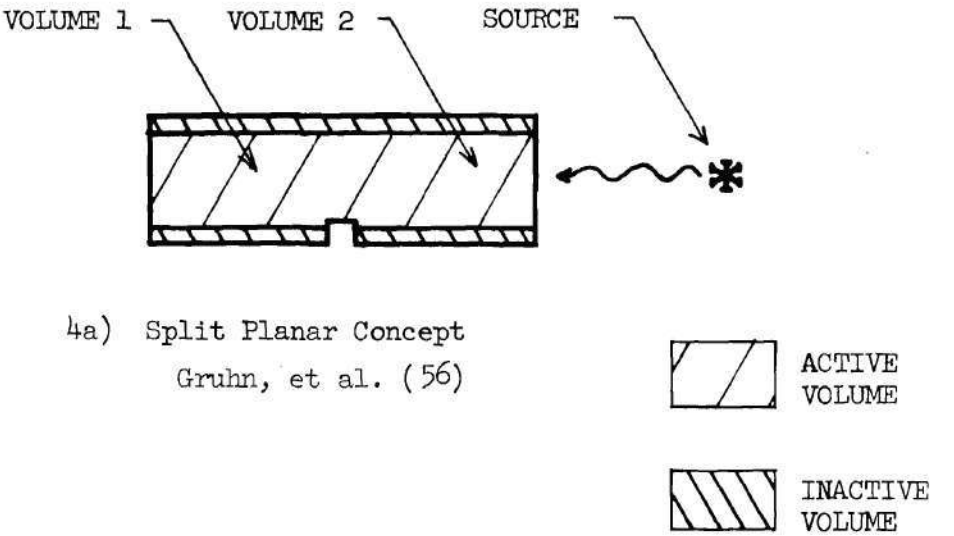

4a) Split Planar Concept
Gruhn, et al. (56)

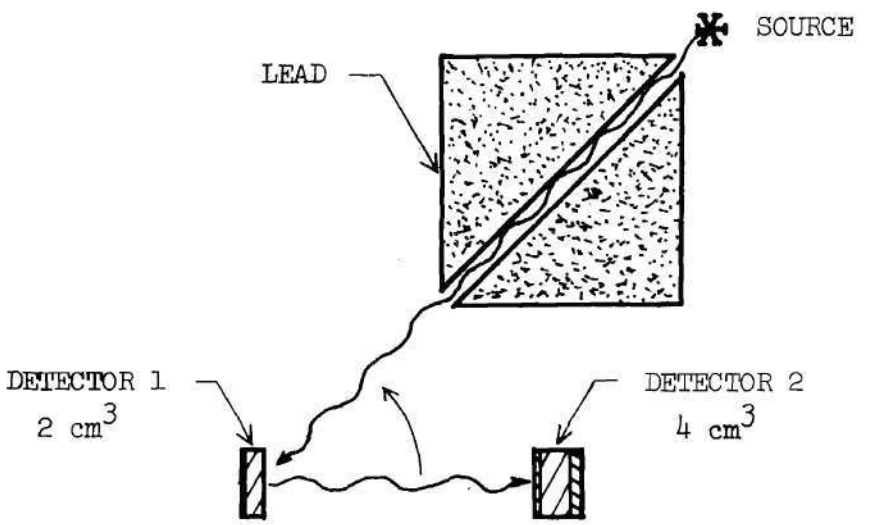

4b) 135° SEPARATED-DETECTOR CONCEPT
Kantele, et al. (58)

Figure 4. Early Concepts for All-Germanium Sum-Coincidence Detectors

find that a 0.076 cm wide cut into the intrinsic region of the planar Ge(Li) detector produces negligible electronic cross talk, as predicted by Hayashi.[57] Thus two essentially independent detector volumes without a separating dead layer are presented to the incident gamma beam. Compton suppression factors (counts) of "10 to 30" are reported for this detector; as scaled from graphs in the report,[56] this corresponds to a Compton suppression factor (height) of about 5.5.

During this same time period, Kantele and Suominen constructed the SCS system shown in Figure 4b in which scattering at a mean angle of 135° is required for coincidence.[58] The efficiency in the coincidence mode is only about one percent of that of the single 2 cm^3 detector, but Compton suppression factors (counts) of "40 to 50" are reported.

At the Eleventh Scintillator and Semiconductor Counter Symposium, Washington, D. C. in February 1968, new SCS detector configurations within single germanium ingots were reported by three independent groups.[59,60,61] As shown in Figure 5, each of these geometries has an internal inactive volume presented by the p-type core. Table 1 summarizes several parameters from the referenced publications for the four SCS detectors fabricated into a single ingot of germanium, and for the anticoincidence system of Camp. To provide a common basis for comparison, the data were scaled from each published spectrum in the same manner; values given may differ somewhat from those given by the authors because of the method of interpretation.

Two recently reported SCS systems[62,63] similar in concept to the collimated source, separate detectors of Kantele, et al.[58] are shown in Figure 6. The data of Hick and Pepelnic[63] for cobalt-60, when scaled in

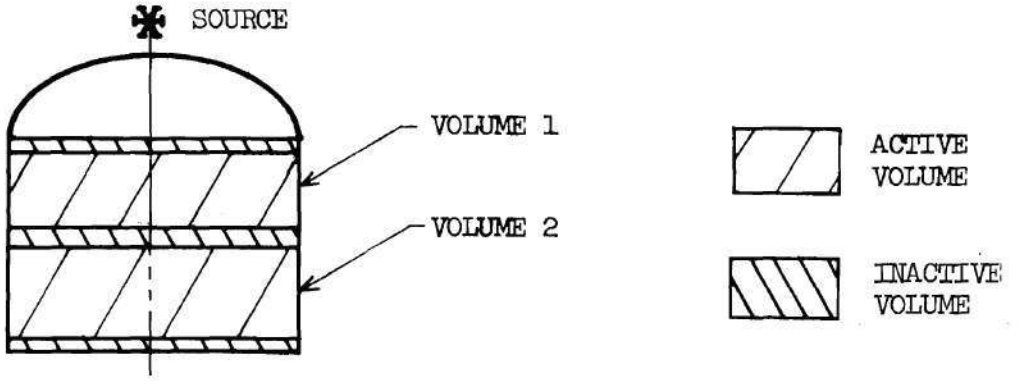

5a) Stacked Planar Design
Sayres, et al. (60)

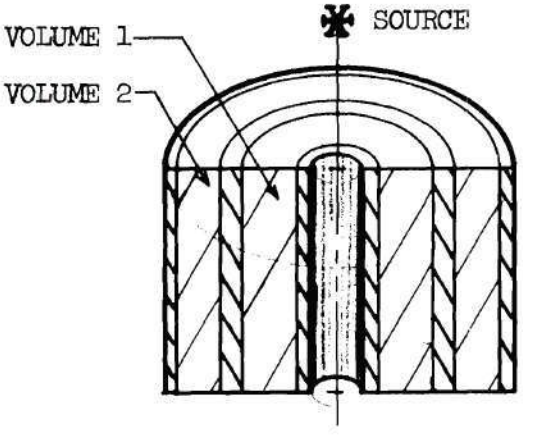

5b) Concentric Cylinder Design
Palms, et al. (61)

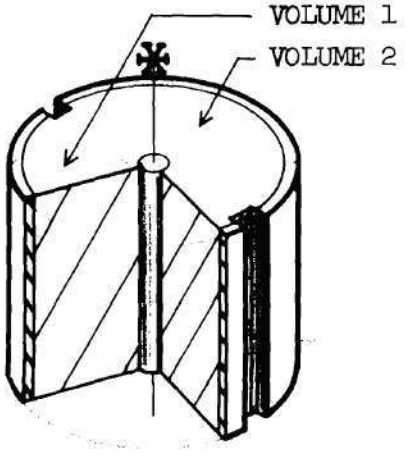

5c) Split Concentric Design
Kraner, et al. (59)

Figure 5. Sum-Coincidence Detectors Reported at the 1968 IEEE Scintillation and Semiconductor Counter Symposium

Table 1. Performance of Selected Anti-Compton Spectrometer Systems

Detector Geometry	Peak-to-Compton Ratio (height)		Compton Suppression Factor (height)	Experimenters	Ref.
	Conventional Mode	Anti-Compton Mode			
Split Planar	1.25	7.0	5.6	Gruhn, et al.	56
Split Coax	10	30	3.0	Kraner, et al.	59
Concentric Coax	2.1	8	3.8	Palms, et al.	61
Stacked Planar	4.6	11	2.4	Sayres, et al.	60
Anticoincidence	11.1	30	2.7	Camp	49

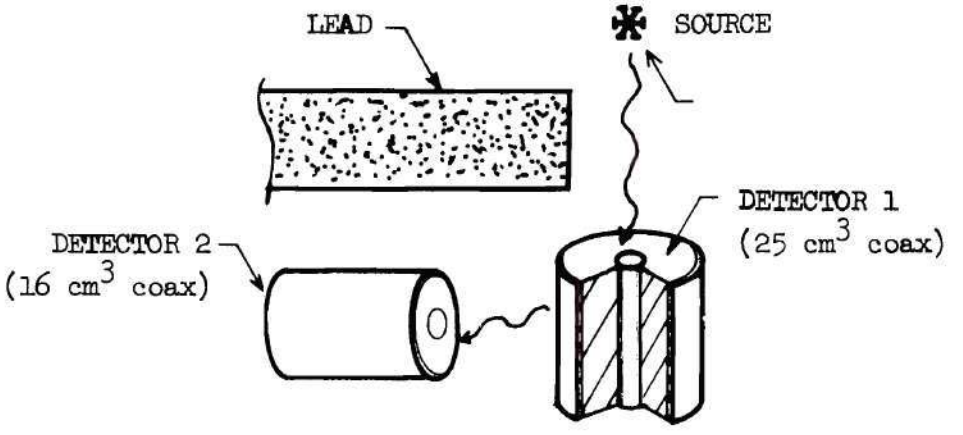

6a) Separated Coaxial Design
Broude, et al. (62)

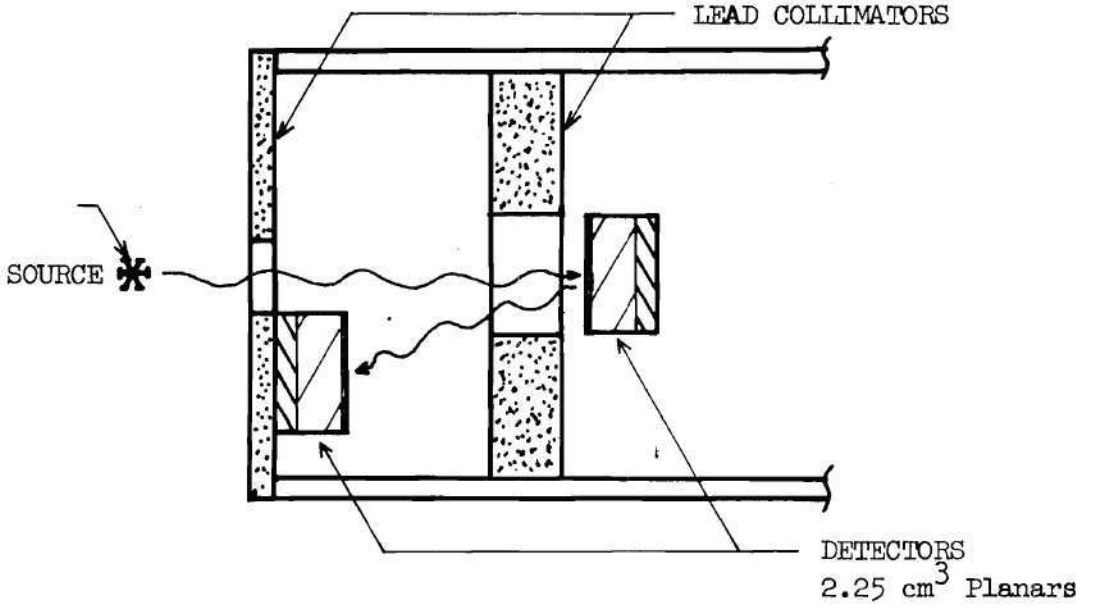

6b) Displaced Planar Design
Hick, et al. (63)

Figure 6. Sum-Coincidence Detectors Using Separate Ge(Li) Detectors and Collimation of the Incident Beam

in the same manner used for Table 1, give a peak-to-Compton ratio (height) of about 200, and a Compton suppression factor (height) of approximately 70.

An examination of the reported geometry and performance of each of these seven sum-coincidence spectrometers led this author to make several observations. First, the Compton suppression capabilities of the sum-coincidence detectors appear to compare favorably in certain cases to that offered by bulkier, more elaborate anticoincidence spectrometers which have a much longer development history.

Secondly, the criteria for analyzing SCS systems and for specifying detector configurations for special Compton suppression applications have not evolved from the previous experimental investigations. It is apparent from the dissimilarity of the existing sum-coincidence detectors that criteria for optimizing the performance of this type of detector system are less than obvious. An intuitive analysis of Compton suppression performance based on the sequential anisotropic interactions of gammas is found to be of limited value in resolving even basic questions such as the desired relative volumes of the active detector regions.

Thirdly, it appeared that the understanding and effective use of Ge(Li) detectors which require multiple interactions would require that a mathematical model be developed which could accurately predict the response of such detector systems. Because of the large number of parameters which are known to influence multiple scattering spectrometer performance, a solely experimental approach appeared to be an inefficient method of extending the investigation.

In view of these three observations, and of the latent benefit

which may be afforded by the multiple scattering concept, the decision was made to conduct the research described in this thesis. For the analysis, optimization, and evaluation of performance of multiple scattering detectors, the decision was made to develop a computerized Monte Carlo model to describe sequential gamma scattering behavior for realistic detector geometries. Consideration was first given to the use of one of several existing Monte Carlo models for predicting detector response to gamma radiation.[64,65,66,67] These models were designed to analyze conventional detectors, and as a result the method of procedure and the output information are not well suited for sum-coincidence detector analysis. In addition, Monte Carlo programs are commonly designed to make maximum use of the features of the particular computing language, processor, and subroutine library of the computer on which the program is run. The direct translation and subsequent modification of an existing model was not attempted, therefore, in favor of developing a special Monte Carlo model and associated computer programs for computers available at Georgia Tech. The reported models did, however, provide a valuable source of information and comparison of techniques and equations used in this work.

Bertolini, et al. have reported a Monte Carlo model developed and used for analysis of a specific sum-coincidence detector geometry.[68] This model computes output spectra only for a parallel gamma beam incident on back-to-back cylindrical planar detectors of the same diameter. Internal inactive volumes and energy resolution are not taken into account in this model.

As a final background note, it must be acknowledged that the ideal semiconductor gamma spectrometer performance used as a basis for the

previous discussions is not realized in practice. Incomplete charge carrier collection, inherent noise sources, statistical fluctuations in carrier production, pulse overlap, and many other effects influence the output from an actual detector.[69] Additional sources of "misinformation" arise in the electronic systems for amplification, pulse height analysis, and data processing of the detector output signal. Each of these sources can produce an observable effect on the gamma spectra recorded by either a conventional or sum-coincidence semiconductor detector system. In order to concentrate this study on Compton suppression by sum-coincidence methods, these higher-order effects are considered only where they would have a significant influence on the performance of actual detector systems.

Objectives of This Research

The specific objectives of this research are:

1) to develop a Monte Carlo model which could provide a quantitative description of multiple gamma scattering in germanium volumes which are typical of volumes for state-of-the-art Ge(Li) detectors.

2) to compute the performance capabilities of a selected variety of Ge(Li) spectrometers operated in the multiple scattering mode as a function of detector volume, internal detector geometry, and energy discrimination requirements for the incident gamma energy range of 300 keV to 3000 keV.

3) to compare computed detector performance to the performance measured with an actual Ge(Li) sum-coincidence detector system in order to establish the range of validity for the Monte Carlo model.

4) to define optimum Ge(Li) spectrometers for operation in the multiple scattering mode, and to compare the Compton interference reduction capabilities of the multiple scattering detectors with those of conventional Ge(Li) detectors with and without anticoincidence shields.

5) to determine the major limitations to the performance of existing detectors based on multiple scattering, and to suggest methods to overcome these limitations.

CHAPTER III

METHOD OF PROCEDURE

The method of procedure used to realize the objectives of this research as given in the previous chapter consisted essentially of four steps. First, the mathematical model describing multiple gamma scattering in a finite solid was developed and programmed for computer calculations. It was desired that the model provide both general information on sequential gamma interactions in detector-sized volumes of germanium and detailed predictions of performance of sum-coincidence detectors of specified geometry and operating conditions.

Because of the finite geometries and the many possible combinations of scattering sequences to be considered, the use of Monte Carlo modeling techniques appeared to be the most practical approach to obtaining the desired data. Monte Carlo modeling as applied here consists of following the progress of one gamma photon at a time from the source, through a scattering sequence in the detector until the photon is either completely absorbed or escapes from the detector volume. The fate of the gamma at each step in the sequence is determined by random sampling from appropriate probability distribution functions representing the options available to an actual photon under similar conditions.

Thus the computed output can include general information on the type and location of the interactions and detailed performance information such as the energy spectrum which would be accumulated by a detector

of prescribed size and operating conditions. Phenomena known to affect detector performance can be included in any required detail, provided a suitable mathematical or tabulated functional dependence of the phenomena can be devised. A summary of characteristics of the model is given in Table 2, and detailed descriptions of the model and computer programs are given in Appendix I.

The accuracy with which the computed performance corresponds to the actual performance depends basically on three factors: the extent to which the pertinent physical phenomena are represented in the model, the accuracy of the mathematical description of the phenomena, and the statistical validity afforded by the number of cases considered in the computation. The influence of the number of cases (incident photons) on the accuracy of the predicted results provides the motivation for streamlining the calculational procedures where possible. Obviously some balance must be established between the number of phenomena considered, the accuracy of the modeling, and the requirement for rapid calculation. The criteria for the programs to be described were chosen as that balance which provides a maximum of information specifically needed for evaluating the SCS concept.

Once the Monte Carlo model had been developed, the second step consisted of establishing the range of validity of this model and of the computer program. Data generated using each major equation of the mathematical model were compared to accepted values from the literature to assure that the equations were valid over the range in which they were to be used. Monitoring computer runs of the Monte Carlo scattering calculation for several thousand interactions were made, with selected

Table 2. Summary of Monte Carlo Program for Study of Ge(Li) Spectrometers Which Require Multiple Interactions

SYSTEM CONSIDERED:

1) Ge(Li) detector of any geometry described by (polar) equations (including central hole)
2) Point or plane source any distance from detector
3) Photon energy 300 keV to 3000 keV
4) Surface or internal dead-layers definable by equations
5) Sum-coincidence or sum-only mode
6) Energy discriminator for either or both active volumes

OUTPUT AVAILABLE FROM COMPUTER PROGRAMS:

1) Spectrum recorded by detector; ideal or with specified FWHM, either active detector volume, sum-coincidence or sum-only. Outputed as tabulation, cards, Cal-Comp plot.
2) Density plot for event locations within detector for selected events.
3) Number distributions for number of scatterings before escape and for number of scatterings before photoelectric absorption.
4) Listing of spatial coordinates and energy lost for each event; output on printer or on mag tape for rapid analysis under variety of detector configurations.
5) Two-parameter energy spectrum of energy in each detector volume for coincidence events.
6) Listing of number of photons not hitting detector, passing through detector or center hole, and total number of photons represented by a given calculation.

COMPUTER REQUIREMENTS:

1) Machine: Burroughs B5500
2) Language: Extended ALGOL
3) I-O requirements in: cards, mag tape
   out: cards, line printer, mag tape, Cal-Comp plotter.

variables being printed each time they assumed a different value. These data were used to ascertain that the calculated results are correct regardless of the order in which the various computing loops are traversed, or correspondingly, to any ordering of the interaction types.

The physical characteristics of an available concentric-cylindrical detector were used in a series of calculations at gamma energies attainable from isotopic sources. The detector system will be described in detail in the section on experimental apparatus. Data were obtained on the experimental SCS system for conditions identical to those postulated for the computer runs. Predicted and actual detector efficiency, output spectrum, and distribution of energy between detector sections were compared at the gamma energies listed in Table 3.

Table 3. Gamma Sources Used in the Experimental Program (ordered in increasing gamma energy)

Energy (MeV)	Isotope	Half-life	Approximate Rate During Use (gammas/second)	Origin
0.320080	^{51}Cr	27.8 d	5.0×10^4	Produced in GTRR
0.661635	^{137}Cs	30.0 y	4.28×10^4	NBS #415
0.703	^{94}Nb	20,000 y	6.74×10^3	NBS #4201-84
0.872	^{94}Nb	20,000 y	6.74×10^3	NBS #4201-84
0.89804	^{88}Y	106.6 d	5.8×10^4	Prepared from solution
1.17323	^{60}Co	5.26 y	1.51×10^5	NBS #8203-60
1.33249	^{60}Co	5.26 y	1.51×10^5	NBS #8203-60
1.368526	^{24}Na	15.0 h	2.5×10^4	Produced in GTRR
1.83613	^{88}Y	106.6 d	5.3×10^4	Prepared from solution
2.75392	^{24}Na	15.0 h	2.5×10^4	Produced in GTRR

The isotopic gamma sources were either obtained from the National Bureau of Standards, produced in the Georgia Tech Research Reactor, or prepared from a cyclotron-produced isotope in solution. Gamma emission rates from the sources prepared at Georgia Tech were measured using a 16 cm^3 Ge(Li) spectrometer for which the efficiency over a broad energy range previously had been determined to within five percent error limits for activation analysis research. The 0.898 and 1.369 MeV gamma components from the yttrium-88 and sodium-24, respectively, are close in energy to the 0.872 and 1.332 MeV gamma components of the NBS sources of niobium-94 and cobalt-60, thus allowing the emission rates of the fabricated sources to be measured at an energy at which the detector efficiency could be established with confidence.

After the capabilities and limitations of the mathematical model had been established, the third step based on the extensive use of the model was initiated. A series of computer runs was outlined to provide answers to specific questions on sequential gamma scattering and on the relationship of selected system parameters to multiple scattering detector performance.

One general question of interest was the number of scatterings to be expected for each incident gamma, since multiple scattering is the essence of this spectroscopy concept. Procedures were devised to show the scattering number distribution and the average gamma energy loss per interaction as a function of the scatter number. A plotting routine for the line printer was devised to give a density plot of interactions within the detector boundaries. Data were then generated for selected cylindrical germanium volumes from radius 0.5 cm, thickness 0.5 cm to radius

2.5 cm, thickness 8.0 cm, and for gamma energies from 300 keV to 3000 keV.

An analysis of the general behavior of sequential gamma scattering with respect to practical detector configurations provided the basis for selecting the gamma energies and external detector geometries of Table 4. The "PD" detectors are hypothetical, but the two "SCS" detectors represent actual detectors.

Table 4. Detector Configurations and Gamma Energies Used in the Analysis of Multiple Scattering Ge(Li) Spectrometers

Detector Number	External Geometry	Radius of Central Hole (cm)	Radius of Detector (cm)	Length of Detector (cm)	Total Volume of Detector (cm^3)
PD1	cylinder	0.0	1.5	1.0	7.1
PD2	cylinder	0.0	1.5	2.0	14.1
PD4	cylinder	0.0	1.5	4.0	28.3
PD22	cylinder	0.0	2.0	2.0	25.1
PD44	cylinder	0.0	2.2	4.0	61.0
SCS #1	cylinder annulus	0.35	1.30	2.2	10.8
SCS #3	cylinder annulus	0.35	1.55	1.8	12.9

Gamma Energies: 320, 662, 1332, 1836, and 2754 keV

For each of the gamma energies and detector volumes, the Monte Carlo model was used to generate a magnetic tape record of the scattering sequences of approximately 18,000 incident gammas interacting more than once in the specified volume. The position coordinates and energy loss were recorded for each gamma interaction, thus providing a record

which could be scanned rapidly to obtain information on the effect of varying other detector parameters. For example, sets of internal geometry coordinates and energy discriminator levels were specified, and the tape record was read to sort the gamma interaction sequences into categories according to tests for location, coincidence, and energy loss criteria. For each reading of the tape, either printed tabulations, punched cards, or Cal-Comp plots were available of the spectra from the separate detector sections, of the ideal sum spectrum, and of the sum spectrum with specified energy resolution. The fate of the gammas not treated by the Monte Carlo scattering (those missing the detector, interacting once only, or passing through the detector) was also calculated and presented as a printed tabulation for subsequent efficiency calculations.

Thus, for each parameter value of the parameter variation study, system performance quantities such as the number of events in the full energy peak and the Compton tail, the peak-to-Compton ratio, the efficiency, and the amount of Compton interference at any energy were available from the computer output. These system performance characteristics were catalogued as a function of the following parameters: total detector volume, incident gamma energy, active volume configurations and ratios, dead layer location and volume, energy discriminator levels, and energy resolution of the system.

Additional information to guide the energy discrimination analysis was obtained by printing a two-parameter array of the energy spectrum from each detector for coincident events only. This display showed the energy distribution between the two detectors for both full energy and

partial energy scattering sequences. It was then a straightforward procedure to determine the number of full energy and partial energy events affected by any combination of energy discriminator or window settings simply by observing the number of counts within the corresponding area on the two-parameter array.

Information from the two-parameter array was also considered in the selection of threshold value settings for parameter variation runs on the experimental SCS system. For various combinations of gamma source energy and discriminator settings, experimental spectra were recorded from which the peak-to-Compton ratios and peak efficiency could be calculated. The system was also operated in the sum-only mode to obtain data for comparing sum-coincidence and sum-only performance. Summations of performance data from both the computer calculations and from operation of the sum-coincidence system are given in Chapter V.

The fourth step in the study was the analysis of the computed and experimental results to establish whether or not multiple scattering spectrometers offer significant Compton suppression capabilities as compared to other techniques. First, the general behavior of sequential gamma scattering was examined to determine if suitable scattering behavior to support coincidence operation can be expected in typical detector volumes of germanium. Secondly, the parameter variation study results were used to establish the importance of various parameters and to determine how the parameters might be fixed to enhance SCS system performance. The performance of optimized systems was estimated, and this performance compared to that attainable with other Compton suppression techniques using Ge(Li) detectors. Finally, observations were made

as to the limitations of Ge(Li) spectrometers based on multiple scattering and on possible methods of minimizing these limitations.

CHAPTER IV

THE EXPERIMENTAL APPARATUS

A sum-coincidence spectrometer system was operated as a part of this research in order to test the validity of the mathematical model and to supplement the parameter variation study. The choice of the detector and sum-coincidence instrumentation was limited by economic considerations to the instrumentation available within Georgia Tech and that provided by the Department of Physics of Emory University. Although the relatively poor energy resolution, efficiency, and Compton suppression of the system prevent the demonstration of optimum sum-coincidence spectrometer capabilities, the performance of the system was adequate for accomplishing both the check of the mathematical model and the experimental parameter variation study. The effect of such factors as energy resolution of the system and inactive volumes inside the detector could be accounted for within the Monte Carlo model.

The discussion of the experimental apparatus is divided into two topics: the detector and the sum-coincidence instrumentation. Additional material describing the experimental system is presented in Appendix II.

The Detector

The experimental Ge(Li) detector and cryostat were fabricated by the Department of Physics of Emory University. The starting material for

fabrication of the detector was a germanium cylinder of 3.1 cm diameter cut from the standard Sylvania No. 4 ingot configuration. Resistivity of the gallium-doped ingot was approximately 35 to 40 ohm-cm, and the dislocation density and minority carrier lifetime were specified by the supplier as $2400/cm^2$ and 350 microseconds, respectively. A cylindrical hole of 0.70 cm diameter was drilled in the center by grinding with a brass tube and Al_2O_3 lapping compound of grit No. 600. A lithium-in-oil suspension was painted onto the interior and exterior cylindrical surfaces, and an n-type layer approximately 400 microns thick was produced on each surface by a 10 minute diffusion at 425°C.

The drifting process was carried out in a water bath at temperatures from 10 to 25°C. The voltage during the lithium drifting operation varied from 100 volts to 1000 volts, and drifting current from 10 milliamperes to 400 milliamperes. A cross sectional sketch of the detector, designated SCS #3, is shown in Figure 7.

The detector was then stored for nine months in the cryostat at liquid nitrogen temperature but without applied bias voltage. In September 1969 the detector, cryostat, and Dewar flask were moved to the Nuclear Research Center at Georgia Tech. Detector resolutions were measured to be 10 keV* and 12 keV, respectively, for the inside and outside detectors, using the instrumentation shown in Figure 8 and listed in Appendix II.

Redrifting operations were performed at Georgia Tech to improve the detector resolution. After the redrifting procedure, the FWHM resolutions were measured to be 5.4 keV and 5.8 keV for the inside and outside

---

*All measured energy resolutions to be quoted are FWHM values for the 1.332 MeV gamma component of cobalt-60 at low count rates.

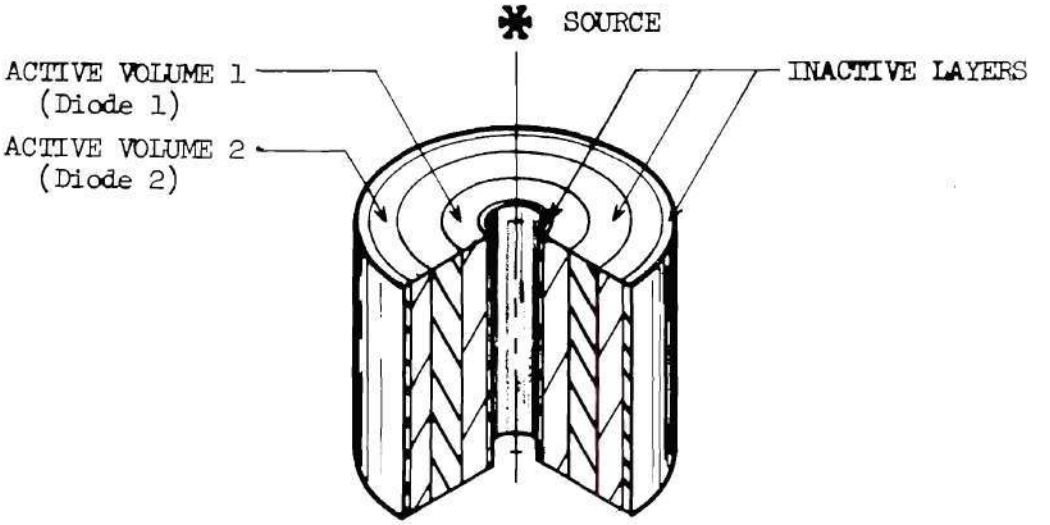

Figure 7. Detector Internal Configuration for Concentric Cylindrical Detector

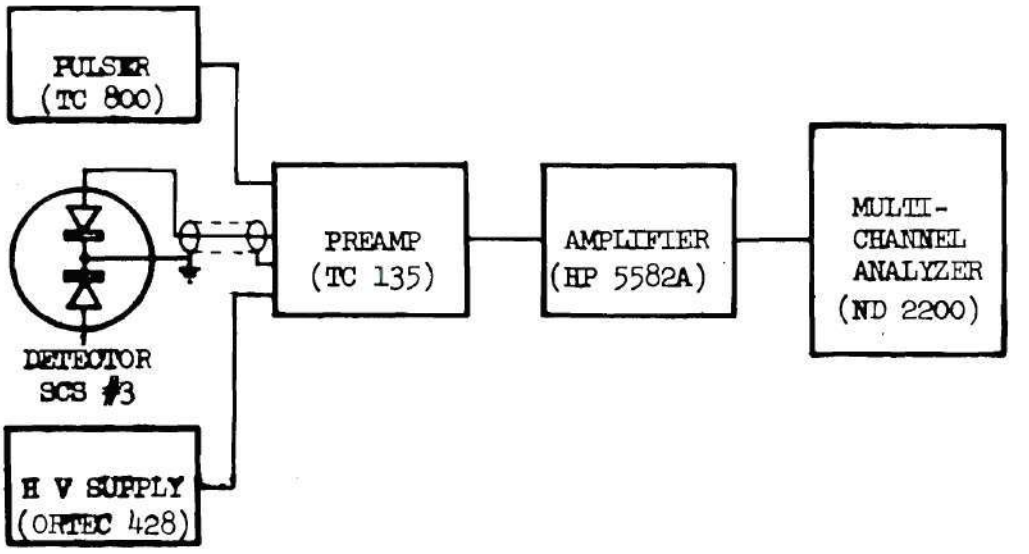

Figure 8. Instrumentation for Energy Resolution Measurements

detectors.

Using the instrumentation shown in Figure 9, the capacitance of each detector section was measured versus applied voltage, giving the values shown in Table 5.

Table 5. Capacitance as a Function of Applied Bias Voltage for Detector SCS #3

Bias Voltage (Volts)	Capacitance (picofarads)	
	Inside Detector	Outside Detector
0	86.4	230
10	31.8	76.0
100	26.2	72.8
200	25.0	72.1
300	24.8	71.8
400	24.8	71.5
500	24.7	71.3
600	24.6	71.1
700	24.6	70.9
800	24.5	70.8

Because the detector was supplied in the cryostat, it was necessary to X-ray the cryostat to determine the outside dimensions of the detector and the exact location of the detector within the cryostat. Figure 10 shows positive prints made from the X-rays and a sketch of the detector mounting based on information supplied by the manufacturer. From these combined sources of information, the external detector dimensions were determined to be as follows: inside radius = 0.35 cm; outside radius = 1.55 cm; length = 1.75 to 1.85 cm; cryostat-to-detector distance = 1.6 cm; outside diffusion depth = 400 microns.

It is necessary for the computation also to know the locations of

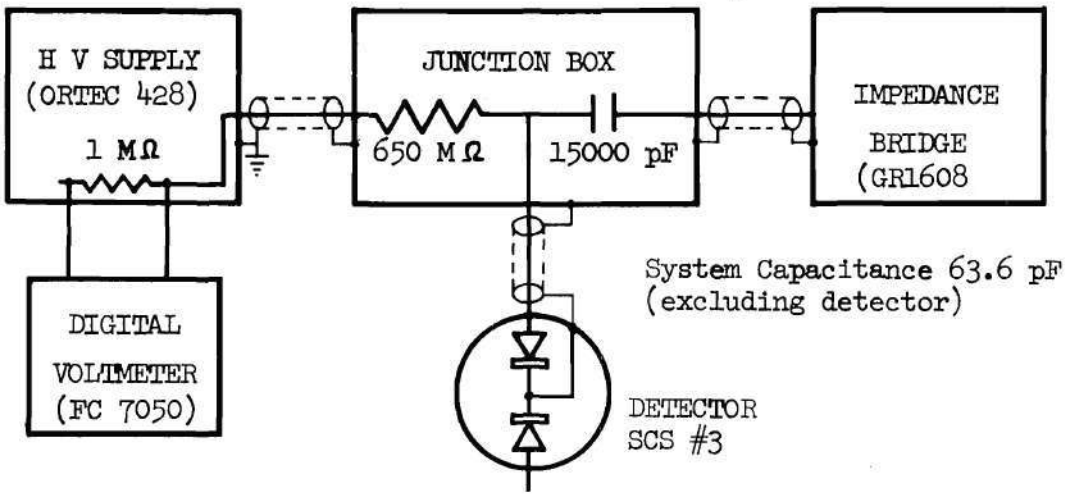

Figure 9. Instrumentation for Detector Capacitance Measurements

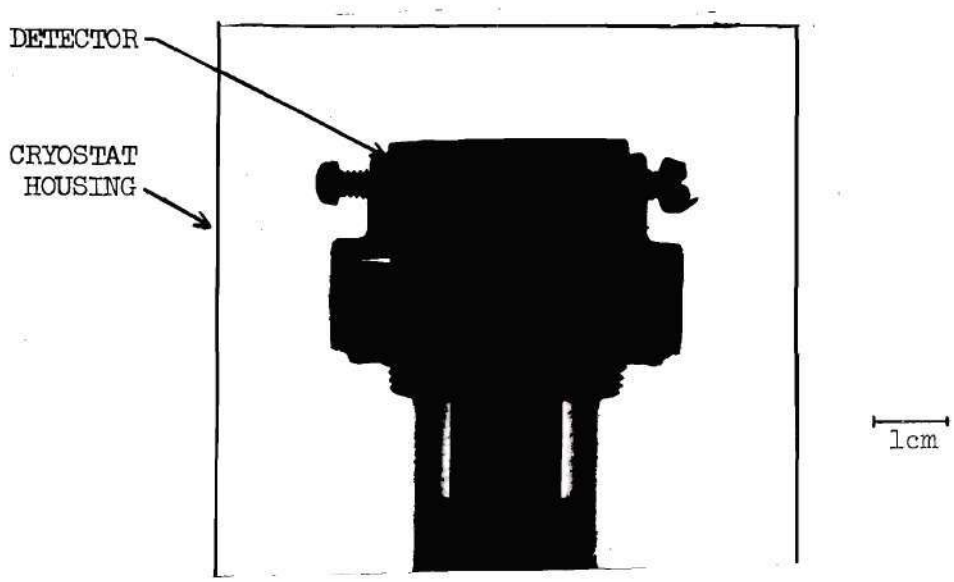

Figure 10. X-Ray Positive Print of Detector SCS #3 and Cryostat

the boundaries of the active detector regions which lie inside the detector. These can be calculated from a knowledge of the capacitance of the detector and of the external geometrical dimensions. The capacitance of concentric cylindrical shells of inside radius, a, and outside radius, b, is given by[70]

$$C = \frac{2\pi\ \epsilon_o \epsilon_r\ L}{\ell n\ (b/a)} \tag{7}$$

where ϵ_o = permittivity of vacuum

= 0.0885 picofarad/cm

ϵ_r = relative permittivity of material between cylindrical boundaries

= 16 for germanium[33]

L = length of cylinder in cm

C = capacitance in picofarads.

Thus, for germanium

$$C = \frac{8.91\ L}{\ell n\ (b/a)}\ \text{picofarad} \tag{8}$$

Using a measured capacitance value from Table 5 and the external dimensions from the previous paragraph, the inside radius R_I and outside radius R_O of the internal dead layer separating the two active detector regions can be calculated.

$$\text{Inside Detector:}\quad C_I = \frac{8.91\ (1.7)}{\ell n\ (R_I/0.390)} = 24.5\ \text{pF}\ ;\quad R_I = 0.73\ \text{cm} \tag{9}$$

$$\text{Outside Detector:}\quad C_O = \frac{8.91\ (1.7)}{\ell n\ (1.51/R_O)} = 70.8\ \text{pF}\ ;\quad R_O = 1.2\ \text{cm} \tag{10}$$

Based on the measurements described, the detector dimensions are as shown in Figure 11. A subsequent attempt to define the junction regions was made by traversing a well collimated gamma beam across a diameter of the detector in steps of 0.1 cm. The geometry defined by this experiment agreed with that shown in Figure 11 to within the resolution limits of this technique, about 0.1 cm.

The dc leakage current for each detector immediately after the redrifting operation was approximately one nanoampere at 800 volts bias. The leakage increased during the data recording period to approximately two nanoamperes and three nanoamperes for the inside and outside detectors, respectively, with an applied bias of 800 volts.

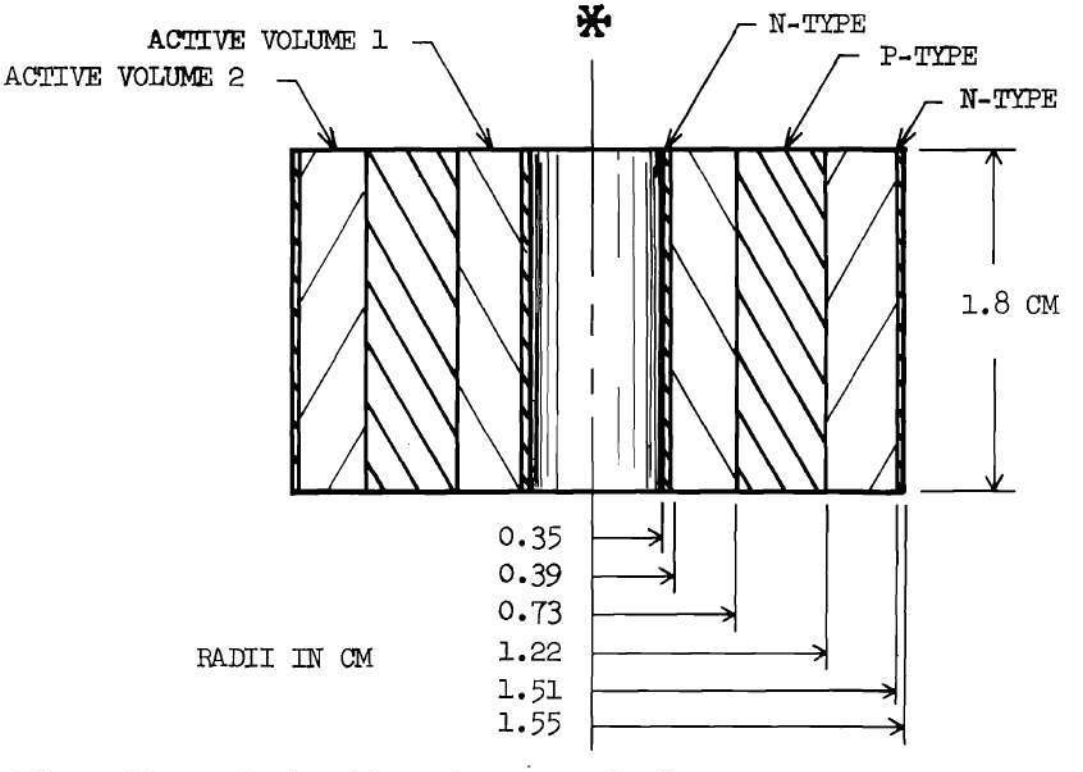

Figure 11. Detector Dimensions for SCS #3 from X-Ray and Capacitance Measurements (Drawing of Detector Cross Section at a Diameter)

The Sum-Coincidence Instrumentation

The function of the instrumentation is to provide a linear output signal proportional to the sum of the gamma ray energy deposited in each detector section for incident gamma rays which deposit energy in both detector sections. Several approaches to achieving this sum-coincidence function were evaluated, and the instrumentation system shown in Figure 12 was selected as a practical system designed for the purposes of this research.

Linear signals from each detector section pass through independent charge-sensitive FET preamplifiers and pulse shaping voltage amplifiers, then are summed in the linear summing amplifier. The linear signal is then fed into a delay amplifier, a linear gate, and into the pulse height analyzer of the multichannel analyzer. The gating signal is derived from a coincidence unit which is driven by the timing single channel analyzers (SCA's).

Sum-coincidence operation of the system proceeds in the following manner. If a photon incident from the source leads to interactions in both detector sections, signals appear simultaneously at the outputs of amplifiers "A" and "B". Coincident logic signals then appear at the outputs of the single channel analyzers, causing the coincidence unit to trigger the gate-and-delay generator, which provides an output pulse of the required time duration for opening the linear gate to pass the linear summed signal from the delay amplifier. To assure that the linear signal and the gate signal arrive in the proper time order at the linear gate, the linear signal may be delayed at the delay amplifier, and the logic signals at the timing single channel analyzers and the gate-and-delay generator.

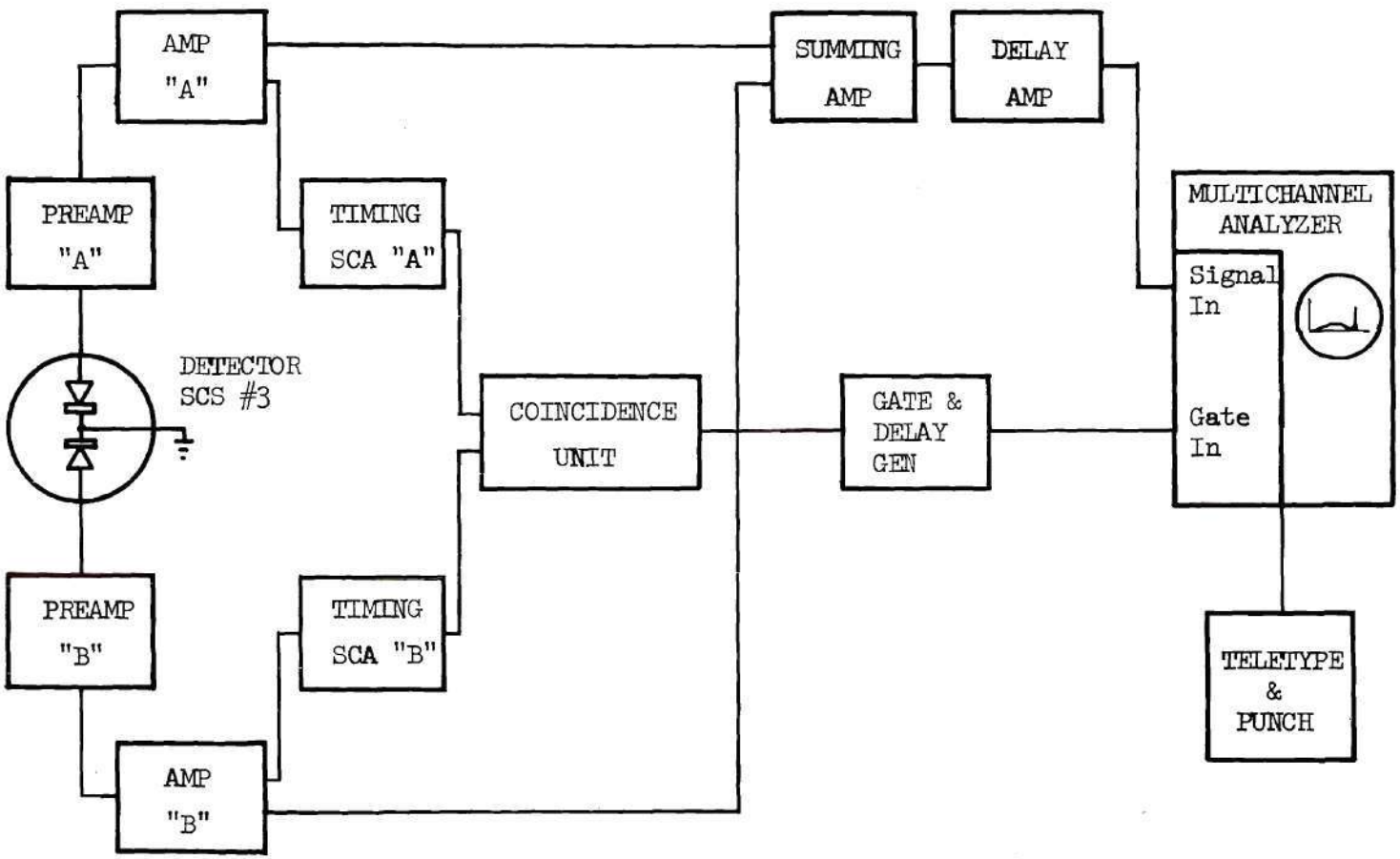

Figure 12. The Experimental Sum-Coincidence Instrumentation

Output spectral data from the 1024 channel analyzer were displayed graphically on an oscilloscope or an x-y plotter, and were recorded on punched paper tape or as a typewritten tabulation.

Two-parameter energy spectra from the two detector volumes were recorded with the instrumentation shown in Figure 13. The coincidence instrumentation from the sum-coincidence system was used to provide gating signals to both pulse height analyzers of the two-parameter system. The two-parameter energy spectra for coincidence events were photographed from the oscilloscope display of the 32 by 32 spectrum.

A list of the specific instruments used in the sum-coincidence and two-parameter systems is given in Appendix II. A photograph of the instrumentation and detector is also contained in the appendix.

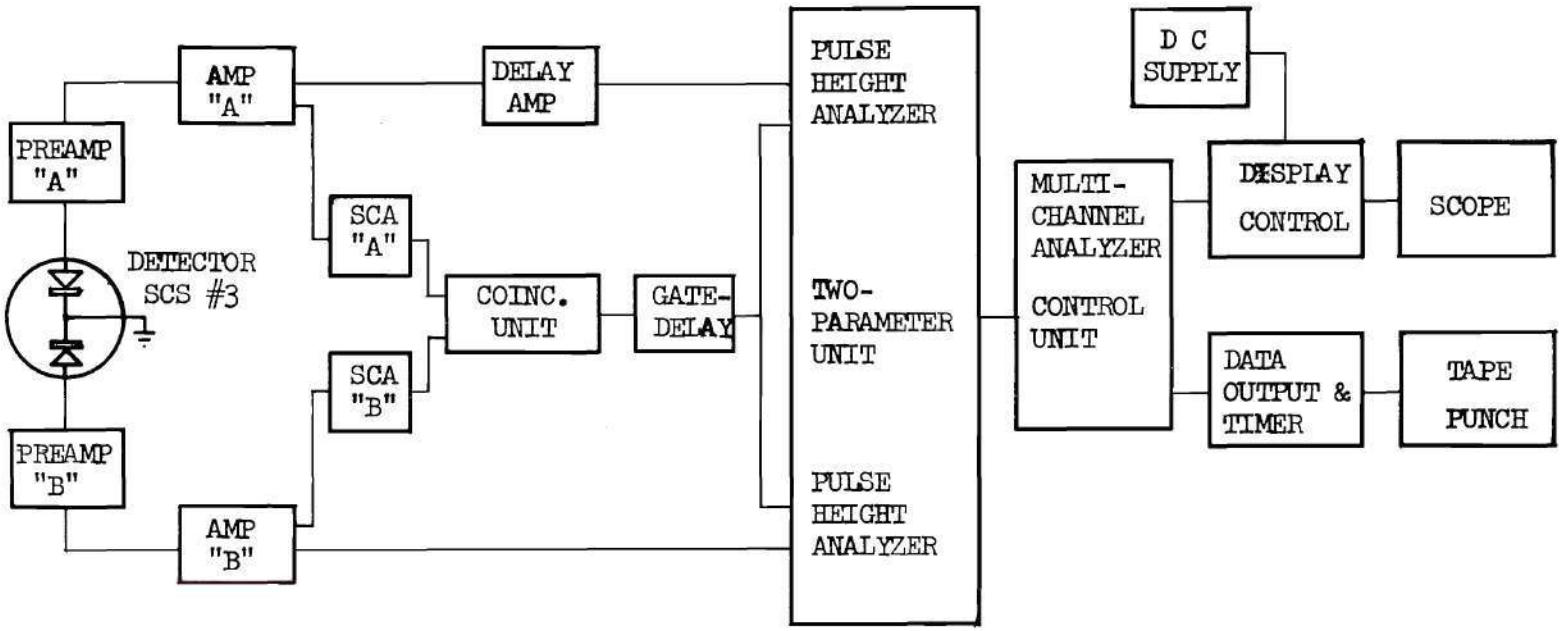

Figure 13. The Experimental Two-Parameter Instrumentation

CHAPTER V

DISCUSSION OF RESULTS

The results of the analysis will be presented in four sections. First, calculated data on the general behavior of gamma scattering in germanium will be discussed as it relates to multiple scattering detector concepts. Secondly, the parameter variation study based on computed results for selected detector geometries will be presented. In the third section, measured sum-coincidence spectrometer performance will be presented and compared to calculated results. Finally, the performance of optimized multiple scattering spectrometers will be discussed and compared to that of conventional Ge(Li) spectrometer systems.

General Observations on Sequential Gamma Scattering in Germanium

As a first step in the analysis, calculations were made to provide a qualitative model of the consequences of gamma scattering in detector-sized volumes of germanium. The following sections present the results of calculations of the geometrical distribution of interactions, of the extent of multiple scattering, and of the energy and range of electrons produced in the interactions. The calculated information is then combined to form a general description of gamma scattering and electron production in finite germanium volumes for incident gamma energies of 300 keV to 3.0 MeV.

Spatial Distribution of Events

In Figure 14, gamma pathlengths in an infinite germanium volume

are given for interaction probabilities of 0.1, 0.5, and 0.9.

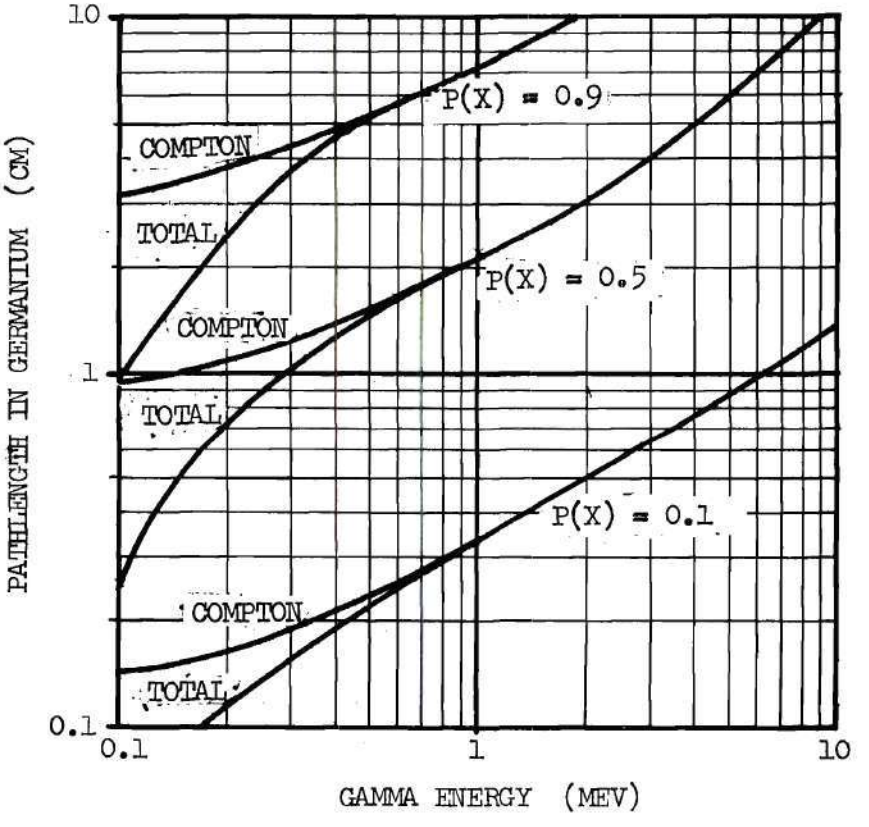

Figure 14. Pathlengths in an Infinite Germanium Sample versus Gamma Energy for Interaction Probabilities of 0.1, 0.5, and 0.9 from Equation $P(X) = (1 - e^{-\Sigma_\gamma X})$

These curves were generated from the equation for the probability of interaction, P(X), based on the linear interaction cross sections:

$$P(X) = (1 - e^{-\Sigma_\gamma X}) \qquad (11)$$

where $P(X)$ = probability of interaction within a linear distance of X cm for a gamma of energy E

Σ_γ = linear interaction cross section (cm^{-1}) for a gamma of energy E

X = distance (cm) in material of linear interaction cross section Σ_γ.

Values of Σ_γ were calculated from the data of Table 2, and corresponding values of distance, X, were calculated and plotted for P(X) values of 0.1, 0.5, and 0.9.

The median path length, P(X) = 0.5, for gammas is seen to vary from about one centimeter at 300 keV to four centimeters at 3.0 MeV. Because detector dimensions are typically of the order of these median gamma pathlengths, the interaction sites would be expected to be distributed throughout the detector volume.

Computed results obtained during calculations with the Monte Carlo model were used to display the interaction locations for initial and subsequent gamma interactions. These plots were used to identify the detector volumes in which the maximum concentration of desired events occurred. In these plots the y-axis represents the centerline of a cylindrical germanium volume, where the gamma source is located above the cylinder on the axis. The ordinate and abscissa are therefore the "z" and "r" directions, respectively, of a cylindrical coordinate system, where interaction events for any "Φ" have been rotated into a single r-z plane.

Specific plots for the first Compton scatter and final photoelectric absorptions for full energy scattering sequences from 662 keV

incident gammas are shown in Figure 15, and for 1332 keV incident gammas in Figure 16. Each density plot given shows the interaction locations of about 3000 gammas which undergo multiple scattering ending in photoelectric absorption. Each star represents the occurrence of one or more events within the corresponding volume increment.

In these cases the 2.5 cm radius and 8.0 cm length of the germanium cylinder were intentionally chosen to be larger than the typical dimensions of germanium detectors. Practical detector dimensions could then be identified as the regions of maximum concentration of interactions for full energy scattering sequences. These plots show that only a minor fraction of events occurs in the lower four centimeters of the cylinder; from other calculated results, less than ten percent of the good event sequences involve interactions in the lower half of the volume for the cases shown. The selection of four cm as the maximum length to be considered in the parameter variation study was based on an analysis of the density plots and the calculated distributions.

Scattering Number Distributions

In order to obtain data on the extent and type of sequential gamma interactions in germanium, computer calculations were performed in which each scattering sequence was categorized according to the number of gamma interactions occurring before total absorption or escape from the volume. Tabulated interaction distribution data for several cases are given in Table 6, where all data have been normalized to 10^6 photons emitted from a gamma source located 2.0 cm above the detector volume. Because the data are normalized to the same number of photons from the source, the table shows the relative number of gammas of various energies which undergo

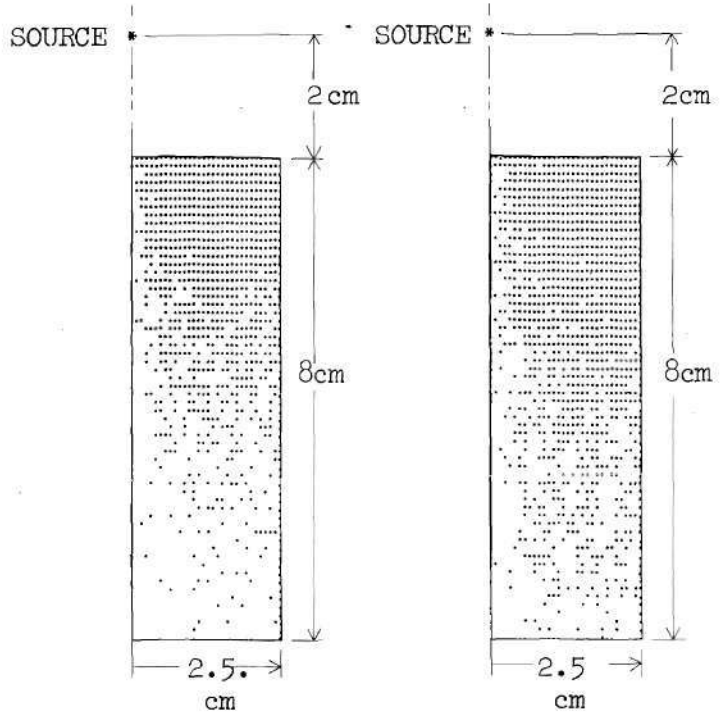

15a) First Compton Interaction

15b) Final Photo-electric

Figure 15. Density Plot for Gamma Interaction Locations for 662 keV Gammas Incident on a Germanium Cylinder

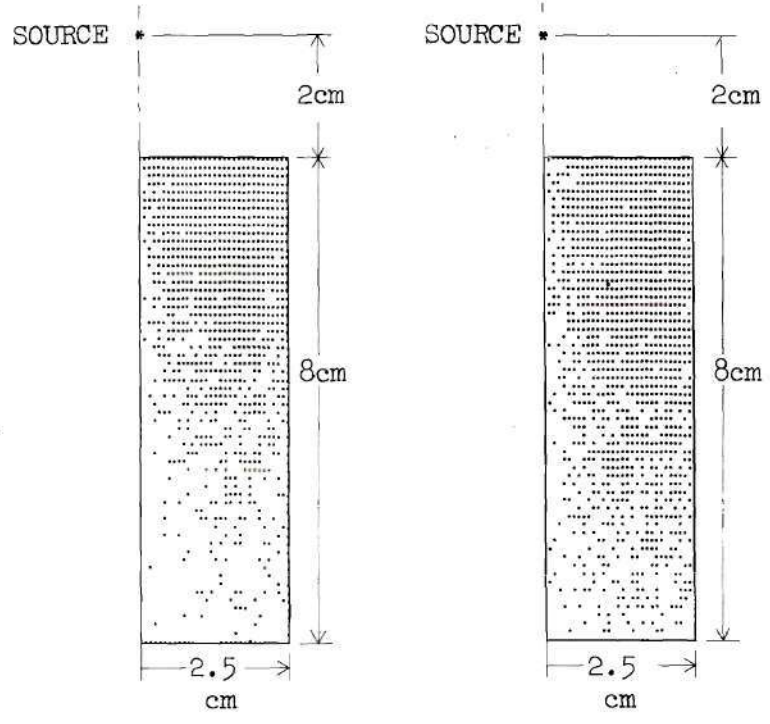

16a) First Compton Interaction

16b) Final Photo-electric

Figure 16. Density Plot for Gamma Interaction Locations for 1332 keV Gammas Incident on a Germanium Cylinder

Table 6. Number of Gammas Which Escape or Are Captured on a Given Interaction Number per 10^6 Gammas from Source

Detector	Gamma Energy (keV)	No. of Interactions before Escape or Capture						
		1	2	3	4	5	6	7
		Escape Distribution						
PD1 (L = 1 cm, R = 1.5 cm)	320	17065	3811	1768	237	48	0	5
	662	16603	3527	759	138	20	0	1
	1332	13542	2491	558	85	21	4	0
	1836	11822	2054	432	77	18	1	0
	2754	9780	1525	323	62	13	2	0
PD2 (L = 2 cm, R = 1.5 cm)	320	18600	5060	1115	272	38	0	7
	662	20002	5422	1394	364	92	15	4
	1332	17127	4238	1142	256	60	16	3
	1836	15300	3636	883	206	69	13	4
	2754	13250	2840	700	158	40	7	3
PD4 (L = 4 cm, R = 1.5 cm)	320	17750	5680	1432	284	99	4	0
	662	20972	6836	1906	598	172	28	6
	1332	18884	5673	1721	450	126	33	4
	1836	17116	5050	1500	419	91	22	8
	2754	14700	3940	1080	274	76	22	9
		Capture Distribution						
PD1 (L = 1 cm, R = 1.5 cm)	320	4286	5333	2045	754	221	56	9
	662	117	657	626	369	138	58	18
	1332	73	411	392	231	86	36	11
	1836	28	284	251	176	69	22	7
	2754	10	174	163	114	48	16	4
PD2 (L = 2 cm, R = 1.5 cm)	320	5675	8218	3568	1643	562	188	24
	662	760	2196	1753	1023	444	181	42
	1332	379	1183	1129	814	378	142	47
	1836	99	636	749	512	230	108	23
	2754	13	294	349	280	138	60	15
PD4 (L = 4 cm, R = 1.5 cm)	320	6466	9610	4746	2481	928	306	50
	662	829	2589	2470	1781	826	309	103
	1332	156	901	1245	912	485	229	106
	1836	43	587	909	699	360	162	75
	2754	20	362	565	463	248	112	38

capture or escape, as well as the number of interactions involved in the typical scattering sequence. In Figure 17, two distributions from Table 6 are plotted to display the general features of the scattering number distribution for partial energy and full-energy event sequences.

From these data it is seen that the most probable fate for an incident gamma is a single Compton or pair production interaction followed by escape of the scattered photon or annihilation photon pair. This one-interaction sequence is the primary source of partial energy events occurring in a germanium detector. By comparison, the sequences in which the entire gamma energy is captured in the detector have a most probable number of interactions of two or three, with four or more interactions also observed to be common. In none of the distributions for sequences ending in capture was the single interaction the most probable sequence.

These results are pertinent to detector concepts based on multiple gamma interactions in showing that abundant multiple scattering accompanies full energy absorption processes, while a major portion of the partial energy events occurs as a single interaction. This behavior is quantitatively shown by the data of Table 7 which gives the fractions and normalized numbers of event sequences which are comprised of a single interaction only. In the range of cases considered, between 69 percent and 84 percent of the partial energy events would be eliminated by rejecting one-interaction sequences, while only about 1 percent to 34 percent of the full energy events would be eliminated. If a fixed number of gammas from the source is chosen as the basis for comparison, the number of partial energy events eliminated by neglecting single interactions exceeds the number of full energy events which would be eliminated by factors of from about 3 at low energies to 100 or more at higher energies.

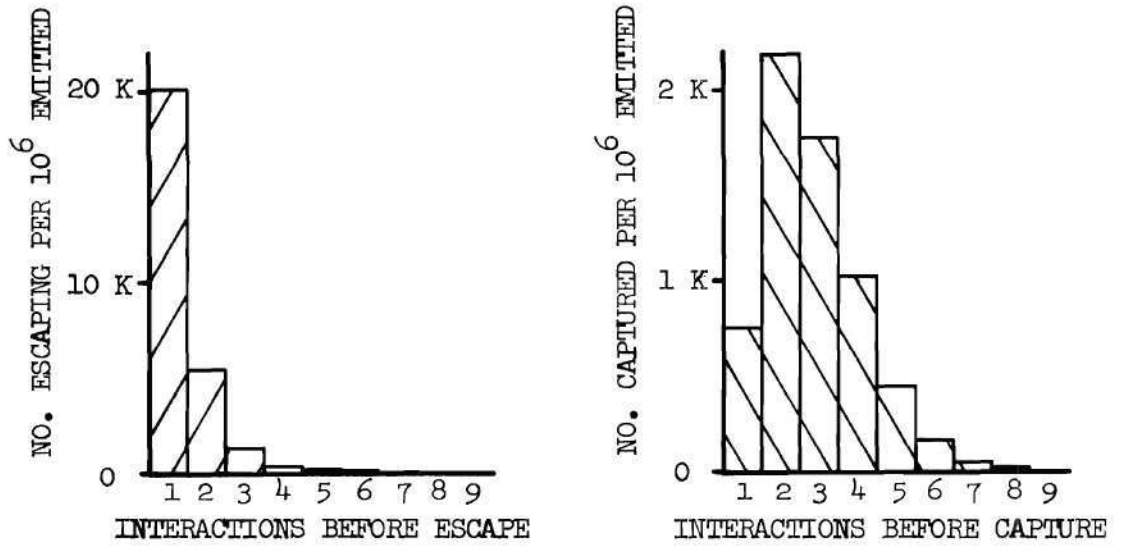

17a) Number Distribution for 662 keV Incident Gammas

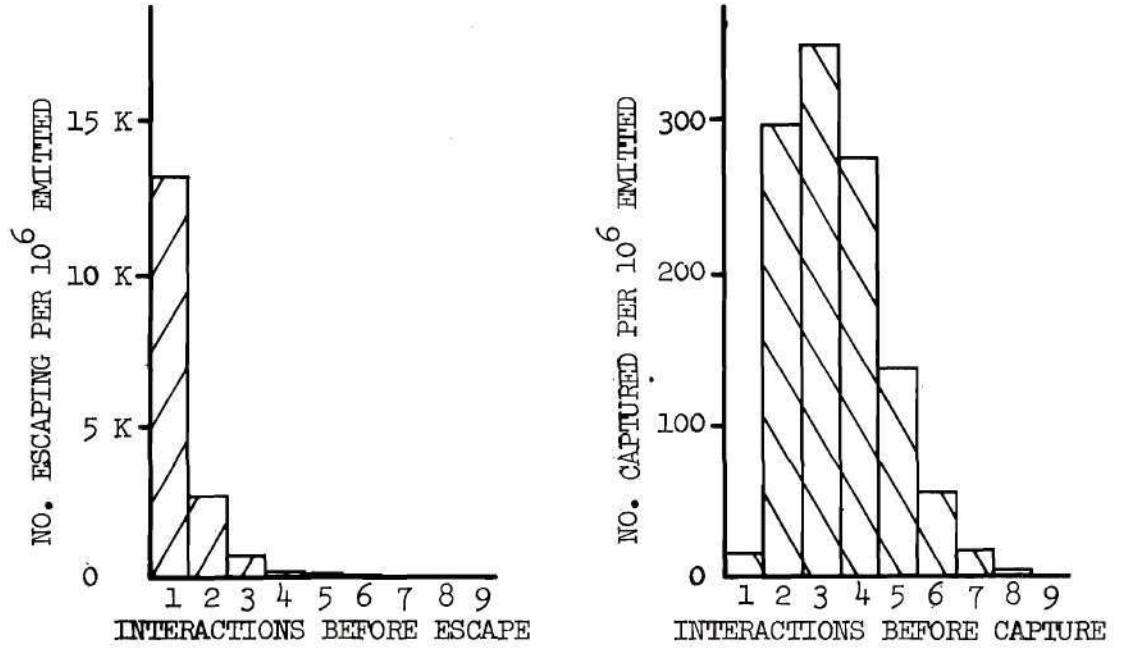

17b) Number Distribution for 2754 keV Incident Gammas

Figure 17. Gamma Interaction Number Distributions for a Germanium Cylinder of Radius 1.5 cm, Length 2.0 cm, and a Source-to-Cylinder Distance of 2.0 cm

Table 7. Full Energy and Partial Energy Gamma Scattering Sequences Comprised of a Single Interaction (source is 2 cm above volume)

Detector Size (cm)		320 keV		662 keV		1332 keV		2754 keV	
Radius	Length	Full	Partial	Full	Partial	Full	Partial	Full	Partial
				Percentage of All Events of That Type					
1.5	1.0	33.7	75.6	15.9	78.9	5.87	81.8	1.96	83.7
1.5	2.0	28.5	74.3	11.9	73.3	4.17	75.0	1.16	77.8
1.5	4.0	26.3	70.0	9.25	68.7	3.84	70.0	1.12	73.2
2.0	2.0	26.9	72.9	11.0	71.2	3.60	73.4	0.60	76.8
				Number per 10^6 Gammas from Source					
1.5	1.0	4286	17065	117	16603	73	13542	11	9780
1.5	2.0	5675	18600	760	20002	110	17127	13	13250
1.5	4.0	6466	17750	829	20972	156	18884	20	14700
2.0	2.0	9130	26867	1309	29879	189	26421	15	20074

It should be noted that the maximum relative peak efficiency for a detector system accepting only multiple gamma interactions as compared to accepting all events is set by the fraction of full energy events lost by neglecting one-interaction sequences. For the cases given, the upper bound on relative efficiency would vary from about 66 percent at 320 keV to greater than 99 percent at 2754 keV. The relative efficiency of an actual detector requiring multiple gamma interactions will be less than the theoretical maximum by the fraction of multiple events which is not recognized as such by the instrumentation system.

Average Energy Loss versus Event Number

In the computer calculations the amount of energy transferred to the electron during each photon-electron interaction was recorded as a function of the interaction number for that incident gamma. After all scattering data were catalogued for a given computer run, the average energy loss per collision versus interaction number was calculated. The calculated average energy loss includes the contribution from all types of interactions which occurred for a given interaction number in all scattering sequences.

Figure 18 shows a plot of the computed average energy loss as defined above versus interaction number for a cylindrical germanium volume of radius 1.5 cm and length 4.0 cm. These data are typical of those calculated for each of the detector volumes of the analysis. Note that the average energy loss per collision for the first interaction is approximately half of the incident gamma energy and that, regardless of the incident energy, the average energy transferred to electrons quickly approaches about 100 keV per collision for subsequent collisions.

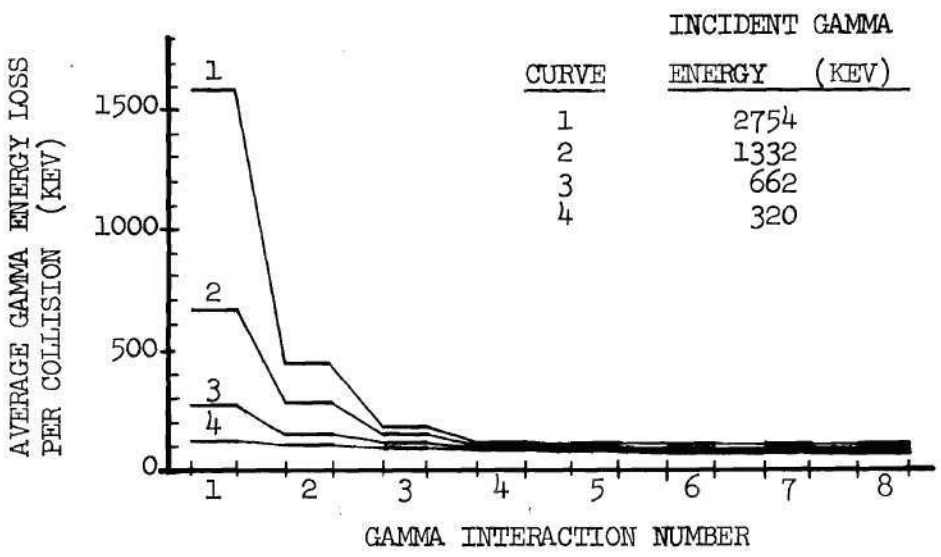

Figure 18. Average Gamma Energy Loss per Collision versus Gamma Interaction Number in a Germanium Cylinder of Radius 1.5 cm and Length 2.0 cm

The range in germanium for electrons within this energy span can be calculated using the empirical electron range-energy equation of Katz and Penfold[71]

$$R\ (mg/cm^2) = 412\ E^{(1.265\ -\ 0.0954\ \ln E)} \qquad (12)$$

where E = electron energy in MeV

For electron energies of 100, 500, and 1000 keV, the calculated electron ranges are 26, 306, and 773 microns, respectively. Based on the small average energy transfer per interaction as indicated from the data of Figure 18, the range of primary electrons is expected to be small compared to the dimensions of the detector volumes considered in this analysis.

Qualitative Description of Multiple Scattering

By the use of the combined calculated results on geometrical gamma interaction locations, scattering number distributions, and average energy transferred to the electrons, a qualitative description of multiple scattering in state-of-the-art germanium detector volumes can be formulated. These comments apply only for the previously defined range of gamma energies and detector dimensions.

First, partial energy gamma scattering sequences are more probable than full energy scattering sequences, and the most likely interaction sequence is a single interaction followed by escape of the scattered gamma or annihilation gammas. Secondly, for full energy scattering sequences, multiple gamma scattering is predominant, with the most probable number of interactions being two or three. On the average, these sequences are comprised of gamma interactions separated by distances of the order of a centimeter for the first one or two interactions, and by distances of millimeters for subsequent interactions.

Thirdly, after the first interaction the energy given to the electron in each gamma interaction is on the average a small fraction of the incident gamma energy. Thus the consequence of a multiple sequence is typically the production of several spatially remote regions of localized charge within the detector volume.

This composite scattering picture indicates that, at least in theory, partial energy events may be suppressed preferentially with respect to full energy sequences by requiring multiple gamma scattering and that the maximum intrinsic loss of peak efficiency is not greater than about one third of the efficiency for accepting all detected events.

The presence of multiple events might be established in germanium detectors by identifying the geometrical region of charge collection or by the pulse shape characteristics caused by different charge transit times. The task then is to define the detector and instrumentation systems which can effectively identify and record the energy of the multiple interaction sequences.

Computer Analysis of Sum-Coincidence Spectrometers

The sum-coincidence gamma spectrometers described in the introductory sections of this report select multiple gamma interaction sequences by requiring coincident interactions in independent active detector volumes. Performance of these sum-coincidence spectrometers is known to depend on several physical parameters of the germanium detector and on energy requirements for accepted gamma events. Computer calculations with the Monte Carlo model were used to provide a basis for characterizing the effect of important parameters and for specifying detector systems which maximize selected performance criteria. Based on a review of the general characteristics of gamma scattering in attainable germanium detector volumes, the detector volumes and gamma energies which were listed previously in Table 4 were selected for the parameter variation studies.

Interaction Mode for Full Energy Events

In the empirical analyses of germanium sum-coincidence spectrometer (SCS) operation as given by previous investigators,[56,60,68,72] the primary interaction mode has been postulated as a large-angle Compton interaction in one detector volume, followed by capture of the low-energy backscattered gamma in the second active volume, as shown in Figure 19a.

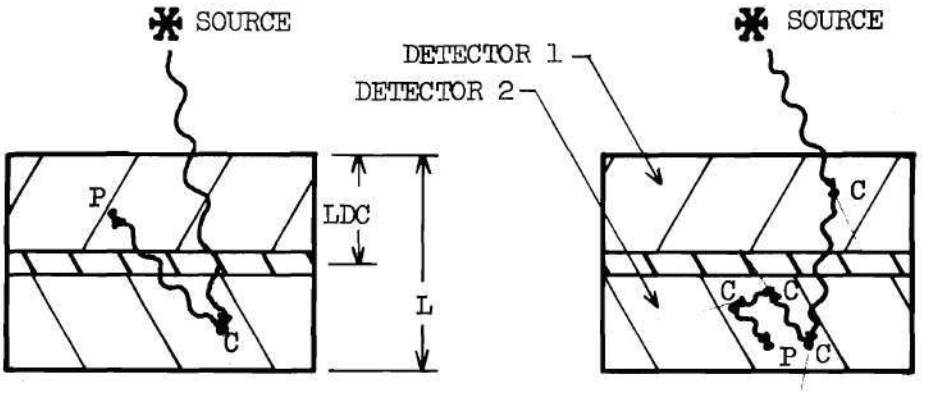

19a) Backscatter Event Mode

19b) Small-Angle Event Mode

Figure 19. Postulated Interaction Modes for Full Energy Events in Sum-Coincidence Spectrometers

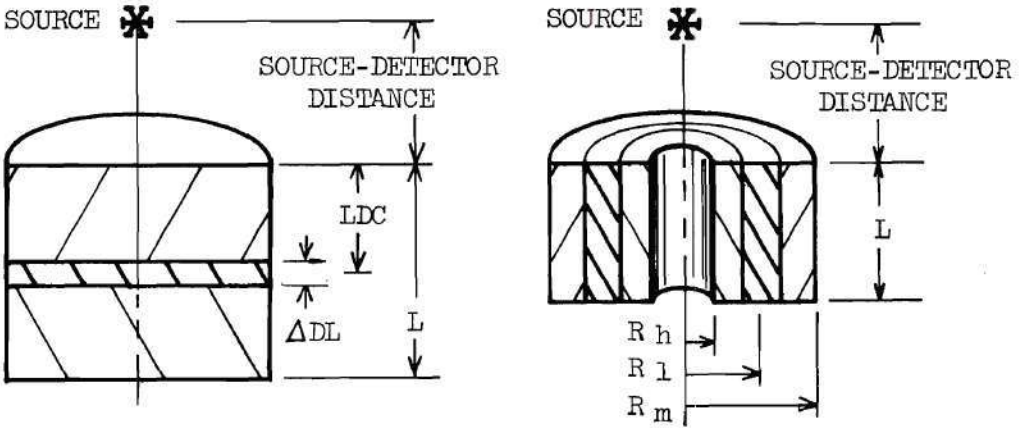

20a) Stacked Planar Configuration

20b) Concentric Cylindrical Configuration

Figure 20. Stacked Planar and Concentric Cylinder Detector Geometries for Sum-Coincidence Spectrometers

Detector configurations and energy discrimination criteria were chosen to maximize the occurrence and detection of the backscatter-capture sequence. Energy requirements of a large energy release in the second detector from the backscatter interaction and a small energy release in the first detector were observed to enhance Compton suppression performance.[56,60]

Early in this study it became apparent that the dominant role of the backscatter interaction mode for SCS operation was in conflict with the computed results of this analysis. The computer program was expanded to give specific output information on the number of good (full energy) and bad (partial energy) gamma interaction sequences originating in each active detector volume. If the backscatter mode were dominant, then a majority of the good events should originate in the second detector volume. The computed results predicted the opposite behavior; the calculated ratios of good events originating in the first volume to those originating in the second volume as given in Table 8 show that, for most cases, only a minor fraction of the full energy events is initiated in the second detector volume.

The success of the energy selection requirements based on the backscatter mode then requires explanation. One possible alternate mode giving approximately the same division of energy between detector volumes is the occurrence of a small-angle Compton event in the first detector followed in the second detector by multiple interactions ending in complete absorption (Figure 19b). The general description of gamma scattering behavior developed in the previous section tends to support this concept. Those data showed that a major fraction of interaction sequences

was initiated by small-angle Compton interactions and that extensive multiple scattering is associated with good events. Both phenomena would be required for the small-angle Compton mechanism to account for an appreciable number of good event sequences.

Table 8. Calculated Ratio of Full Energy Events Initiated in Volumes 1 and 2 for Selected Detector Geometries and Gamma Energies (see Figure 19a)

Detector Geometry		Ratio = $\frac{\text{No. Initiated in Volume 1}}{\text{No. Initiated in Volume 2}}$			
Dimensions (cm)	LDC (cm)	Gamma Energy in keV			
		320	662	1332	2754
R = 1.5	0.25	1.37	1.06	0.953	0.913
L = 1.0	0.45	1.45	1.11	0.997	0.988
	0.65	1.61	1.32	0.983	0.989
R = 1.5	0.45	2.57	2.02	1.90	1.49
L = 4.0	0.95	3.91	2.71	2.52	1.80
	1.95	5.88	4.00	2.92	2.43
	2.95	5.88	3.70	2.69	2.11
R = 2.0	0.25	2.11	1.63	1.43	1.15
	0.75	2.63	1.97	1.73	1.41
	1.25	2.97	2.17	2.13	1.73
	1.75	2.18	2.22	1.60	1.62

It may appear that the small-angle mechanism for good multiple interaction events is in conflict with the data presented in Figure 18. Those data showed that the average gamma energy loss per collision for the first interaction was approximately one half of the incident gamma energy. From equation 3, however, the Compton scattering angle for the loss of one half of the energy of a 2754 keV gamma is calculated to be only 35.5 degrees. In addition, the data of Figure 18 include not only

full energy multiple scattering sequences but also partial energy sequences and one-interaction absorptions in which the entire energy of the gamma is captured.

The computed results also indicate that other scattering sequence types contribute significantly to the total number of full energy events. For concentric cylindrical active detector regions with the source on the axis above the detector, approximately equal numbers of good events were calculated to be initiated in each active region.

Detector Volume and Volume Ratios

Because of the difficulty in relating the physical characteristics of a detector to the behavior of that detector in the sum-coincidence mode, the configurations of previous SCS detectors have largely been determined by the preferences of the experimenter and by the shape of the germanium ingot to be lithium drifted. Using the Monte Carlo model, data have been calculated to establish the relationship of physical detector parameters to Ge(Li) detector performance in the sum-coincidence mode. As discussed in Chapter II, the sum-coincidence mode requires that coincident events be detected in electrically independent active detector volumes.

For the range of external detector volumes given in Table 4, the internal active volumes were defined by specifying the location of the horizontal or vertical inactive region separating the active volumes, as shown in Figures 20a and 20b. Calculated absolute peak efficiencies as a function of the position of a horizontal dead layer of 1.0 mm thickness are given for three detectors in Figure 21. The absolute peak efficiency

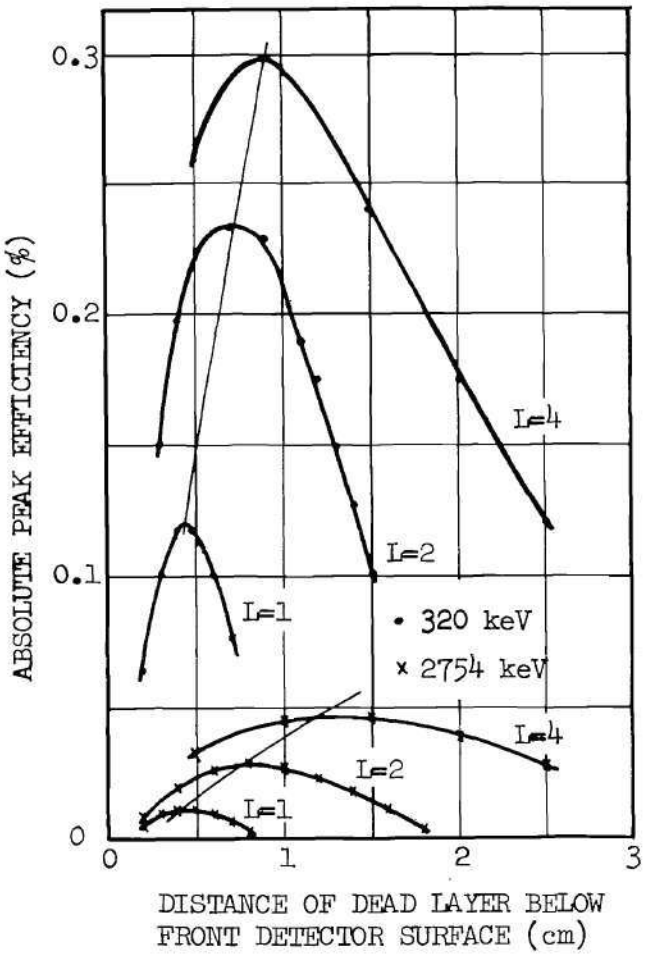

Figure 21. Calculated Absolute Peak Efficiencies versus Location of a 1 mm Thick Dead Layer for Sum-Coincidence Operation of Stacked Planar Detectors

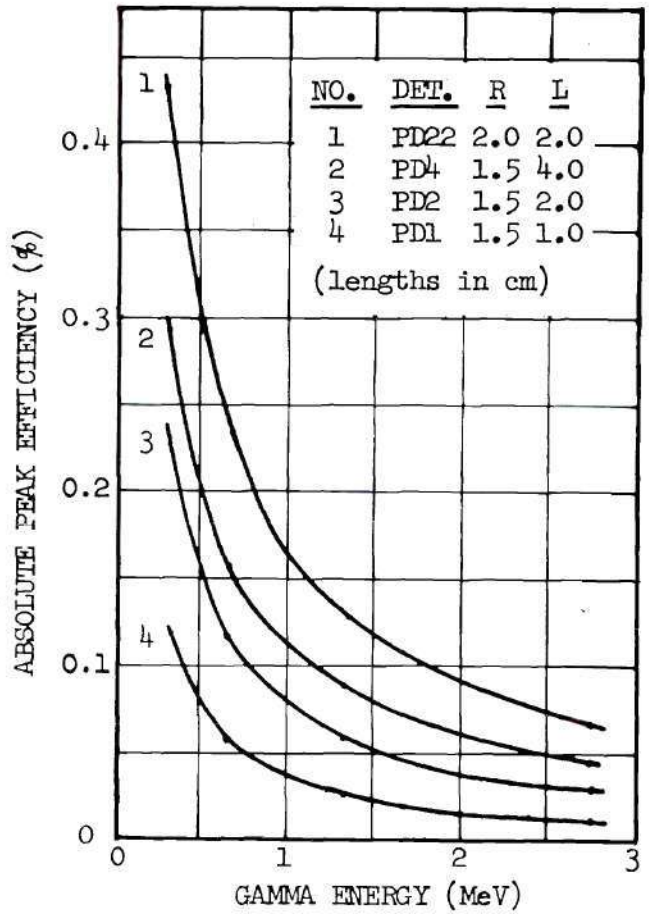

Figure 22. Calculated Absolute Peak Efficiencies versus Gamma Energy for Sum-Coincidence Operation of Optimized Stacked Planar Detectors

is defined as the number of recorded counts in the full energy peak, divided by the total number of gammas of that energy emitted from the source. For the data given, the source-to-detector distance was 2.0 cm. Efficiency curves for the intermediate energies fall in a regular manner between the curves shown for 320 keV and 2754 keV.

The efficiency data show that, for maximum efficiency, the volume of the front detector should be about 0.4 of the total detector volume for overall detector lengths of 2 cm or less. For detector lengths of 2 cm to 4 cm the optimum thickness for the front detector varies from about 0.9 cm at 320 keV to about 1.2 cm at 2754 keV. The maximum efficiency position of the separating layer was observed to be insensitive to the radius of the detector for radii of less than 3 cm.

Peak-to-Compton ratios, given in Table 9, are less sensitive than is the efficiency to the location of the 1.0 mm thick separating layer and hence to the volume ratios. The broad maxima observed for these peak-to-Compton data appear to occur for nearly the same locations of the separating inactive layers as do the efficiency maxima from Figure 21.

The conditions for location of the separating inactive layer which give maximum efficiency, as taken from Figure 21, were used in calculations of absolute efficiency versus gamma energy for SCS operation of four detector configurations. Figure 22 is a plot of these calculated full energy peak efficiencies for an assumed separating dead layer thickness of 1.0 mm. Source-to-detector distance was again assumed to be 2.0 cm. The data show that the peak efficiency doubles over the entire energy range when the detector length is increased from 1.0 cm to 2.0 cm, but that an additional increase of 50 percent or less is gained by increasing

Table 9. Calculated Peak-to-Compton Ratios (counts) versus Dead Layer Position for Sum-Coincidence Operation (see Figure 20 for detector geometry specifications)

Detector	Stacked Planar Data			Concentric Cylindrical Data		
	LDC (cm)	P/C Ratio (counts) 320 keV	2754 keV	R1 (cm)	P/C Ratio (counts) 320 keV	2754 keV
PD1 (R = 1.5, L = 1.0)	0.15	0.86	0.13	0.2	0.93	0.23
	0.35	0.88	0.15	0.4	1.3	0.20
	0.55	0.87	0.15	0.7	1.3	0.24
	0.65		0.11	0.9	1.1	0.20
	0.75	0.75		1.2	0.91	0.19
PD4 (R = 1.5, L = 4.0)	0.45	1.3	0.21	0.2	1.4	0.3
	0.95	1.4	0.22	0.4	1.5	0.27
	1.45	1.4	0.23	0.7	1.3	0.28
	2.45	1.1	0.21	0.9	1.2	0.24
	3.45	0.85	0.16	1.2	0.91	0.19
PD44 (R = 2.2, L = 4.0)				0.4	1.8	0.42
				0.7	2.0	0.43
				1.0	1.7	0.41
				1.3	1.6	0.36
				1.6	1.3	0.34

the length from 2.0 cm to 4.0 cm. By increasing the radius of the detector from 1.5 to 2.0 cm for a 2.0 cm length, a much larger efficiency gain is realized. Although the total volume of detector PD22 is less that that of PD4, the efficiency is greater. These data indicate that, for SCS operation, increasing the length of this type of detector beyond about 2.0 cm yields diminishing returns in efficiency but that increasing the surface area presented to the source appears to yield efficiency increases nearly proportional to the added area.

Absolute efficiency data were also calculated for the external detector dimensions of Figure 21 but with concentric cylindrical active regions as shown in Figure 20b. For these cases the parameter varied was the location of the cylindrical annular inactive volume. Figures 23a and 23b show the absolute peak efficiencies versus the radial positions of a 1.0 mm thick annular dead layer for energies of 320 keV and 2754 keV, respectively. Observe that the radial position of the separating dead layer which gives maximum efficiency is nearly independent of the detector length and that the increase in efficiency with increasing length is significantly greater than for the horizontal separating layer cases. Peak-to-Compton ratios (counts) as taken from calculated spectra for concentric cylindrical volumes are given in Table 9 along with the stacked planar detector data. The peak-to-Compton performance for the concentric cylindrical configurations excels that for the stacked planar geometries, especially for the 4.0 cm detector length. The application of these data to selecting detector geometries for specific gamma energy measurements will be discussed in a later section.

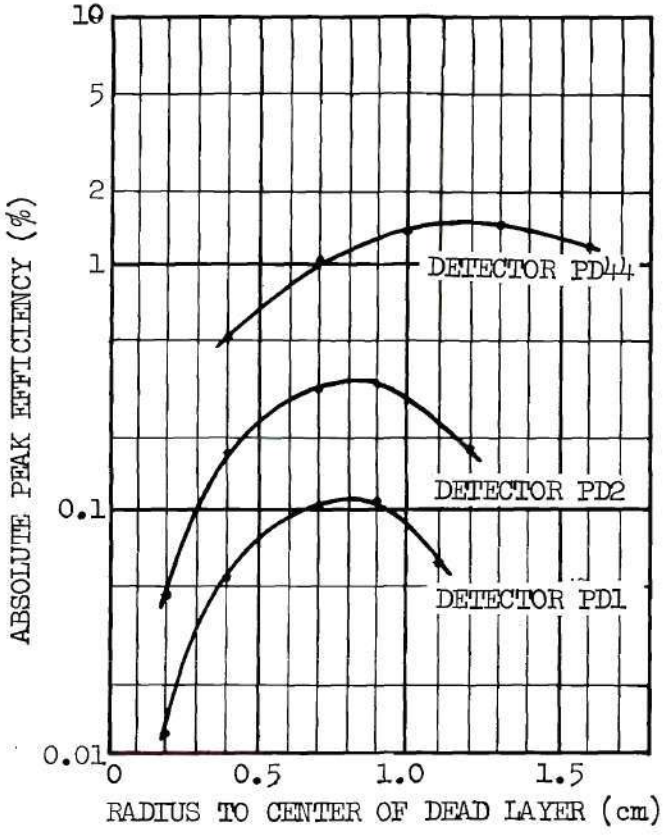

23a) 320 keV Data

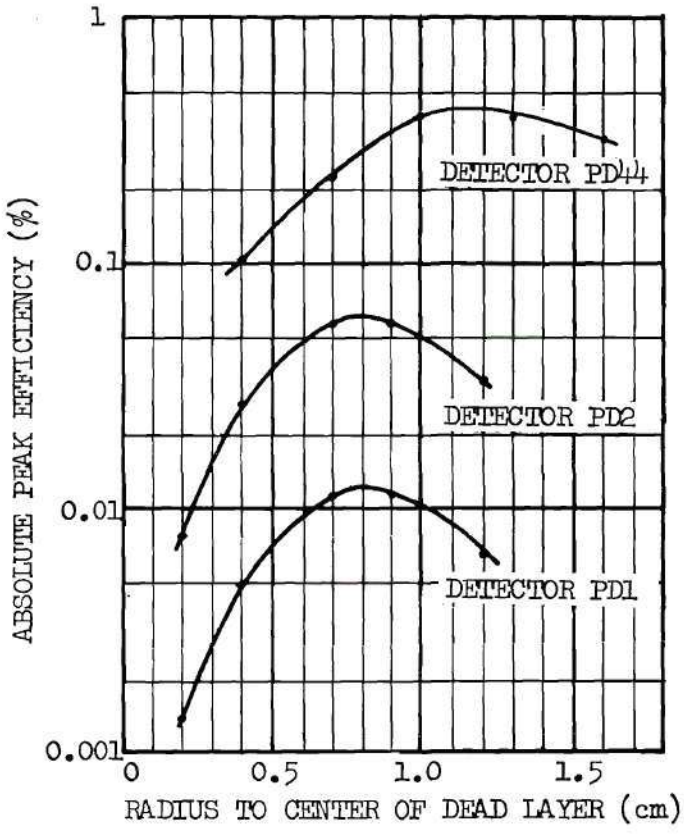

23b) 2754 keV Data

Figure 23. Calculated Absolute Peak Efficiencies versus the Location of a 1 mm Thick Dead Layer for Sum-Coincidence Operation of Concentric Cylindrical Detectors

Inactive (Dead) Layer Thickness

The general description of gamma scattering in germanium as given in a previous section indicates that extensive multiple interactions accompany full energy scattering sequences. In view of the expected pathlengths of gammas as given in Figure 14, the incidence of interaction of gammas traversing the inactive layer separating the active volumes would be expected to result in the shifting of a number of potential full energy events into the partial energy category. Monte Carlo calculations which provided quantitative data on the phenomenon confirmed that detector performance is strongly dependent upon the thickness of the dead layer separating the active detector volumes.

Figures 24 and 25 show the dependence of absolute full energy peak efficiency and peak-to-Compton ratio, respectively, on the thickness of the separating dead layer. The plotted data are for detector PD1 with the dead layer located as shown in Figure 24. These data, which are typical for all geometries of this study, show that efficiency can be reduced by factors of more than four and peak-to-Compton ratio by more than two by increasing the thickness of the dead layer from zero to 5.0 millimeters.

The presence of dead layers in previous SCS detectors probably accounts for a portion of the poor efficiency displayed by these systems. Detector fabrication techniques which eliminate the dead layer[56,59] would appear to offer superior low energy performance for sum-coincidence systems.

Energy Partitioning Between Detector Volumes

The previous experimental studies of SCS systems have demonstrated

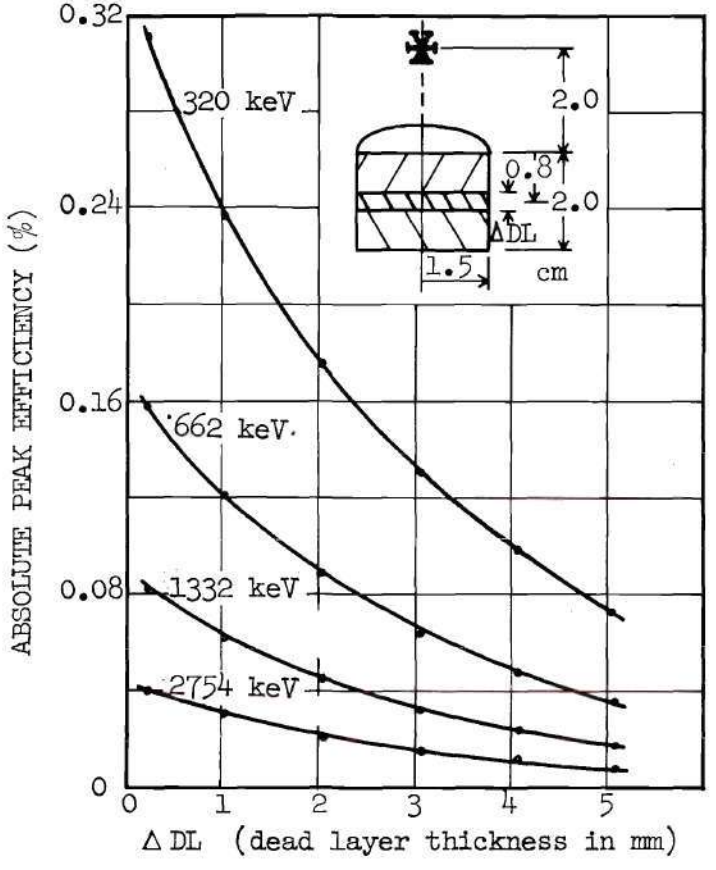

Figure 24. Calculated Absolute Peak Efficiency versus Dead Layer Thickness for Sum-Coincidence Operation of a Stacked Planar Detector

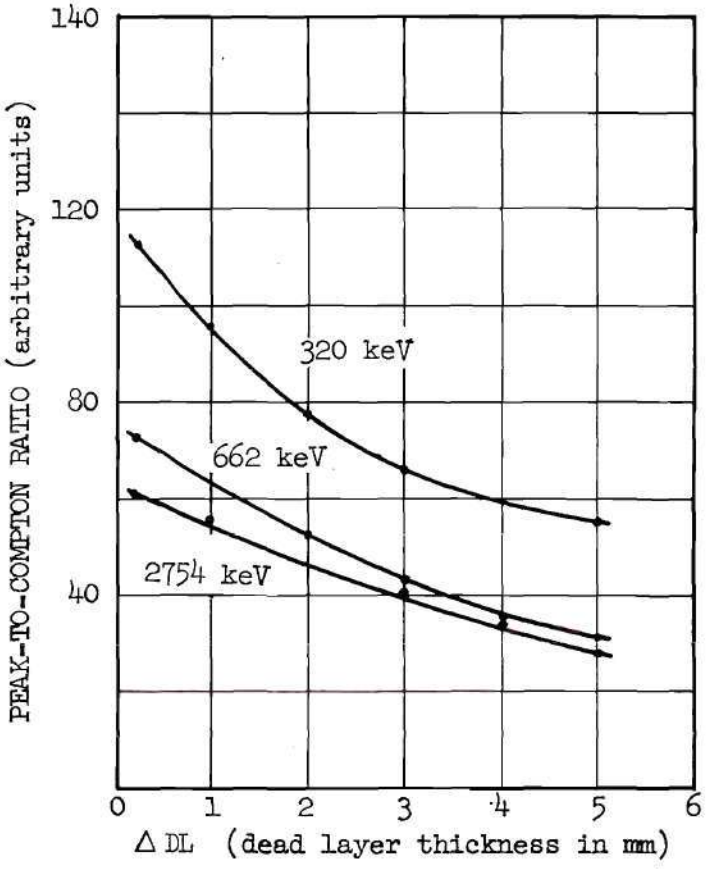

Figure 25. Calculated Peak-to-Compton Ratio versus Dead Layer Thickness for Sum-Coincidence Operation of a Stacked Planar Detector

that peak-to-Compton ratios can be improved by discriminating against detector signals which fall within specified energy ranges. As a means of analyzing the effect on detector performance of energy discrimination criteria, the mathematical model was programmed to display a two-parameter spectrum of the energy recorded in one detector versus the energy recorded in the second detector for coincidence events only.

Figure 26 is a diagram showing the expected location of gamma events as displayed on the two-parameter spectrum. Each gamma which interacts in both detector volumes contributes to the energy surface a "point" which has a y-coordinate determined by the energy (E_1) deposited in volume 1 and an x-coordinate determined by the energy (E_2) deposited in volume 2. In a sum-coincidence system the signal from the two detectors is summed linearly before the energy analysis operation. In the conventional one-dimensional display of the summed energy spectrum, counts at a particular energy, E_s, are contributed by any partitioning of energy between the two volumes which combines to give the energy E_s. Note that, on the energy surface, points of constant E_s lie along a diagonal line intercepting each axis at the energy E_s.

As shown in Figure 26, when the sum of the energy from the detectors, E_s, represents the total energy of the incident gamma, E_T, a count is produced which falls on the "full energy" diagonal line defined by $E_1 + E_2 = E_T$. Partial energy scattering sequences ($E_1 + E_2 < E_T$) which satisfy the coincidence requirement produce a count which falls below the full energy diagonal line. Low-level discrimination is the exclusion of all events below a line parallel to one axis and intersecting the other axis at the energy threshold. An energy window on either detector volume

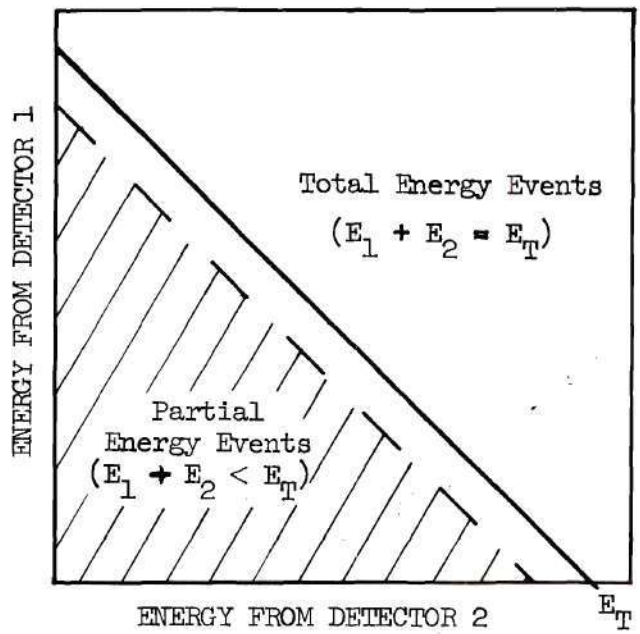

Figure 26. Location of Recorded Gamma Events on a Two-Parameter Energy Spectrum of Coincident Events from Electrically Independent Detector Volumes

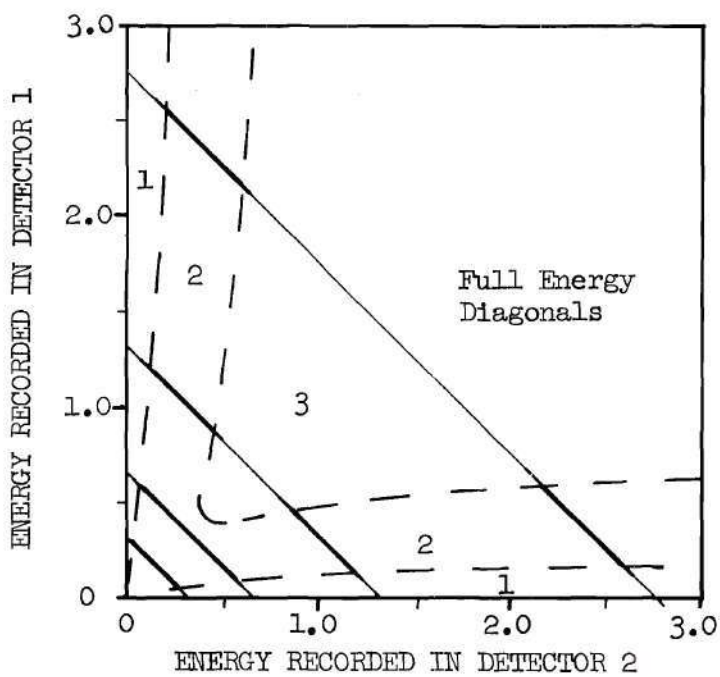

Figure 27. Location of Full Energy Event Concentrations on the Two-Parameter Energy Spectra (region 2 is the region of concentration of full energy events)

would identify those events falling between two lines perpendicular to the energy axis for that detector volume and intersecting the axis at the energy bounds of the window. Simultaneous energy windows on each detector output would define a rectangular energy "surface" of events to be accepted or rejected.

For either experimental or computed detector operation, the two-parameter spectrum was recorded by dividing the x-axis and y-axis (one for each detector volume) into regular energy increments and sorting each coincident set of events into the energy "square" defined by the energy increment satisfied in each of the two detector volumes. In the computer output, the two-parameter spectrum is simply a two-dimensional array in which each element is the number of events meeting the simultaneous energy requirements for that square. In the two-parameter spectra to be presented, the constant energy diagonal line is broadened into a "zone" because the diagonal may pass through adjacent incremental energy squares.

The analysis of a variety of computed two-parameter spectra showed that the full energy events tended to be concentrated at certain locations along the full energy diagonals. This localization of full energy events is illustrated in Figure 27. In the two-parameter display, the full energy diagonals (only) for several incident gamma energies are diagramed. Regions of concentration of events occur where the diagonals pass through the zones designated as region 2. For low-energy gammas, full energy events tend to concentrate near the center of the diagonal but, as the energy increases, a distinct separation of events occurs into two portions of the diagonal. The location of the partial energy events

on the energy surface and observations of how selective energy discrimination can be applied will be discussed by a summary review of the computed spectra.

Computed spectra for radial and horizontal dead layer detector geometries are given in Figures 28 and 29 for 320 keV and 662 keV gammas, respectively. The full energy diagonal zone is indicated by the two diagonal lines which enclose all of the full energy counts. For the radial dead layer geometry, symmetrical energy distributions along the diagonals are observed in the detectors because the gammas incident onto either active volume require approximately the same angular deflections to initiate a successful scattering sequence. Note that discriminator thresholds of up to 150 keV on the output of each volume would leave intact a majority of the full energy peak counts.

The horizontal dead layer cases show a shift toward a concentration of energy in the lower detector volume, and at 662 keV, the beginning of the split into two regions on the full energy diagonal can be identified. Partial energy events are seen to be localized in the regions corresponding approximately to scatter at the Compton edge energy in one detector volume, with a low energy Compton event in the other volume.

As may be seen in Figure 30, the localization of events into two regions of the energy surface is more pronounced for 1332 keV gammas. At 2754 keV, the two localized energy zones are in evidence, along with a "double-escape" phenomenon for partial energy events as shown in the two-parameter spectrum of Figure 31. A true double-escape would not be detected by a sum-coincidence system since it involves only a single

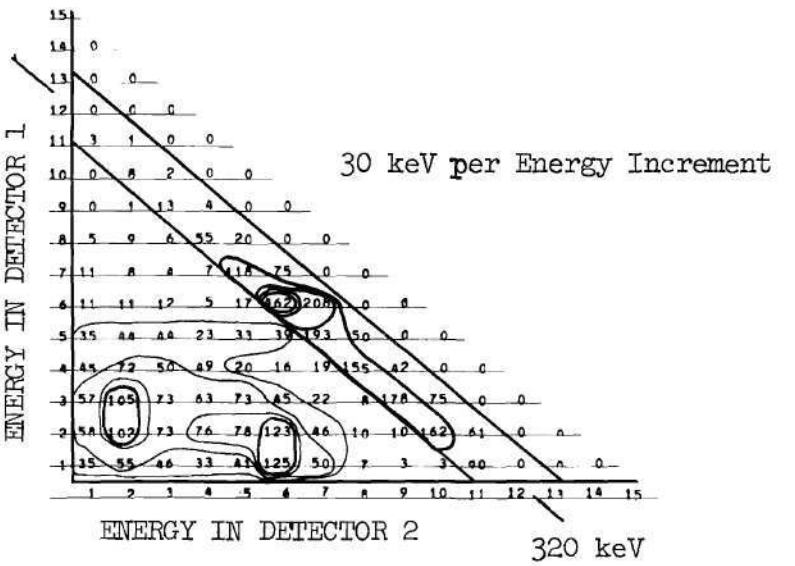

28a) Stacked Planar Geometry

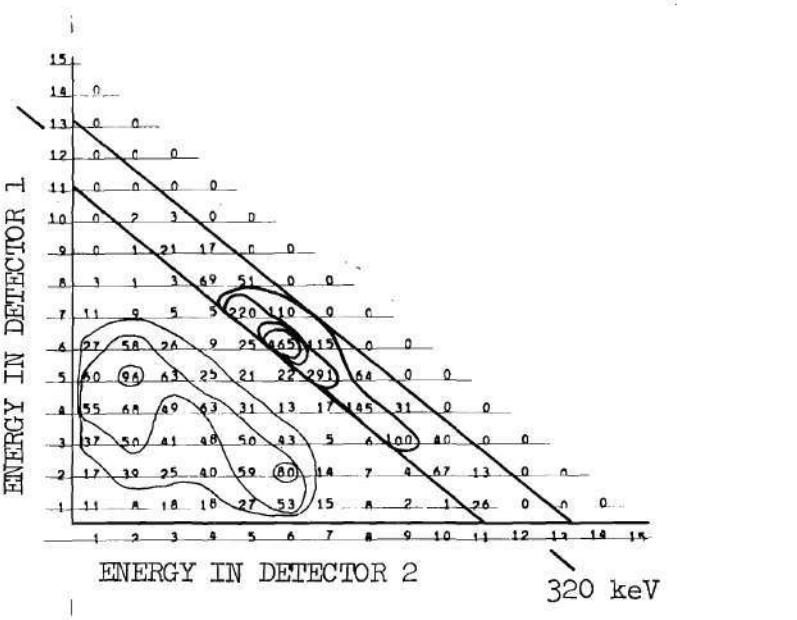

28b) Concentric Cylindrical Geometry

Figure 28. Two-Parameter Energy Spectra for 320 keV Gammas (constant-count contour lines shown)

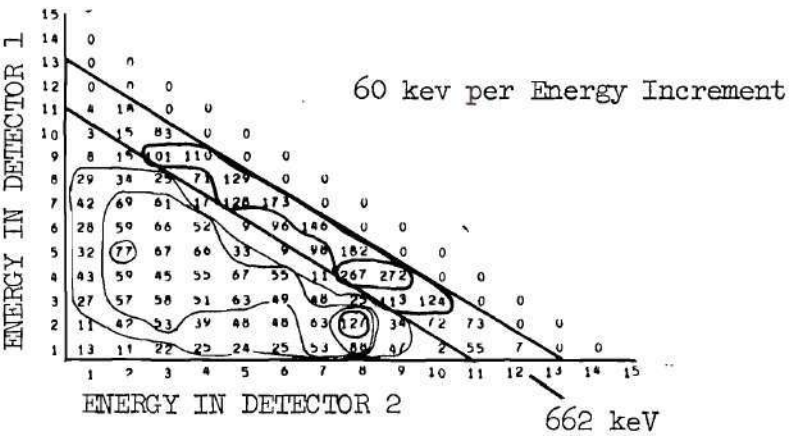

29a) Stacked Planar Geometry

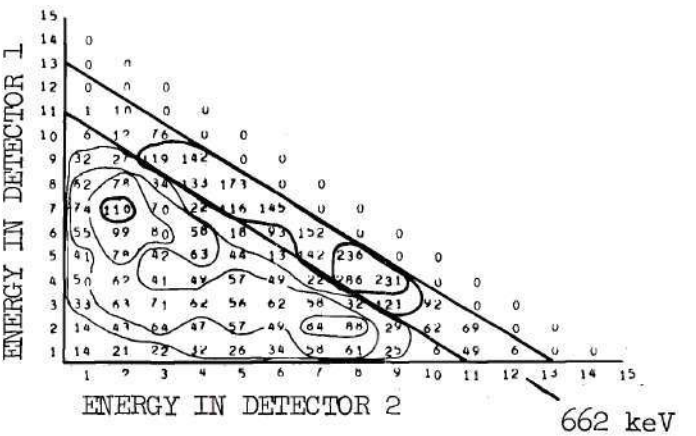

29b) Concentric Cylindrical Geometry

Figure 29. Two-Parameter Energy Spectra for 662 keV Gammas (constant-count contour lines shown)

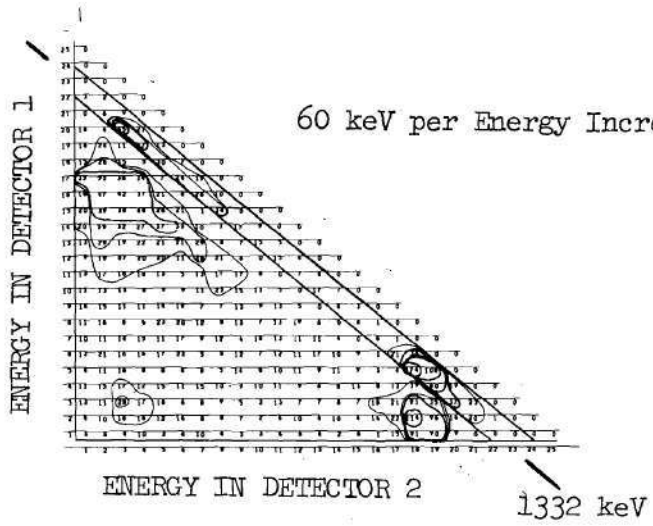

30a) Stacked Planar Geometry

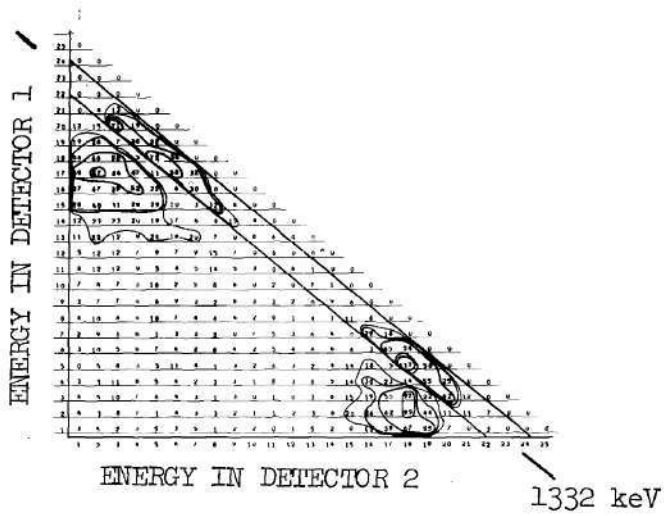

30b) Concentric Cylindrical Geometry

Figure 30. Two-Parameter Energy Spectra for 1332 keV Gammas (constant-count contour lines shown)

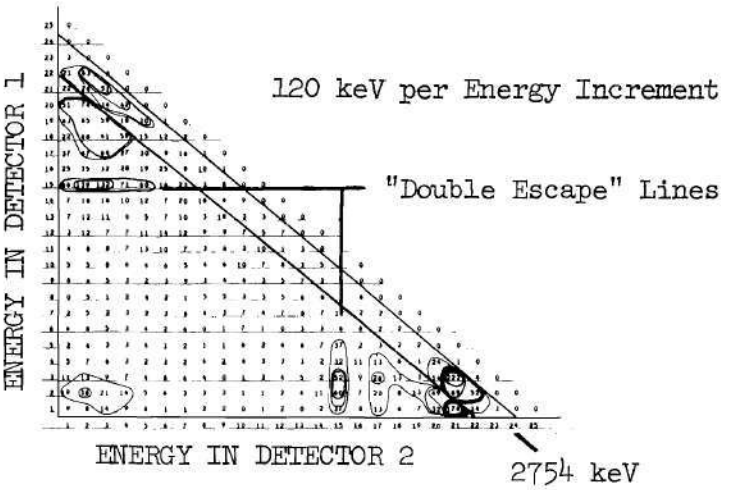

31a) Stacked Planar Geometry

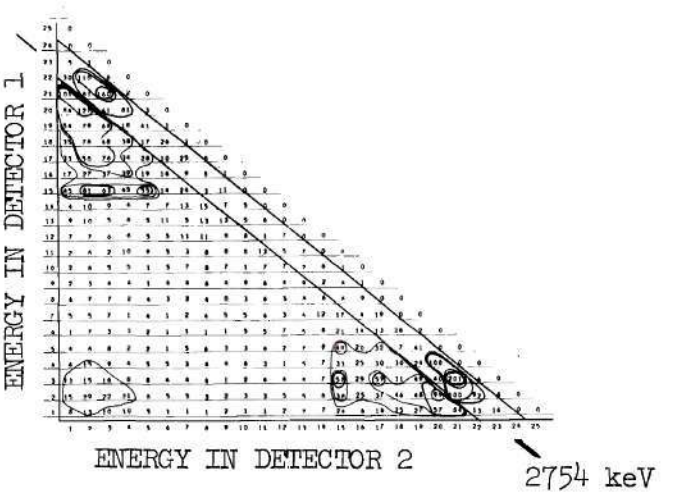

31b) Concentric Cylindrical Geometry

Figure 31. Two-Parameter Energy Spectra for 2754 keV Gammas (constant-count contour lines shown)

interaction. The prominent concentration of events at approximately 1.75 MeV in both detector volumes is probably the result of a pair-production event in one volume, followed by a Compton scatter or complete absorption of one annihilation gamma in the other volume. On the summed single-dimensional energy spectrum this phenomenon produces what has been referred to by Camp[72] as the "strange hump" which would "produce a highly discontinuous background, becoming intolerable for anything more than simple spectra."

For all experimental two-parameter spectra, the counts comprising a given full energy peak must also fall along a single constant energy diagonal whose width is determined by the energy resolution of the system. Regions of concentration of partial energy events through which the constant energy diagonal passes contribute the plateau upon which the full energy peak appears in the summed spectrum. Thus, for a sum-coincidence system, performance improvement is realized either by selecting regions of concentration of full energy events or rejecting regions of concentration for partial energy events.

In general, this may be accomplished by rejecting events in energy regions 1 and 3 of Figure 27. Region 1 is eliminated by imposing lower energy threshold settings on both detector outputs. From the computer results, threshold levels in the range of 100 keV to 200 keV appear to maximize the peak-to-Compton ratio while eliminating an acceptable number of full energy events. Table 10 gives an example of the effect of imposing symmetrical threshold levels on a stacked planar detector of 1.5 cm radius by 2.0 cm length for 1332 keV gammas. Note that a symmetrical discriminator level of 150 keV gives the greatest peak-to-Compton ratio,

while at the same time reducing the efficiency by only 15 percent.

Counts in Region 3 of Figure 27 are eliminated by requiring that the recorded energy does not simultaneously exceed a specified upper limit in both detector volumes.

Selective elimination of localized regions of partial energy events on the energy surface may be used to eliminate known interference contributions. As an example, the hump from the "double escape" events of Figure 31 may be eliminated by setting narrow energy windows on each detector output at the double escape energy. Such selective discrimination would reject full energy events only at the intersections on the energy surface of the narrow energy window zones and the full energy diagonals.

The preferential selection of full energy events also can be accomplished by setting two-dimensional windows on the energy surface to accept events from regions of concentration of full energy events along the constant energy diagonal. Regions of concentration can be identified from data such as those presented in Figures 28 through 31.

Table 10. Calculated Peak-to-Compton Ratio and Relative Efficiency versus Discriminator Level

Disc. Level (keV)	Peak/Compton Ratio	Relative Efficiency
0	59	1.0
50	85	0.98
100	88	0.95
150	97	0.85
200	91	0.72
250	64	0.47
300	58	0.37
400	60	0.25

R = 1.5 cm; L = 2.0 cm; source distance = 2.0 cm, 1.0 mm horizontal dead layer at 0.8 cm; 3 keV FWHM resolution.

Experimental Results

As a supplement to the computer study, experimental data for operation of SCS systems were obtained and correlated with the calculated results. Comparisons were made of the general shape of the energy spectrum, of the peak efficiency, and of the energy partitioning between detector volumes.

For all efficiency calculations, between 500 and 2500 counts were recorded in the full energy peak during computer runs for experimental correlation and performance optimization. The maximum statistical error in calculated efficiencies was about 14 percent based on a confidence limit of three standard deviations. Possible error limits of ten percent were estimated for the experimental measurements; ten percent error limits have also been used by other experimenters in sum-coincidence studies.[61] For comparing computed and measured spectra the uncertainty in the actual energy resolution introduces additional error if the two spectra are normalized based on the height of the full energy peak or if peak-to-Compton ratios (height) are calculated. If the peaks are Gaussian, an assumed FWHM resolution of 6.0 keV for an actual resolution of 7.0 keV would introduce a 12.5 percent error in the normalization factor. For an assumed 2.0 keV FWHM resolution and an actual resolution of 3.0 keV, the normalization error would be 25.5 percent.

Figure 32 is a comparison of the computed and measured spectra shapes for sum-only and sum-coincidence operation of a concentric cylindrical detector. This detector had an outside radius of 13 mm, a central hole of 3.5 mm, and a length of 22 mm. The radial thickness of each active volume was 3.5 mm and the thickness of the separating dead layer

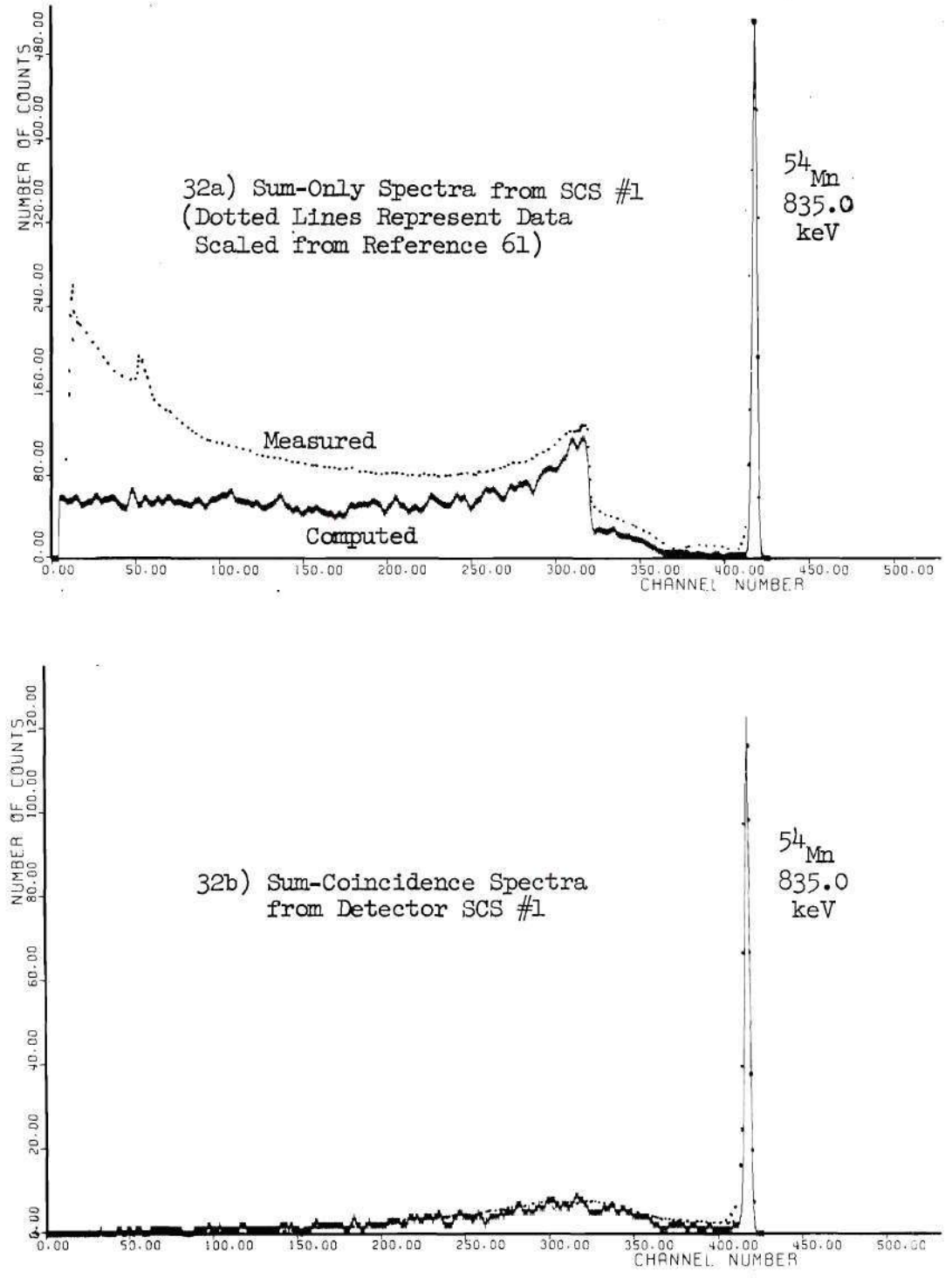

Figure 32. Measured and Computed Energy Spectra of the Sum-Coincidence Spectrometer System Described in Reference 61

was 2.5 mm. The computed spectra are Cal-Comp plots of data generated by the Monte Carlo model, and the measured spectra were scaled directly from a previous publication.[61] Essential features of the spectra such as peak-to-Compton ratio and ratio of peak heights for sum-only and sum-coincidence operation are seen to be in good agreement. The general shape of the spectra is also very similar except for the low-energy end of the sum-only spectrum. In the low-energy region the difference is caused by scattering from surrounding materials and by loss mechanisms within the actual SCS detector which are not considered in the computer model.

Using the detector and instrumentation described in Chapter IV, measurements of absolute peak efficiency for sum-only and sum-coincidence operation were made for gamma energies of 320 keV to 2754 keV. Computed efficiencies for this detector configuration for the same source energies compare with the measured values as shown in Figure 33. The observed differences between measured and calculated performance are within the possible error related to uncertainties in the actual dimensions of the inactive internal volumes of the detector. Note that the calculated efficiencies as compared to measured values are greater for sum-only operation and less for sum-coincidence operation. Thus the relatively poor efficiency for sum-coincidence operation tends to be magnified by the computer results.

Experimental data were also obtained to verify the behavior of the partitioning of energy between detector volumes as predicted by the Monte Carlo model. The two-dimensional energy surface presentation of coincidence events, which was described in detail in the previous section, will

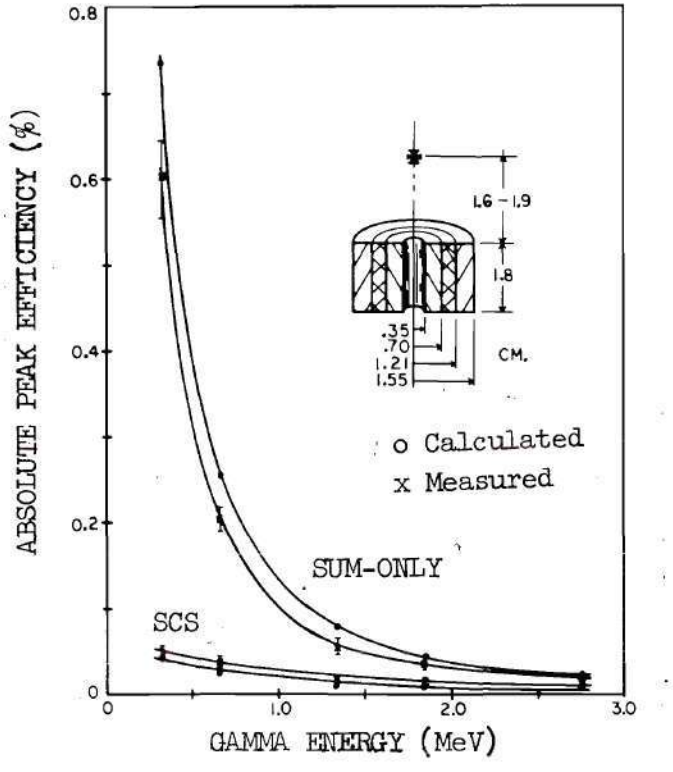

Figure 33. Calculated and Measured Peak Efficiency versus Energy for Concentric Cylindrical Detector SCS #3 in the Sum-Only and Sum-Coincidence Modes

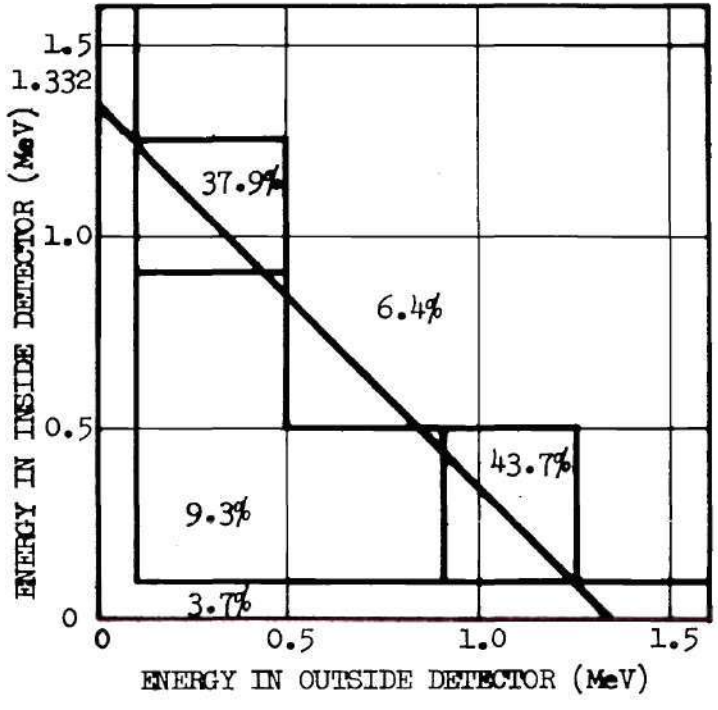

Figure 34. Measured Energy Partitioning Between Active Volumes of Concentric Cylindrical Detector SCS #3 for 1332 keV Gammas

be used to display the measured sum-coincidence spectrometer performance. One of the significant features of the two-parameter spectra as predicted from the computed results was the concentration of full energy events into two regions along the diagonal line representing the capture of the entire energy of the incident gamma.

Figure 34 shows a two-dimensional energy surface which has been divided into five zones as indicated by the zone boundary lines. For detector SCS #3, coincidence events recorded for the 1332 keV gamma of cobalt-60 contributed counts to the five energy zones as shown in the plot. As is shown by a comparison of the percentage number in each zone with the corresponding area of the computed data of Figure 31, the distribution of events on the surface is as predicted by the Monte Carlo model.

Table 11 lists the results of a comparison of measured and computed relative peak efficiency as a function of the energy discriminator threshold. The data of this table indicate that the computed threshold behavior is in good agreement with the experiment and that the previously suggested threshold levels of 100 keV to 200 keV eliminate substantially more partial energy events than full energy events.

Measured and computed two-parameter spectra are presented for comparison in Figure 35. Each dot on the energy surface display signifies the presence of more than a specific number of events in that energy square; each increase in dot size indicates an increased number of counts in that square by a factor of two. The measured spectrum was taken from the detector designated SCS #3 and is the two-parameter spectrum for the 1173 keV energy component of cobalt-60. Although the calculated spectrum

Table 11. Normalized Efficiencies for Equal Discriminator Settings on Each Active Volume of SCS #3 for 1332 keV gammas

Threshold Energy (keV)	Measured Relative Peak Efficiency	Computed Relative Peak Efficiency	Computed Fraction of Bad Events Remaining
0	1.00*	1.00	1.00
100	0.96	0.96	0.56
200	0.74	0.81	0.25
300	0.31	0.34	0.11
400	0.15	0.16	0.05
500	0.06	0.06	0.02

*extrapolated data point based on computed behavior

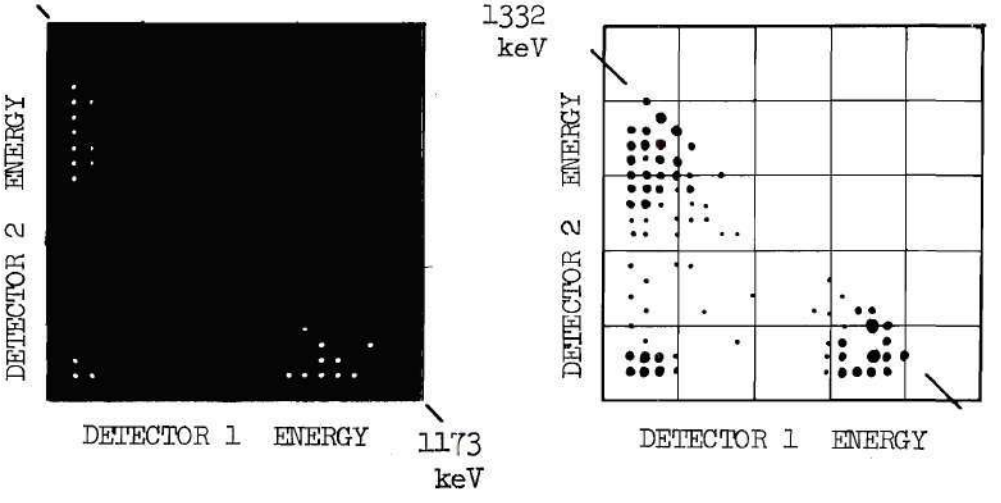

a) Measured Spectrum

b) Calculated Spectrum

Figure 35. Measured and Calculated Two-Parameter Energy Spectra for Cobalt-60 with Detector SCS #3

is for a gamma energy of 1332 keV, the energy difference is so slight that the spectrum distributions should be very similar. In each spectrum the two components resulting from an initial scatter in either coaxial detector volume can be readily identified. The low-energy component near the origin is probably the result of a small angle Compton scatter in each detector volume, followed by the escape of the twice-scattered gamma.

Figure 36 gives measured two-parameter energy spectra as recorded with detector SCS #3 for incident energies ranging from 320 keV to 2754 keV. The 320 keV and 662 keV spectra were for sources having only a single monoenergetic gamma and show the central concentration of full energy events on the constant energy diagonal. Although the yttrium-88 and sodium-24 sources have two monoenergetic gamma components, the splitting of full energy events into two localized regions is still apparent. These experimental spectra confirm the computed energy distribution behavior as illustrated in Figures 28 through 31. Note that the sharp "double-escape" lines predicted by the Monte Carlo model are apparent in the measured spectra for both the 1836 keV and 2754 keV gamma components. A narrow energy window on each detector volume would eliminate this interference component.

Operation of the detector in the sum-coincidence mode led to the observation of another source of extraneous spectrum components. For the gamma sources emitting more than one gamma per disintegration (cobalt-60, yttrium-88, sodium-24), a significant background plateau was in evidence in the summed energy spectrum, as shown for cobalt-60 in Figure 37. The measured two-parameter spectrum for cobalt-60 as given in Figure 38 shows that events above the 1332 keV constant energy diagonal appear to corres-

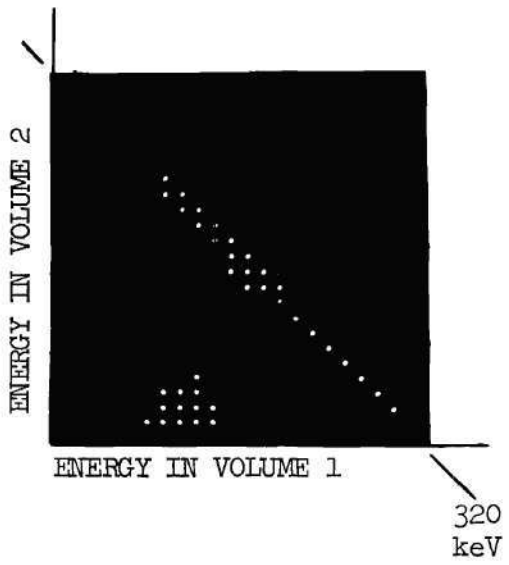

36a) Chromium-51 Spectrum

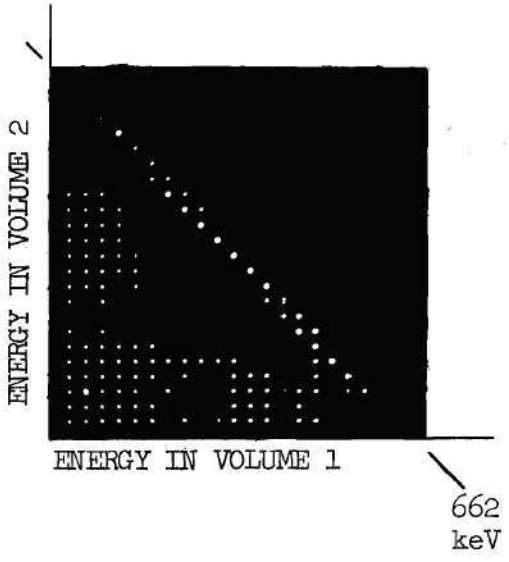

36b) Cesium-137 Spectrum

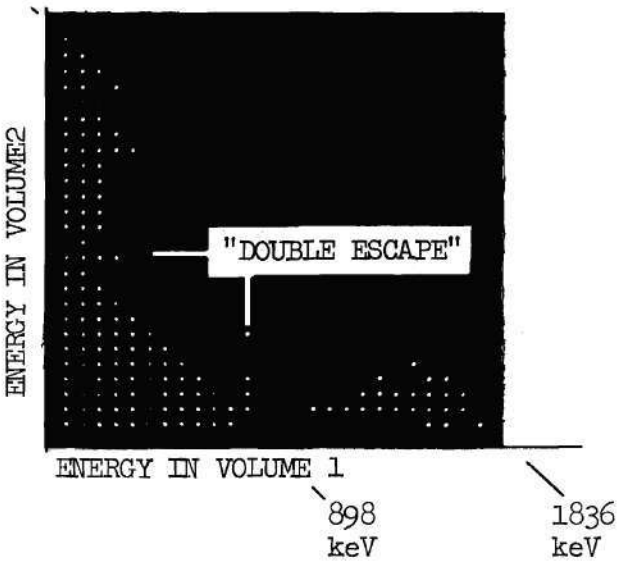

36c) Yttrium-88 Spectrum

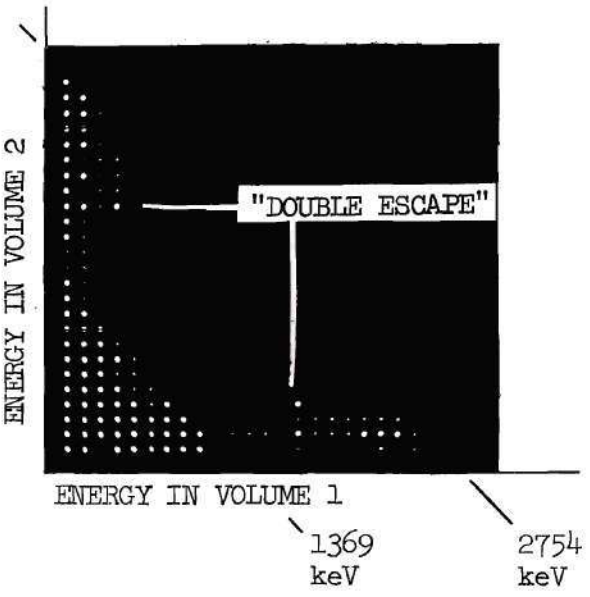

36d) Sodium-24 Spectrum

Figure 36. Measured Two-Parameter Energy Spectra for Four Isotopic Sources with Detector SCS #3

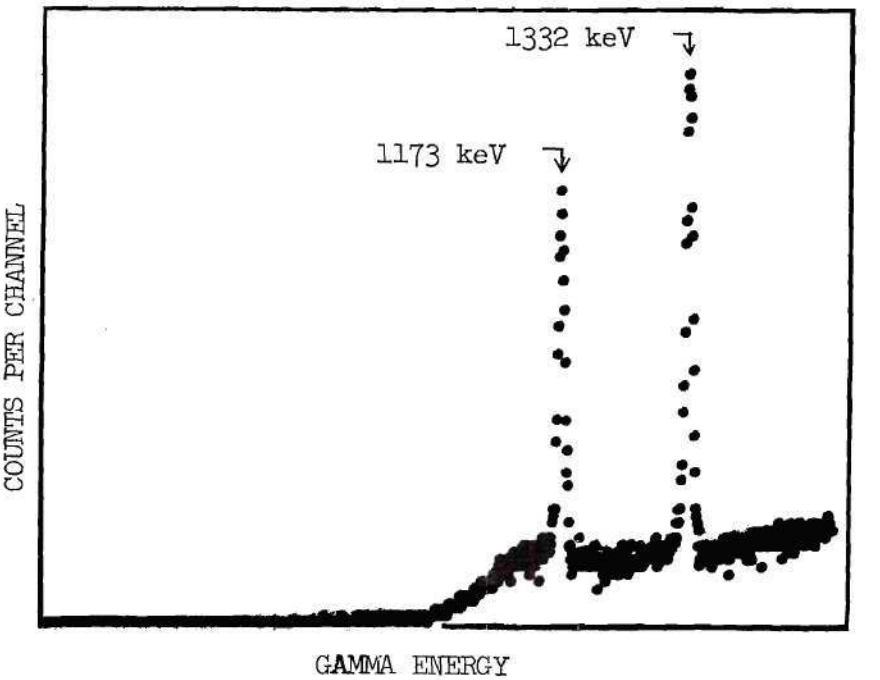

Figure 37. Measured Sum-Coincidence Energy Spectrum for Cobalt-60 with Detector SCS # 3 (Discriminators at 500 keV).

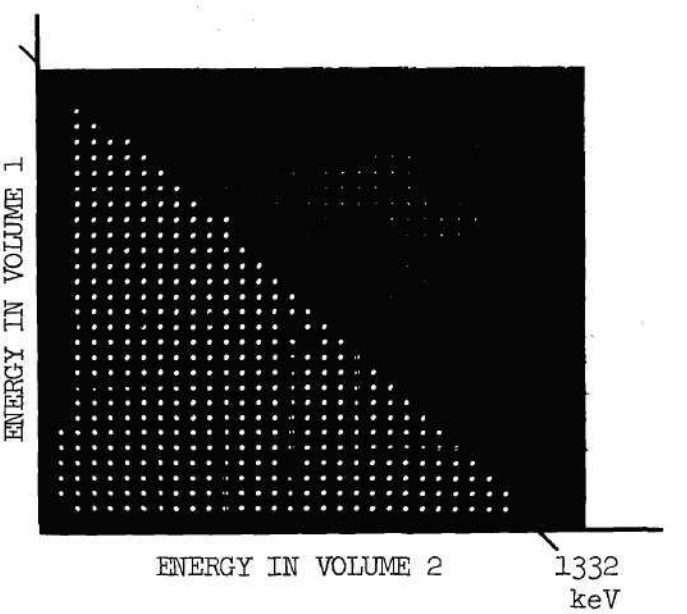

Figure 38. Measured Two-Parameter Energy Spectrum for Cobalt-60 with Detector SCS # 3.

pond to coincidence events in which the two simultaneous gammas interact in different active volumes of the SCS detector. An order-of-magnitude type of calculation was made to determine whether coincident events from the separate gammas are of sufficient probability to account for the observed behavior. For the geometry of the measurement with cobalt-60, the computer results indicate that 3.3 percent of the photons interact one or more times in the detector. From the measured and calculated detector geometry, the fractions of the inside and outside active volumes are 0.17 and 0.50, respectively, of the total volume. The fraction F of the total number of disintegrations for which the coincidence requirements would be satisfied by the separate gammas is

$$F = \left(\begin{array}{l}\text{Fraction of disintegrations}\\ \text{for which both gammas inter-}\\ \text{act in detector}\end{array}\right) \times \left(\begin{array}{l}\text{Probability of}\\ \text{interaction in both}\\ \text{active volumes}\end{array}\right) \qquad (13)$$

$$= (0.033 \times 0.033) \times (2 \times 0.17 \times 0.50)$$

$$= 1.8 \times 10^{-4}$$

For these same conditions, the measured full energy peak efficiencies are 1.7×10^{-4} and 1.1×10^{-5} for symmetrical energy discriminator thresholds of 100 keV and 500 keV, respectively. Thus the total number of events from coincident gammas will approximately equal the number of peak events for low energy thresholds and will greatly exceed the number of peak events as the energy thresholds are increased.

The interference contribution from coincident gammas would be present for any isotope which emitted multiple gammas within the coincidence resolving time of the SCS system. The interference contribution is not count-rate dependent but depends only on the probability of

satisfying the geometry and energy requirements for coincidence events. For SCS systems the interference could be minimized by selective energy discrimination on the energy surface, or by locating the source further from the detector. As the source-to-detector distance is increased, the full energy peak would decrease linearly with the interaction probability, while the efficiency for the detection of true coincident gammas would decrease as the product of the interaction probabilities for the single gamma components.

Note that anticoincidence systems for Compton suppression also are affected by true coincidence gammas from the source. The response of an anticoincidence system is different, however, in that full energy events in the Ge(Li) detector are not recorded when the coincident gamma is captured in the larger shield detector.

Comparative Performance of Multiple Scattering Spectrometers

In the previous sections the effect of parameters which control the performance of multiple scattering spectrometer systems has been described. These results may now be applied to the comparison of multiple scattering detectors versus conventional detector systems and to the definition of detector systems which maximize overall spectrometer performance in the multiple scattering mode.

For the sum-coincidence detectors defined in Table 4, the detector efficiencies in the sum-coincidence mode as compared to sum-only operation of the same detector can be seen from the data of Table 12. Stacked planar detector geometries were assumed, with a 1.0 mm dead layer separating the active volumes and 400 micron dead layers on the external planar

surfaces. The relative efficiency in the sum-coincidence mode as compared to that in the sum-only mode is observed to vary from about 10 percent at 320 keV to about 30 percent at 2754 keV. The peak-to-Compton ratios (height) for 1332 keV gammas for an assumed 3.0 keV FWHM resolution are also given in Table 12.

Table 12. Calculated Efficiency and Peak-to-Compton Data for Sum-Only and Sum-Coincidence Operation

Detector	Operating Mode	Calculated Absolute Peak Efficiency Energy (keV)					P/C Ratio 1332 keV 3 keV FWHM 100 keV Disc
		320	662	1332	1836	2754	
PD1	S-O	1.1	0.27	0.091	0.062	0.037	6.8
	S-C	0.12	0.05	0.023		0.011	47
PD2	S-O	1.8	0.58	0.22	0.16	0.097	12
	S-C	0.23	0.12	0.061		0.030	60
PD4	S-O	2.3	0.82	0.37	0.26	0.18	16
	S-C	0.24	0.15	0.083		0.05	63
PD22	S-O	3.1	1.0	0.45	0.31	0.20	14
	S-D	0.43	0.24	0.13		0.07	99

These data will be compared by the use of the figure-of-merit developed as equations 5 and 6 on page 19. The assumption will be made that the peak efficiency is the same at 1332 keV as for the Compton-edge energy at 1100 keV since the efficiency difference is small as may be seen from Figure 33. The figure-of-merit becomes

$$\text{FOM} \propto n_{E_1} \sqrt{\frac{R_{21}}{n_{E_2}}} \approx \sqrt{n_{E_1} R_{21}} \qquad (14)$$

Table 13 gives calculated FOM values from the data listed in Table 12 for sum-only, sum-coincidence, and sum-only with anticoincidence shields assumed to reduce the Compton peak by factors of 2 and 5 without reducing the peak efficiency. Sum-coincidence operation appears to offer improved performance over the sum-only mode except for detector PD4, a detector of 4.0 cm length. Anticoincidence operation with Compton suppression factors of approximately two with these detectors appears to be the breakover point above which the anticoincidence mode is favored.

Table 13. Figure-of-Merit Values for E_2 = 1332 keV, E_1 = 1100 keV (Compton edge)

Operating Mode	Detector PD1	Detector PD2	Detector PD4	Detector PD22
Sum-Only	0.79	1.57	2.40	2.48
Sum-coincidence	1.03	1.92	2.29	4.00
Anticoincidence (2)*	1.11	2.22	3.40	3.51
Anticoincidence (5)*	1.76	3.86	5.37	5.55

*Compton suppression factor

The results presented in Tables 12 and 13 were specialized by determining the Compton interference only at the energy of the Compton edge and by including the 1.0 mm dead layer. In an attempt to define a more realistic spectroscopy case for comparison, a detector configuration was chosen as having performance characteristics representing the state-of-the-art (1970) for Ge(Li) detectors. The hypothetical detector geometry

shown in Figure 39 was selected.

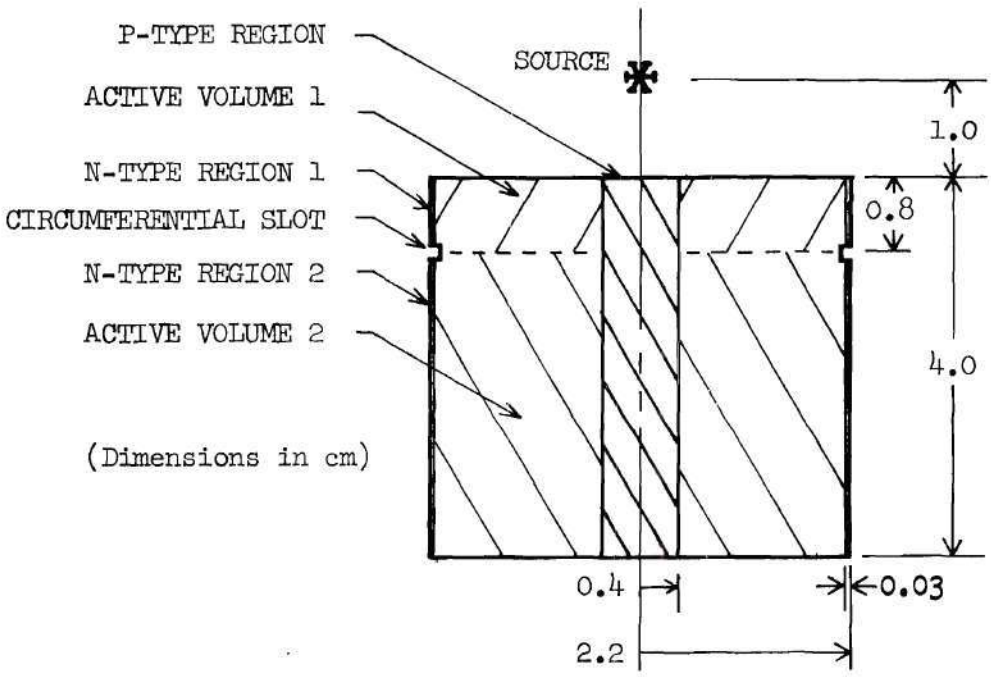

Figure 39. Configuration for Hypothetical Detector PD44

The active detector volume was about 59 cm^3 and the resolution was assumed to be 3.0 keV FWHM. For sum-coincidence operation the detector was assumed to function as two electrically independent volumes as effected by the presence of a circumferential slot through the outside contact region as shown in the sketch. Calculated peak efficiency and peak-to-Compton (height) data for sum-only and sum-coincidence operation of the detector are given in Table 14.

Table 14. Calculated Performance of Detector PD44 in the Sum-Only and Sum-Coincidence Modes

Energy	Absolute Peak Efficiency		(Peak/Compton) height 3 keV FWHM, 100 keV Disc.	
(keV)	Sum-Only	Sum-Coincidence	Sum-Only	Sum-Coincidence
320	8.2	0.84	30	> 500
662	3.4	0.86	26	91
1332	1.6	0.53	23	82
1836	1.2	0.40	22	82
2754	0.8	0.30	23	70

Calculations of the full energy peak efficiency and the Compton plateau "efficiency" at that energy from each higher energy component were made for energies of 320, 662, 1332, 1836, and 2754 keV. Energy thresholds of 100 keV on each output were applied in the calculation. Although the Compton reduction factor is significantly greater for the sum-coincidence system, the figure-of-merit as shown in Table 15 favors the sum-only detector in most of the sample cases. In the cases where sum-coincidence performance excels, anticoincidence Compton suppression by factors of two to four on the sum-only mode would equal the sum-coincidence performance.

The predominant emphasis on efficiency occurs because the figure-of-merit is proportional to efficiency at the peak energy of interest but is proportional only to the square root of the peak-to-Compton ratio. Thus the superior peak-to-Compton ratios of the sum-coincidence system are more than offset by the efficiency reduction when compared to sum-only operation of the same detector. Note that these comparative figures-of-merit hold for any counting time, so long as it is the same for both

operating modes.

Table 15. Figures-of-Merit for Detecting Gamma E_1 on the Compton Plateau of Gamma E_2 for Detector PD44

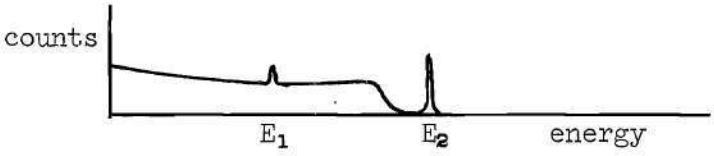

Energy (keV)		Figure-of-Merit	
E_1	E_2	Sum-Only	Sum-Coincidence
320	662	33	16
	1332	59	57
	1836	70	61
	2754	107	62
662	1332	24	23
	1836	30	53
	2754	42	91
1332	1836	40	12.9
	2754	24	45
1836	2754	11	16

As an indication of the effectiveness of the parameter variation study, the performance of hypothetical detector PD2 and actual detector SCS #3 were compared. Although the germanium volume of the two is approximately the same, the efficiency of the optimized detector PD2 is about three times that of detector SCS #3 for all energies. The figure-of-merit also is about three times greater for detector PD2. A comparison of the performance of detector SCS #3 with that of optimized detector PD44 shows that the optimized detector, although five times larger in volume, offers an efficiency advantage of 10 and an increase in figure-of-merit of about 25.

Based on an analysis of the computed results, the efficiency reduction is seen to represent the major performance limitation of sum-coincidence detectors that can be fabricated by conventional lithium drifting techniques. In an attempt to determine whether the inherent efficiency limitation on all multiple scattering concepts is as restrictive as that shown for the postulated sum-coincidence systems, the efficiency data of Table 16 were calculated. Table 16 lists the calculated sum-only and sum-coincidence efficiencies for the previously specified operating conditions for detectors PD22 and PD44 and also the theoretical maximum peak efficiency for multiple scattering operation of these two detectors.

Table 16. Calculated Efficiencies for Detectors PD22 and PD44 for Various Operating Modes

Energy (keV)	Detector PD22			Detector PD44		
	S-O	M M-S	S-C	S-O	M M-S	S-C
320	3.1	2.22	0.43	8.2	6.3	1.3
662	1.0	0.90	0.24	3.4	3.1	0.93
1332	0.45	0.44	0.13	1.6	1.6	0.55
1836	0.31	0.30		1.2	1.2	
2754	0.20	0.20	0.07	0.82	0.82	0.31

S-O = Sum-Only; M M-S = Maximum Multiple-Scattering; S-C = Sum-Coincidence

The data for the maximum attainable efficiency in the multiple scattering mode are predicated on the assumption that all multiple events are recorded except those with interactions in an inactive volume of the detector. It may be seen from the data that the fraction of multiple scatter-

ing events detected by the sum-coincidence systems is less than one third of the theoretical maximum value.

Improvements in the general performance of sum-coincidence spectrometers therefore appear to depend upon the development of detector designs which more effectively sense multiple events. From the analysis, several possible methods for accomplishing this objective can be recognized. All non-essential inactive volume within the detector should be eliminated, as for example the central core of detector PD44. Concentric detectors with the source placed in the central void volume would maximize the detector surface area, which has been shown to be of importance. Another technique to enhance multiple event detection is the use of many electrically independent regions within the detector rather than only two as in the cases presented here. For example, additional circumferential slots could be cut into detector PD44 and each isolated region operated as a separate active volume. Energy discrimination in three or more dimensions then would be possible. The practical limits on such techniques are the loss of energy resolution in the detector and the requirement for multiple coincidence and summing circuitry. Separate detectors might also be employed if fine-gain adjustments are provided to correct for the different charge sensitivity of each detector and external window thicknesses are minimized.

If pulse shape discrimination or other means of sensing multiple events can be devised for conventional semiconductor detectors, then the efficiency limitations imposed by the sum-coincidence approach can be circumvented. However, the advantages of energy discrimination in more than one dimension would be lost.

Multiple scattering detectors can also be used in conjunction with anticoincidence systems to achieve further reduction of Compton interference. Because single-interaction events in the multiple scattering detector are rejected, the anticoincidence detector would not be required to detect the once-scattered, high energy gammas but only the lower energy gammas which escape after two or more interactions.

In summary, for Ge(Li) detectors of less than about 30 cm^3 in total volume, the sum-coincidence operating mode offered Compton interference reduction compared to that of anticoincidence systems with Compton suppression factors of from two to five. For state-of-the-art Ge(Li) gamma spectrometers in the 60 cm^3 volume range, the sum-coincidence operating mode as compared to sum-only operation offers superior performance only in isolated cases. The poor relative efficiency of sum-coincidence spectrometers is their major performance limitation. Efficiency improvements appear to be realizable through special detector configurations and energy discrimination techniques or, to a greater extent, by alternative methods of sensing multiple events within a single detector volume.

CHAPTER VI

CONCLUSIONS

The objectives of this research have been realized in that the physical basis for multiple scattering Ge(Li) detectors has been defined, parameters which control spectrometer performance have been categorized, and the practical performance capabilities of multiple scattering detectors have been evaluated. Approaches for achieving additional improvement in the Compton interference reduction attainable from multiple scattering Ge(Li) spectrometers have been suggested.

The objectives were achieved through a combined theoretical and experimental program. A Monte Carlo model was developed which calculates gamma scattering behavior for either sum-coincidence or sum-only Ge(Li) spectrometers. Computed detector performance for the gamma energy range of 320 keV to 2754 keV is shown to be in good agreement with measured performance of sum-coincidence spectrometer systems.

For the range of germanium detector volumes and gamma energies considered in this study, the following conclusions can be made based on the results presented in this thesis:

1. The extent and nature of multiple gamma scattering in detector sized volumes of germanium are adequate to support Compton suppression concepts based on multiple scattering. Full energy interaction sequences are characterized by an average of approximately three gamma interactions separated by distances of the order of a centimeter, and only a minor

fraction of full energy events would be eliminated by requiring multiple interactions. On the other hand, a single interaction followed by escape of the scattered gamma is the most probable sequence for partial energy events which contribute interference counts to the recorded gamma energy spectrum.

2. Parameter variation study results presented in this thesis provide a basis for selecting sum-coincidence detector configurations and energy discrimination criteria for reducing Compton interference for gamma spectroscopy applications. Specifically, the dependence of full energy peak efficiency and peak-to-Compton ratio upon detector geometry parameters and energy selection requirements have been categorized for sum-coincidence operation of stacked planar and concentric cylindrical detector geometries. A severe performance reduction is shown to be caused by internal inactive layers between active volumes, which appears to favor separate-detector spectrometers with thin interface dead layers, or configurations which entirely eliminate the dead layer.

3. Except for isolated combinations of gamma energies, spectrometers based on sum-coincidence operation do not appear to offer advantageous Compton interference reduction as compared to state-of-the-art Ge(Li) detectors. This conclusion is based on comparative performance calculated for sum-only and sum-coincidence operation of a hypothetical 60 cm^3 coaxial Ge(Li) detector. For Ge(Li) detectors of up to 2 cm in length and about 25 cm^3 in volume, sum-coincidence operation was calculated to give an equivalent Compton suppression factor of about two.

4. The efficiency reduction which represents the major performance limitation for sum-coincidence spectrometers is not an inherent

characteristic of multiple scattering spectrometers, and probably can be overcome by the development of alternate methods of identifying multiple interactions within a Ge(Li) detector system. Possible alternate methods include pulse shape identification or optical transition detection which could be correlated to multiple gamma interactions. Additional peak-to-Compton performance can be realized over that offered by any existing sum-coincidence detector by setting energy discrimination requirements based on the distribution of events on the two-parameter surface as discussed in this thesis.

APPENDIX I

THE MONTE CARLO MODEL AND COMPUTER PROGRAM

Major Equations and Computational Techniques

Although the basic Monte Carlo techniques for radiation are fairly standard, the methods used to obtain the important scattering parameters are usually developed to fit the particular system to be studied. Methods used in this investigation are described in the following subsections. Exact equations or approximations methods were used rather than table searching or interpolation for all quantities needed in the calculations.

Cross Section Equations

Photoelectric. The most accurate theoretical cross section equations for photoelectric interaction in low Z elements appear to be those of Pratt, et al.[73,74] These equations are derived using approximate Coulomb wave functions, with up to 40 terms being carried in the wave function expansion. Roy and Reed[41] show that the photoelectric cross section values calculated from these equations agree within about ten percent with experimental values except at the k-shell edges. The equations are not well suited for rapid computer calculations, however. A form of the equations written for computer calculations by Walker and Clement[75] still contains several quantities which must be generated by slow-running machine functions involving expansions: exponentials, logs, functions to non-integer powers, and inverse trigonometric functions. The difficulty of efficient computing with the Pratt equations prompted

the investigation of empirical equations to calculate linear photoelectric cross sections explicitly for germanium over the restricted energy range of interest in this research. A form of the linear cross section equation based on the work of Heitler[76] is commonly given in semiconductor detector reference texts[33]:

$$\sigma = 10^{-33}\ N\ Z^5\ (h\nu)^{-3.5} \text{ barns/atom} \tag{15}$$

$$= (0.03245)\ (h\nu)^{-3.5} \text{ for germanium} \tag{16}$$

where σ_{PE} = linear absorption cross section for photoelectric event, (cm^{-1})

N = number of absorber atoms per cm^3

Z = atomic number of absorber

$(h\nu)$ = incident photon energy in MeV

Cross sections calculated from equation 16 are plotted in Figure 40 along with experimental values from the recent compilation by Storm and Israel.[44] Using the same equation form as equation 16 and cross sections at 15 keV and 500 keV from Storm and Israel, an attempt was made to derive an empirical equation giving a more accurate fit to experimental data than that given by equation 16. The resulting equation is given as equation 17.

$$\sigma_{PE} = (0.0596)\ (h\nu)^{-2.92} \text{ barns/atom} \tag{17}$$

$$= (0.00264)\ (h\nu)^{-2.92}\ cm^{-1} \tag{18}$$

As can be seen in Figure 40, equation 17 gives an excellent fit to the experimental data over the range of photon energy of interest in this

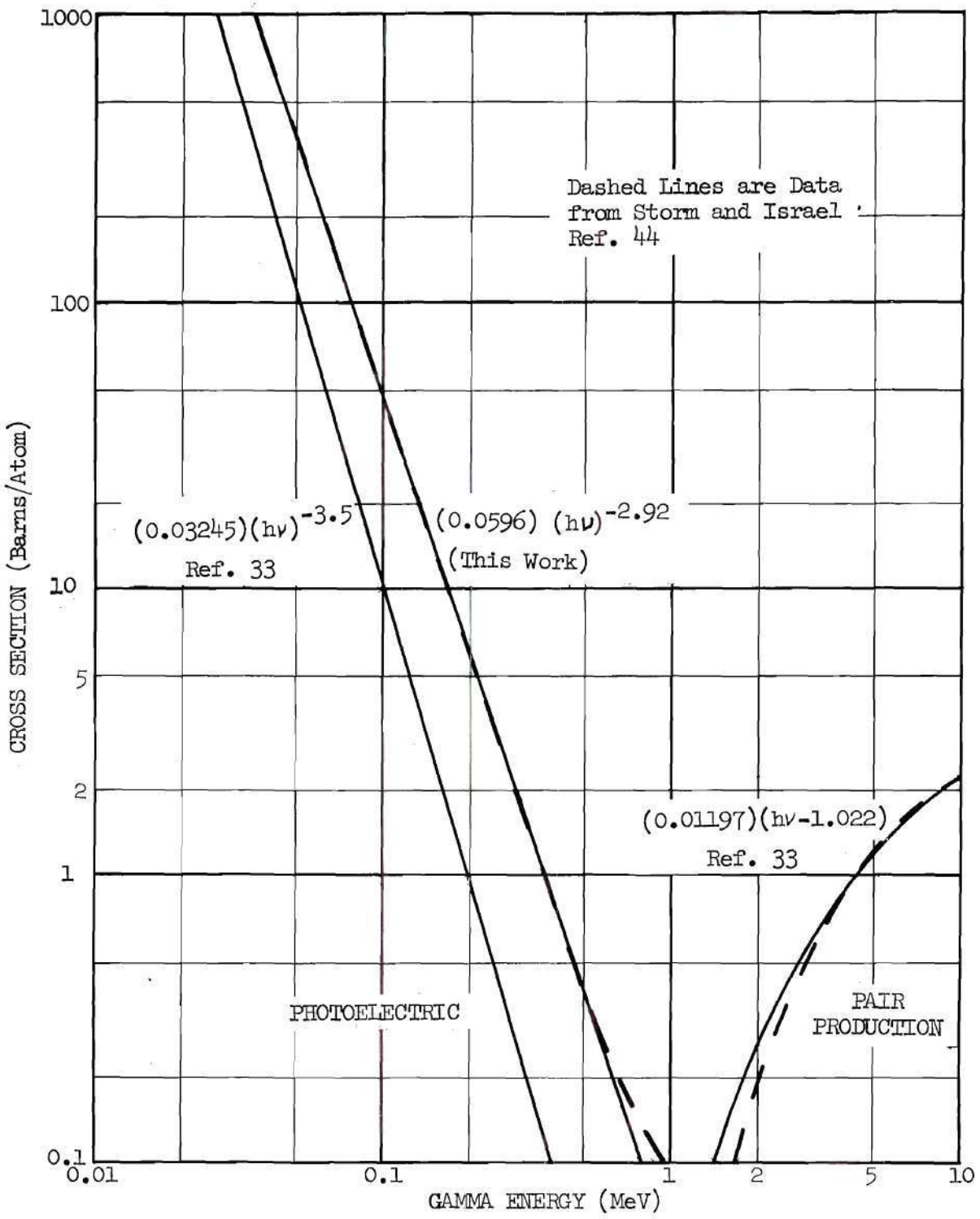

Figure 40. A Fit of Calculated Cross Section Values to Experimental Data of Storm and Israel (Reference 44)

study. Because the simplicity of the equation also gives a relatively rapid calculation time, this equation form is used in the mathematical model.

Compton. Cross sections for Compton scattering are calculated using a form of the Klein-Nishina equations which has been integrated with respect to solid angle to give the total collision cross section. This equation, as expressed by Evans,[40] is:

$$\sigma_c = 2\pi r_o^2 \left\{ \frac{1+\alpha}{\alpha^2} \left[\frac{2(1+\alpha)}{1+2\alpha} - \frac{1}{\alpha} \ln(1+2\alpha) \right] + \frac{1}{2\alpha} \ln(1+2\alpha) \right. \qquad (19)$$

$$\left. - \frac{1+3\alpha}{(1+2\alpha)^2} \right\} \frac{\text{cm}^2}{\text{electron}}$$

where σ_c = total collision cross section for Compton scattering

r_o = classical electron radius

α = energy of incident gamma normalized to electron rest energy.

For germanium, with Z=32 and an atom density of 4.41×10^{22} atoms/cm^3, the equation may be expressed in linear cross section units (cm^{-1}) by replacing the constant ($2\pi r_o^2$) with the numerical constant (0.70355). This form of Compton cross section equation is used in the mathematical model.

Pair Production. As was the case with the photoelectric cross section equations, the complexity of the equation form for the best available pair production equations would extend the computing time by an amount not justified by the increased accuracy over simpler equation forms. The accurate equation forms for this case are those of Hough[77] which are based on correction terms to the Bethe-Heitler equations.[78]

Roy and Reed[41] note that agreement with experimental values is observed to be within five to ten percent except near the pair production threshold, where errors of 200 to 250 percent are reported by Rama Rao, et al.[79] Figure 40 shows experimental pair production cross sections from Storm and Israel[44] and cross sections calculated from equation 20 as given by Dernalley and Northrup.[33]

$$\sigma_{pair} = NZ^2 \ (h\nu - 2m_o c^2) \qquad (20)$$

$$= (0.01197) \ (h\nu - 1.022)$$

Since the cross sections calculated from equation 20 are accurate to within ten percent over the energy range of significant pair contribution, this simpler equation form is used in the calculations.

Compton Scattering Angle Section

Several methods for selecting scattering angles from the Klein-Nishina distribution were evaluated in an attempt to find a fast, accurate calculating procedure. The probability distribution function versus scattering angle for selected energies is shown in Figure 41. Data points for these curves were calculated from an integral form of the Compton cross section equation as given by Davisson[42]:

$$\sigma_{\theta_o} = \int_o^{\theta_o} \int_o^{2\pi} \sigma(\theta, \Phi) \ d\Phi d\theta \qquad (21)$$

$$= \pi r_o^2 \ \{[2\alpha^2 \ (1-\alpha-\alpha \cos\theta_o)^2]^{-1} [4+10\alpha+8\alpha^2+\alpha^3 \qquad (22)$$

$$- (4+16\alpha+16\alpha^2+2\alpha^3) \cos\theta_o + (6\alpha+10\alpha^2+\alpha^3) \cos^2\theta_o$$

$$- 2\alpha^2 \cos^3\theta_o] + \alpha^3(\alpha^2-2\alpha-2) \ \ell n(1+\alpha-\alpha \cos\theta_o)\}$$

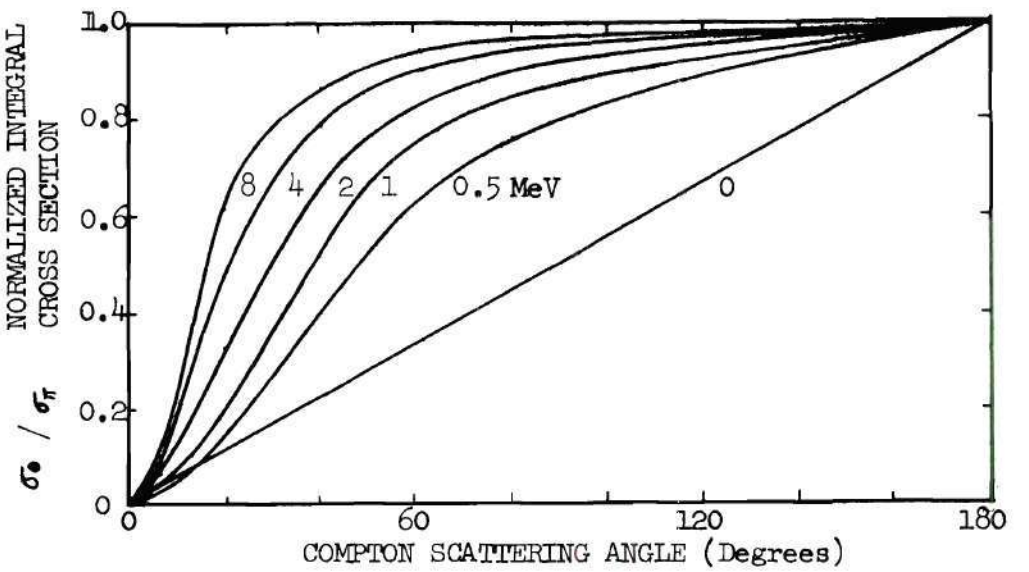

Figure 41. Compton Scattering Angle versus Integral Compton Cross Section Normalized to 180° Scattering (equation 22)

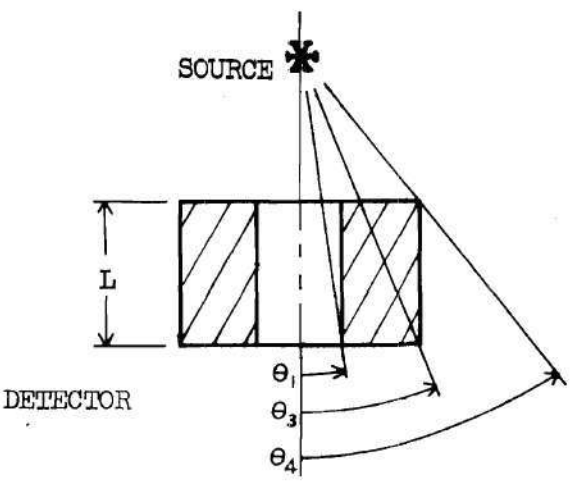

Figure 42. Source and Detector Geometry for Calculating Geometrical Losses

where σ_{θ_o} = cross section for the number of photons scattered within a cone of half angle θ_o

θ = angle between Compton scattered photon direction and incident photon direction

Φ = azimuthal scattering angle about incident photon direction.

The smooth behavior of the probability distribution function $(\sigma_\theta/\sigma_\pi)$ suggests that a series approximation of relatively few terms might give a good fit to the data of Figure 41. A least squares method for fitting an N-dimensional surface with orthogonal polynomials[80] was used to develop and test power series equations for Compton scattering angle. Power series coefficients for the two independent variables were calculated based on an input rectangular grid of 651 data points generated by iterative calculations using equation 22. Table 17 shows the variance in scattering angle versus the order of the terms and the energy range.

Table 17. Variance of Compton Scattering Angle Calculated from Power Series Approximation

Energy Range (MeV)	Order of Terms		Variance (degrees)
	Energy Terms	Normalized Cross Section Terms	
0 - 3.0	5	10	6.6
0.4 - 3.0	3	3	13.10
	3	4	9.41
	3	5	3.138
	3	6	1.996
	3	7	0.5169
	3	8	0.3129
	3	9	0.0827
	4	9	0.0621
	5	10	0.0707
0 - 0.3	3	5	1.57
	5	5	1.57
	10	5	1.65

As may be seen from the table, a test of energy range and computation with a series of greater than 25 terms are required to calculate accurate scattering angle values by this method.

A procedure for determining θ by iterating on θ in equation 22 until the error in cross section was less than a specified value was also tested. Values of θ to within 0.1 degree could be determined with an average of less than six passes through the equation.

Faster calculations were possible, however, by using a variation of the regression method described by Snow.[67] In contrast to the lengthy calculating procedure of the regression method described by Kahn,[81] the method of Snow involves only a few calculations. The principle of the method may be explained in geometrical terms. If coordinates are selected at random from a rectangular area whose ordinate boundaries are the zero and the maximum of a probability density function and whose abcissa boundaries are the limits of the independent variable, then those points under the probability density function (PDF) curve represent a true random sampling from that probability density. In effect, one "throws darts" at the rectangle and accepts the abcissa value if the corresponding ordinate value falls below the PDF curve.

The regression method as applied by Snow to sampling for scattering angle from the Klein-Nishina distribution for an incident photon of energy $h\nu$ proceeds as follows. Random number RN_1 (0-2 range) is selected and set equal to $(1 - \cos\theta)$, which represents selection from a uniform density function in θ. The corresponding energy, E, and normalized differential cross section P are then calculated.

$$E = 1/(1 + \alpha(1 - \cos\theta)) = 1/(1 + \alpha(RN_1)) \qquad (23)$$

where $\alpha = \frac{h\nu}{m_o c^2}$

$$P = E^2 \left[E + E^{-1} + ((RN_1)(RN_1 - 2))\right] \qquad (24)$$

A second random number, RN_2, normalized to P_{max} (2 in this case), is selected. If $P \geq RN_2$, then the coordinates selected are under the PDF curve. The value of θ represented by RN_1, or $\theta = \cos^{-1}(1 - RN_1)$, therefore represents an angle selected from the Klein-Nishina distribution for the energy of the incident photon. If $P \leq RN_2$, the process is repeated beginning with the selection of RN_1 until a coordinate set under the PDF curve is chosen.

As would be expected from an analysis of Figure 41, the procedure is most efficient at low energies and, indeed, approaches unity as the photon energy approaches the uniform PDF for zero photon energy. Using Advanced Algol on the Burroughs B5500 computer, the θ value selection time averaged 6 milliseconds for $h\nu$ = 100 keV and 20 milliseconds for $h\nu$ = 5 MeV. A probability distribution function constructed from 10,000 probability density function values calculated by this technique agreed to within one degree with the distribution function calculated from equation 22.

Random Number Generator

A pseudo random number generator based on the multiplicative method first introduced by Lehmer[82] was developed and tested for this Monte Carlo model by Carr.[83] The generator is of the form:

$$X_{n+1} = A\, X_n \pmod{2^B}$$

where $X_i = i^{th}$ random number

$A = 7{,}000{,}001{,}000{,}003_8 = 481{,}036{,}599{,}299_{10}$

$B = 39$

The constants A and B were chosen by the criteria described by Jansson[84] and Gannon and Schmittroth[85] to give maximum period and simplified (octal) multiplication. The value for B was chosen as the maximum numerical value which could be stored in the 39-bit length mantissa of the 48-bit word used on the B5500 computer. With X_0 chosen to be an odd number, the period is shown by Jansson[84] to be 2^{B-2}, or approximately 1.4×10^{11} for the A and B values given.

For 100,000 numbers generated by this method, the mean normalized random number was 0.4997607. Frequency distribution tests were performed by cataloging 10,000 numbers from each of ten runs into 1000 sub-intervals of the normalized random number range. The Chi-squared test of the frequency distribution was satisfied for a 95 percent confidence level by each group.

The length-of-run distribution test, observed to be the most discriminating test of random number generators by at least two investigators[83,85] was also applied. An occurrence of K consecutive numbers forming a monotonic increasing (or decreasing) sequence which is broken by the $K + 1^{st}$ number constitutes a run of length K. Chi-squared, as calculated for the length-of-run distribution of ten runs of 10,000 numbers each fell within the 95 percent confidence interval for all cases.

Calculation of Geometrical Losses

The gammas which are considered in the Monte Carlo calculation represent a biased sample of only the gammas from the source which intercept the germanium volume and have a pathlength of less than the longest dimension of that volume. The number of gammas excluded from the Monte Carlo procedure is calculated once at the beginning of each computer run so that the fate of all gammas from the source can be determined. The uninteresting no-interaction cases are then excluded from the probability distribution functions presented to the incident gamma in the Monte Carlo calculations.

For the geometry of the source and detector shown in Figure 42, the fraction of gammas which intercepts the cylindrical annulus of germanium is given by:

$$F_i = \frac{\int_0^{2\pi}\int_{\theta_1}^{\theta_4} \sin\theta \, d\theta d\Phi}{\int_0^{2\pi}\int_0^{\pi} \sin\theta \, d\theta d\Phi} = \frac{\cos\theta_1 - \cos\theta_4}{2} \qquad (25)$$

Of the number which intercept the germanium volume, the fraction F_p which has a pathlength greater than the maximum pathlength in the germanium is:

$$F_p = F_i \cdot \exp(-\sigma \cdot P_{max}) \qquad (26)$$

where σ = linear cross section for interaction at the energy of the incident gamma

P_{max} = maximum pathlength in the detector by a photon from the source = L(detector length)/$\cos\theta_3$.

The fraction of gammas considered in the Monte Carlo routine then becomes:

$$F_{mc} = F_i - F_p \tag{27}$$

$$= \left[\frac{\cos\theta_1 - \cos\theta_4}{2}\right] [1 - \exp(-\sigma L/\cos\theta_3)]$$

Because the number of gammas which interact in the detector is specified as an input parameter, the total number of gammas from the source which produce this number of interacting gammas must be calculated:

$$N_{total} = \frac{N_{mc}}{F_{mc}} = \frac{2N_{mc}}{(\cos\theta_1 - \cos\theta_4)(1 - \exp(-\sigma L/\cos\theta_3))} \tag{28}$$

The N_{total} value is used for efficiency calculations at the end of the Monte Carlo calculation in which the number of events in each category has been determined.

The Computational Procedure

An abbreviated flow diagram of the Monte Carlo model for the interaction of gamma photons in a germanium sample is given in Figure 43. Five variations on this basic calculational procedure were programmed to provide the specific information needed for the analysis of multiple scattering detector concepts. A brief discussion of the major steps of the calculation is given below. Topic numbers refer to the block numbers on the diagram.

1. Read Input Data: The fixed parameters for the germanium detector (or volume) and gamma source are entered into the program memory.

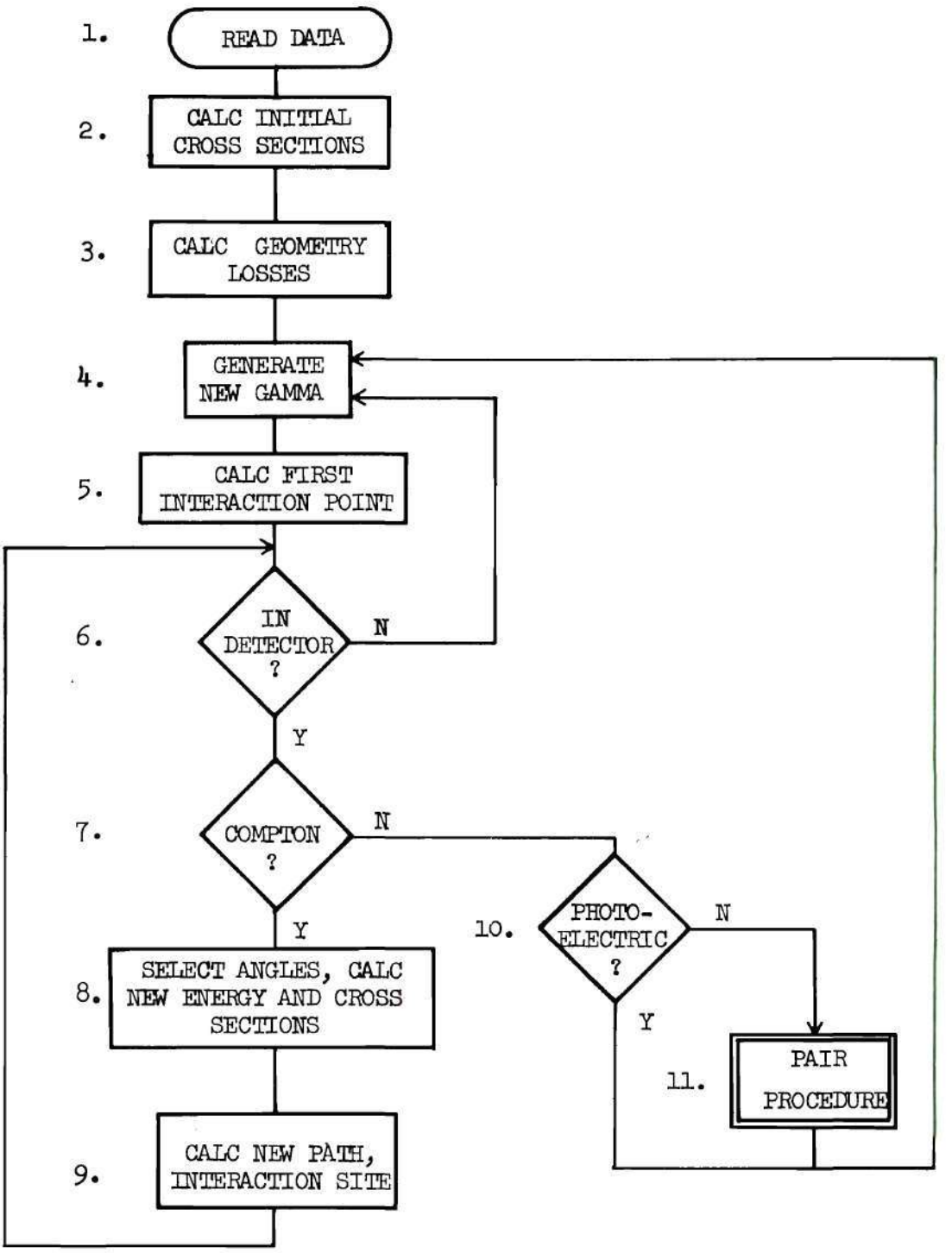

Figure 43. Computer Calculation Flow Diagram for Basic Monte Carlo Calculation

Depending on the type of calculation, the input information might include the incident photon energy, the dimensions of the source, external and internal dimensions of the detector, location dimensions, and the number of photons to be considered.

2. Calculate Initial Cross Sections: Linear interaction cross sections for Compton, photoelectric, and pair production interactions for the initial photon energy are calculated. The cross section values, along with the geometrical information of the next step, are stored for repeated use throughout the calculation since they are needed for each new photon from the (monoenergetic) source. A new set of initial cross sections is calculated only when incident photons of another energy are to be added to the accumulated information. The order in which photons of different energy enter the calculation does not affect the final computed result.

3. Calculate Geometrical Losses: Using the input geometrical data from step 1, the angular limits are calculated for which the photon from the source would be outside the solid angle subtended by the detector, would pass through any central holes, or would pass through selected regions of the detector. The probability of passing through the detector without an interaction is also calculated. Calculations are then made to determine the fraction of photons not interacting in the detector so that this uninformative type of event need not be considered in the Monte Carlo calculation. The total number of photons from the source corresponding to the number allowed to interact in the detector volume is also calculated to provide efficiency information.

4. Generate New Photon: This step is essentially the resetting of the mechanism for logging the progress of an incident photon and the selection of the incident direction for the new photon. For other than a point source, the origin of the photon on the source is selected by a random sampling of the available source geometry. The incident angular coordinates of the photon to the detector are selected from an isotropic distribution restricted to the solid angle of the detector based on the information generated in the previous step.

A counter is also advanced at this point to record the total number of incident photons and to terminate the calculation if a preset number has been reached.

5. Calculate First Interaction Point: Using the calculated total interaction cross section, a weighted probability distribution function for photon path length in the sample is defined. A unique path length is then obtained by equating a random number* to the probability and calculating the corresponding path length. The interaction location is then determined from geometrical considerations which include the elimination of path length traversed before interception of the detector. Void volume inside or outside of the detector is assumed to be vacuum in these calculations.

6. In-Detector Test: The interaction coordinates are tested to determine whether or not the photon interaction is within the prescribed detector boundaries. If so, then a random number representing the inter-

---

*All random numbers are assumed to be distributed over the interval from zero to unity unless otherwise stated.

action type is chosen for testing against the normalized cross sections in steps 7 and 10.

7. Compton Test: If the interaction random number is less than the Compton cross section normalized with respect to the total cross section, the interaction is deemed to be a Compton scatter. If the random number is greater, then control is transferred to step 10, a similar test for photoelectric interaction. The Compton interaction is the first tested, since the probability of Compton interaction is greater over the energy range of interest in this study.

8. Select Angles, Calculate New Energy and Cross Sections: If the photon interaction is a Compton scatter, then the scattering angle with respect to the direction of the photon is selected from an appropriate probability density function by the regression technique. The azimuthal angle is picked from a density function assumed to be uniform. A coordinate rotation is then performed to relate the angles back to a fixed cylindrical system within the detector. The Compton scattering angle is used to calculate the energy of the scattered photon, which in turn is used to calculate the new cross sections for the photon.

9. Calculate New Path Length, Interaction Location: A path length is selected by the method described in step 5, but based on the cross sections for the scattered photon of reduced energy. The new interaction location is then calculated, and program control is transferred back to step 6 to check the location coordinates against the detector boundaries. Note that the Compton event loop (steps 6 through 9) will be traversed as many times as a Compton interaction is selected in step 7; the calculations for a photon cannot terminate in this loop.

10. Photoelectric Interaction Test: If the Compton test result of step 7 was "false," and the photon energy is greater than 2 $m_o c^2$, then a test is made against the normalized photoelectric cross section. If the photoelectric interaction test is "true," the event is logged in some manner and control is directed back to step 4, the generation of a new photon. A "false" result at this point is taken to be a pair production interaction, and control progresses to step 11.

11. Pair Procedure: For a pair production event, the kinetic energy given to the pair is assumed to be dissipated at the location of the pair interaction. The positron-electron annihilation is assumed to create two oppositely directed, isotropically distributed annihilation gammas at the initial interaction location. One annihilation gamma is followed until it either escapes from the detector volume or is completely absorbed. The calculations are similar to those of steps 6 through 9, except that now the possibility of pair production is excluded because the energy of an annihilation gamma is less than the pair production threshold energy.

Upon completion of calculations for the first annihilation gamma, a coordinate rotation is performed at the original pair interaction site to produce a second annihilation gamma oppositely directed from the first. This second gamma is then followed until escape or absorption. The multiple events are logged and program control is returned to step 4 for the generation of a new incident photon.

Although the ordering of certain steps in the calculation is modified in the computer program, the same basic steps outlined in the previous paragraphs are followed. A saving of computing time was realized by pre-

senting one sequence of calculations for the initial photon interaction, then a second sequence for follow-on interactions. This approach allowed the use of pre-calculated values and of simplification based on certain symmetries for calculations involving the photon incident from the source.

Several versions of both the Monte Carlo scattering calculation and the programs to interpret scattering information into detector performance were written. The versions of the Monte Carlo program which did or did not contain provisions for considering a central cylindrical void volume are designated by a "C" or "P", respectively, in the program label. All versions are similar in the treatment of the gamma scattering process. The programs are identified in Table 18.

Listings of programs "DC3" and "DCTAL" follow the table. Major steps in the programs have been identified, and typical data output is given.

Table 18. Computer Programs Used in the Detector Analysis

Label	Description	Output
DC1	M C program for gamma scattering; lists all coordinates, angles, cross sections, path lengths, etc. for checking equations and program.	Tabulated listing
DC2, DP2	M C programs for gamma scattering; lists scattering information and gamma spectrum for sum-only operation of specified detector with internal dead layers.	Tabulation, Density Plot, Punched Cards
DC3, EP3	M C programs for gamma scattering of multiple events only; records position and energy loss of each interaction site onto magnetic tape for given source energy and location; records coded event type and sequence length in space between sequences.	Magnetic Tape, Tabulation
DCTAL DPTAL	Program to read tapes from DC3 and DP3 for SCS operation with specified internal detector geometry, energy discriminator settings, and energy resolution; lists one- and two-parameter energy spectra and tabulated performance information.	Tabulation
DCTAP DPTAP	Program similar to "tally and list" program, except that instructions for Cal-Comp Plot of one dimensional spectra are included.	Cal-Comp Plot
CPLOT	Program to read and plot spectra from punched cards; accepts cards from sum-only programs DC2 and DP2.	Cal-Comp Plot

Listing of Monte Carlo Program "DC3"

```
%COMPILE XXXXXXX/DC3     ALGOL          ,01E600904          WALKER D M          0
%PROCESS=075;   IO=030                                                        10
%COMMENT SCRATCH TAPE REQUIRED,                                               20
%COMMENT  TAPE       TAPE  OUT  "CD184"   PLEASE SAVE                         30
%DATA,                                                                        40
BEGIN                                                                         50
                                                                              60
%%%%%%%%%        DECLARATIONS                                                 70
FILE IN KRD (2,10);                                                           80
FILE OUT DMWO 15(2,15);                                                       90
SAVE FILE MTFL 2          "CD184"  (2,1023,1023, SAVE 2);                     100
FORMAT FMA("# EVENTS LOADED ON TAPE =  ",I6),                                 110
       FMB(I5,3F10.6),                                                        120
         FRID(5R10.6,I6),                                                     130
       FMRZF(2I10,3F10.6,/);                                                  140
FORMAT                                                                        150
  TFMB(/,"INCIDENT ENERGY(MEV)=  ",R10.6,X10,"RHOLE(CM)= ",R7.3,X10,          160
     "RMAX(CM)=  ",R7.3,//,"SOURCE TO DETECTOR DISTANCE(CM)=  ",              170
     R7.3,X10,"DETECTOR THICKNESS(CM)=  ",R7.3),                              180
  TFMC(//,X20,"NUMBER INTERACTING IN DETECTOR =  ",          I9,              190
       //,X20,"NUMBER PASSING THROUGH DETECTOR =  ",          I9,             200
       //,X20,"NUMBER OF PHOTOELECTRIC FIRST EVENTS =  ",     I9,             210
       //,X20,"NUMBER ESCAPING AFTER ONE COMPTON EVENT =  ",  I9,             220
     //,X20,"AVERAGE ENERGY LOSS FOR ONE COMPTON ONLY (MEV)=  ",R10.6,        230
       //,X20,"NUMBER INTERACTING TWO OR MORE TIMES =  ",     I9,             240
       //,X20,"NUMBER PASSING THROUGH HOLE =  ",              I9,             250
       //,X20,"NUMBER OUTSIDE DETECTOR SOLID ANGLE =  ",      I9,             260
       //,X20,"TOTAL NUMBER OF PHOTONS FROM SOURCE =  ",      I9);            270
INTEGER   M,N;                                                                280
INTEGER    J,NUSTO,EZIT,PPZTO,PEZTO,K,PASS,L;                                 290
INTEGER  ADRES;                                                               300
REAL   EEDA,KEVCH;                                                            310
REAL KIND,NUMB,PETO;                                                          320
REAL HNUZS,CSTHZ,SGPE,FEEZ,NTOTL,PF2;                                         330
REAL   HNUZ,SIGCO,SIGPE,SIGPP,SIGTO,SGNCO,SGNPE,SGNPP,RHOLE,RMAX,D,THIK,     340
       ALFA,DL1,DL2,DL3,DL4,HETO,DISTO,RN1,RN2,MFHOL,MFTO,PMAX,MTF1,          350
       RN3,PLZ,RN4,DLR,PLTOZ,R7,ZZ,DLRZ,THTAZ,HNU,ALFM,EE1,SGTO,              360
       SGCO,SCPE,SGPP,REEZ,ALF,BETA,BZ,PLTO,PLTH,PL,R,Z,BHOL,PLIH,            370
       SA,SB,CA,CB,PROB;                                                      380
REAL  ALFP,BTAP,SAP,CAP,SBP,CBP,RN5,RHOLA,HNUS,EFS;                           390
REAL    A,B,E,SIGMA,SNTHZ,SRA,CAZ,SAZ,BITA,SRHNU,PO,THETA;                    400
REAL   RHOL,RL,ZL;                                                            410
INTEGER AI;                                                                   420
    ARRAY AR,AZ,AE[0:1022];                                                   430
INTEGER  ONECO;                                                               440
REAL EE;                                                                      450
REAL ENCO;                                                                    460
REAL  PLH,DA,SING,MFT;                                                        470
INTEGER  S1,S2;                                                               480
REAL     F,G,KOR;                                                             490
$ CARD
$$ A A100                                                                      0
   WRITE (FILE[OBL],15,A[*])%                                              16400
                                                                        99999999
$ CARD LIST
DEFINE LIM= RHOLE,RMAX,(D+THIK),D#;                                           500
LABEL   MO,NOMO;                                                              510
LABEL   PES;                                                                  520
LABEL SCAT1;                                                                  530
LABEL  NUHNU,REGN34,FIND,COZ,PEZ,NOHOL,TALLY,COMPTN;                          540
LABEL  PAIR,NUHIT;                                                            550
                                                                              560
```

```
%%%%%%%%%          MAGNETIC TAPE LOADING PROCEDURE                    570
                                                                      580
PROCEDURE  MTO(R,Z,EE);                                               590
REAL R,Z,EE;                                                          600
BEGIN                                                                 610
OWN INTEGER I,T,H;                                                    620
IF I = 1023 THEN BEGIN                                                630
     WRITE(MTFL,1023,AR[*]);                                          640
     WRITE(MTFL,1023,AZ[*]);                                          650
     WRITE(MTFL,1023,AE[*]);                                          660
     I ← 0;                                                           670
     H ← H + 1;                                                       680
     T ← 1023 + T;                                                    690
   IF H = 10 THEN                                                     700
BEGIN                                                                 710
     H ← 0;                                                           720
              TIMM(DMWD,1);%                                          730
END;                                                                  740
     IF T > 61400 THEN GO TO TALLY;                                   750
END;                                                                  760
     AR[I] ← R;     AZ[I] ← Z;     AE[I] ← EE;     I ← I + 1;        770
  END MTO;                                                            780
                                                                      790
%%%%%%%%%          ARCSIN AND ARCCOS PROCEDURES                       800
                                                                      810
REAL PROCEDURE ARCSIN(X);                                             820
REAL X;                                                               830
BEGIN                                                                 840
LABEL L1;                                                             850
REAL  X2,X3,X4,X5,X6,X7,TA,TB,TC,SX;                                  860
IF ABS(X)≥1.0 THEN                                                    870
BEGIN                                                                 880
ARCSIN←1.5707963268×SIGN(X);                                          890
GO TO L1;                                                             900
END;                                                                  910
IF X=0 THEN                                                           920
BEGIN                                                                 930
ARCSIN←0;                                                             940
GO TO L1;                                                             950
END;                                                                  960
     SX ← ABS(X);                                                     970
     X2 ←SX ×SX;  X3 ← X2 ×SX;  X4 ← X2 × X2;                         980
     X5 ← X2 × X3;   X6 ← X3 × X3;   X7 ← X3 × X4;                    990
     TA ← 1.5707963050 - .2145988016 ×SX  + .0889789874 × X2;        1000
     TB ← -.0501743046 × X3 + .0308918810 × X4 -.0170881256 × X5;    1010
     TC ← .0066700901 × X6 - .0012624911 × X7;                       1020
       ARCSIN ← (1.5707963268 - (TA + TB + TC ) × SQRT(1-SX)) × SIGN(X);1030
L1: END OF ARCSIN;                                                    1040

REAL PROCEDURE ARCCOS(X);                                             1050
REAL X;                                                               1060
BEGIN                                                                 1070
COMMENT CALCULATES THE ARCCOSINE BY CALLING ON ARCSIN(X) AND USING THE 1080
CONVERSION FORMULA ARCCOS(X) = PI/2 - ARCSIN(X). ARCSIN(X) MUST HAVE  1090
BEEN PREVIOUSLY DECLARED. WRITTEN BY HOWARD CARR OF NRC ON 5/4/68;    1100
REAL PI;                                                              1110
LABEL L1;                                                             1120
PI←3.1415926536;                                                      1130
IF X≥1.0 THEN                                                         1140
BEGIN                                                                 1150
ARCCOS←0;                                                             1160
GO TO L1;                                                             1170
END;                                                                  1180
IF X≤-1.0 THEN                                                        1190
BEGIN                                                                 1200
ARCCOS←PI;                                                            1210
GO TO L1;                                                             1220
END;                                                                  1230
PI←PI/2.0;                                                            1240
ARCCOS←PI-ARCSIN(X);                                                  1250
L1: END OF ARCCOS;                                                    1260
```

```
                                                                        1270
%%%%%%%%%%      RANDOM NUMBER GENERATOR PROCEDURE                       1280
                                                                        1290
REAL PROCEDURE RN;                                                      1300
BEGIN                                                                   1310
COMMENT THIS PROCEDURE GENERATES PSEUDO RANDOM NUMBERS NORMALIZED       1320
BETWEEN 0 AND 1. IT USES THE MULTIPLICATIVE METHOD. WRITTEN BY HOWARD E 1330
CARR OF NRC ON 4/4/68;                                                  1340
OWN REAL N,R,S,Z,ZZ;                                                    1350
IF S#481036599299 THEN                                                  1360
BEGIN                                                                   1370
N+5497558138B7;                                                         1380
R+112193164491;                                                         1390
S+481036599299;                                                         1400
Z+ZZ+0.0;                                                               1410
END;                                                                    1420
DOUBLE(R,Z,S,Z,X,+,ZZ,R);                                               1430
WHILE R.[45:3] = 0 DO                                                   1440
BEGIN                                                                   1450
R+7&R[12:9:36]&ZZ[9:45:3];                                              1460
ZZ+Z&ZZ[12:9:36];                                                       1470
END;                                                                    1480
RN+R/N;                                                                 1490
END RN;                                                                 1500
                                                                        1510
%%%%%%%%%%      KLEIN-NISHINA ANGLE SELECTION PROCEDURE                 1520
                                                                        1530
PROCEDURE KN(EIN,THETA);                                                1540
REAL EIN,THETA;                                                         1550
BEGIN                                                                   1560
REAL  RN1,RN2,ALF,E,P;                                                  1570
LABEL  PICK;                                                            1580
PICK:                                                                   1590
    RN1 + RN x 2;   RN2 + RN x 2;                                       1600
    ALF + EIN/.511;                                                     1610
    E + 1/(1 + ALF x RN1);                                              1620
    P + E x E x (E + (1/E) + (RN1 x (RN1 - 2)));                        1630
      IF RN2 > P THEN GO TO PICK;                                       1640
    THETA + 57.295779513 x  ARCCOS( 1 - RN1);                           1650
END KN;                                                                 1660
                                                                        1670
%%%%%%%%%%          BEGINNING OF CALCULATION                            1680
                                                                        1690
WRITE (OMWD[NO1,<" ">);                                                 1700
                                                                        1710
%%%%%%%%%%          READ INPUT DATA                                     1720
                                                                        1730
MO: READ  (KRD,FRID,      HNUZ,RHOLE,RMAX,D,THIK,NUSTO)[NOMO1  ;        1740
     J + 0;                                                             1750
     RN1 + RN;                                                          1760
          NUSTO + 0;                                                    1770
          FZIT + ONECO + 0;                                             1780
     ALFA + HNUZ / 0.511;                                               1790
                                                                        1800
```

```
%%%%%%%%%%          CALCULATE INITIAL CROSS SECTIONS                    1810
                                                                        1820
   SIGCO+0.70355x(((1+ALFA)/(ALFAxALFA))x((2x(1+ALFA)/(1+2xALFA))-      1830
          ((LN(1+2xALFA))/ALFA)) + (LN(1+2xALFA))/(2xALFA)-             1840
          ((1+3xALFA)/((1+2xALFA)x(1+2xALFA))));  %EVANS P684           1850
   IF HNUZ ≤ 1.02 THEN SIGPP + 0  ELSE SIGPP + .01197 x(HNUZ - 1.02);   1860
     SIGTO + SIGCO + SIGPE + SIGPP;                                     1870
     SGNCO + SIGCO / SIGTO;                                             1880
   SGNPE + (.00263717 / (HNUZ * 2.92)) / SIGTO;   %REV 9/10/69          1890
     SGNPP + SIGPP / SIGTO;                                             1900
                                                                        1910
```

```
%%%%%%%%%%          CALCULATE GEOMETRY LOSSES                          1920
                                                                       1930
        DISTO ← D + THIK;                                              1940
        DL1 ← ARCTAN (RHOLE / DISTO ) ;                                1950
        DL2 ← ARCTAN (RHOLE / D);                                      1960
        DL3 ← ARCTAN (RMAX / DISTO);                                   1970
        DL4 ← ARCTAN (RMAX / D);                                       1980
        MFHOL ← (1 - COS(DL1))/2;                                      1990
        HFTO ← (COS(DL1) - COS(DL4)) /2;                               2000
        MFTO ← 1 - HFTO;                                               2010
        PMAX ← THIK / COS(DL3);                                        2020
        MTF1 ←(EXP(-SIGTO × PMAX))×HFTO ;                              2030
       MFT ← (1-(MTF1/HFTO));                                          2040
         NTOTL ← ( NUSTO/(1- MTF1 - MFTO));                            2050
        HNUZS ← SQRT(HNUZ);                                            2060
            RHOL ← RHOLE;                                              2070
                                                                       2080
%%%%%%%%%%          NEW GAMMA FROM SOURCE                              2090
                                                                       2100
NUHNU;   J ← J+1;          K←0;                                        2110
     MTO(KIND,NUMB,PETO);                                              2120
                                                                       2130
%%%%%%%%%%      CALCULATE FIRST SCATTER INFORMATION                    2140
                                                                       2150
 SCAT1:                                                                2160
          NUSTO ← NUSTO + 1;                                           2170
     KIND ← NUMB ← PETO ← 0;                                           2180
     RN1 ← RN × MFT;  % ELIMINATES PATH GREATER THAN PMAX              2190
      PLZ ← -LN(1 - RN1) / SIGTO;                                      2200
      RN2 ← RN × HFTO + MFHOL;                                         2210
     CAZ ← ( 1 - 2 × RN2);                                             2220
     DLR ← ARCCOS (CAZ);                                               2230
     ALF ← (3,1415926536 - DLR);                                       2240
     SAZ ← SIN(DLR);                                                   2250
      IF DLR > DL2 THEN GO TO REGN34;                                  2260
      PLTOZ ← PLZ + (RHOLE / SAZ);                                     2270
      GO TO FIND;                                                      2280
REGN34:  PLTOZ ← PLZ + (D/ CAZ);                                       2290
 FIND:  RZ ← PLTOZ × SAZ;                                              2300
     ZZ ← PLTOZ × CAZ;                                                 2310
                                                                       2320
%%%%%%%%%          TEST FOR INITIAL EVENT IN DETECTOR                 2330
                                                                       2340
IF RZ > RMAX OR ZZ > DISTO THEN                                        2350
BEGIN                                                                  2360
     EZIT ← EZIT + 1;                                                  2370
     GO TO SCAT1;                                                      2380
END;                                                                   2390
                                                                       2400
%%%%%%%%%      TEST FOR COMPTON (INITIAL PHOTOELECTRIC NOT ALLOWED)   2410
                                                                       2420
```

```
                                                                       2430
        RN3 ← RN            ;                                          2440
       IF RN3 < SGNCO THEN GO TO COZ;                                  2450
                                                                       2460
```

```
COMMENT     FIRST PAIR PRODUCTION CALCULATION;                              2470
                                                                            2480
BEGIN                                                                       2490
LABEL  ANHNU,NAHOL,REHIT,INDET,WORK,SCATA,NSHOL,EXPP;                       2500
          KIND ← -2;                                                        2510
      EE ← HNUZ - 1.022;  R ← RZ;  Z ← ZZ;                                  2520
      MTO(R,Z,EE);                                                          2530
      ALFP ← 3.14159265 × RN ;                                              2540
      BTAP ← 3.14159265 × RN ;  %BTAP IS INSIDE ANGLE                       2550
          M ← 0;                                                            2560
        SAP ← SIN(ALFP);                                                    2570
        SBP ← SIN (BTAP);                                                   2580
        CAP ← COS(ALFP);                                                    2590
        CBP ← COS(BTAP);                                                    2600
      BHOLA ← ARCSIN (RHOL / RZ);                                           2610
ANHNU:   HNU ← .511;     N←2;      PLTO←0;                                  2620
      K ← 0;                                                                2630
      ALF ← ALFP;                                                           2640
      ALFM ← 1;                                                             2650
      RL ← RZ;      ZL ← ZZ;                                                2660
      PL ← -(LN(1-RN)) / .45  ;                                             2670
         IF BHOLA <ABS(BTAP)  THEN GO TO NAHOL;                             2680
      PO ← SQRT (( RHOL×RHOL) - (RZ×RZ× SBP×SBP));                          2690
      PLTH ← (( RZ× CBP - PO) / SAP);                                       2700
         IF PL < PLTH THEN GO TO NAHOL;                                     2710
PLTO ← PL + (2× PO / SAP);                                                  2720
NAHOL:  IF PLTO > 0 THEN PL ← PLTO;                                         2730
      PLH ← PL × SAP;                                                       2740
      Z ←ZZ - (PL×CAP);                                                     2750
      R ← SQRT ((RZ×RZ) + (  PLH × PLH  ) - (2×RZ× PLH  ×CBP));             2760
REHIT:                                                                      2770
   IF R > RMAX OR ( Z < 0  OR Z > DISTO )   THEN                            2780
BEGIN                                                                       2790
      IF M = 1 THEN GO TO EXPP;                                             2800
      M ← M + 1;                                                            2810
          GO TO ANHNU;                                                      2820
END;                                                                        2830
INDET:  IF N ≠ 2 THEN GO TO WORK;                                           2840
       SGCO ← 0.435;                                                        2850
      SGPE ← 0.0186;  %REV 9/1/69                                           2860
      SGTO ← 0.4536;  % REV 9/1/69                                          2870
       SA ← SAP;                                                            2880
       SB ← SBP;                                                            2890
       CA ← CAP;                                                            2900
       CB ← CBP;                                                            2910
WORK:RN5 ← RN × SGTO;                                                       2920
         IF RN5 < SGCO THEN GO TO SCATA;                                    2930
           PETO ← PETO - 1;                                                 2940
      EE ← HNU;                                                             2950
      MTO(R,Z,EE);                                                          2960
         M ← M+1;                                                           2970
         IF M>1 THEN GO TO EXPP;                                            2980
      ALFP ← 3.14159265 - ALFP ;                                            2990
      BTAP ← BTAP - 3.14159265 ;                                            3000
       CAP ← -CAP;                                                          3010
      SBP ← -SBP;                                                           3020
      CBP ← -CBP;                                                           3030
                GO TO ANHNU;                                                3040
```

```
SCATA: PROB ← RN5 × SGTO / SGCO;                                        3050
       NUMB ← NUMB + 1;                                                 3060
       SRHNU ← SQRT(HNU);                                               3070
       KN(HNU,THETA);                                                   3080
       CSTHZ ← COS ( THETA / 57.2957795131);                            3090
       SNTHZ ← SIN ( THETA / 57.2957795131);                            3100
          HNUS ← (.511 × ALFM) / (ALFM × (1 - CSTHZ) + 1);              3110
       ALFM ← HNUS / .511;                                              3120
       EE ← HNU - HNUS;                                                 3130
       MTO(R,Z,EE);                                                     3140
      SGCO+0.70355×(((1+ALFM)/(ALFM×ALFM))×((2×(1+ALFM)/(1+2×ALFM))-    3150
                ((LN(1+2×ALFM))/ALFM)) + (LN(1+2×ALFM))/(2×ALFM))-      3160
                ((1+3×ALFM)/((1+2×ALFM)×(1+2×ALFM))));                  3170
       SGPE ← .00263717 / (HNUS * 2.92); %REV 9/1/69                    3180
         SGTO ← SGCO + SGPE;                                            3190
       DA ← ARCCOS((R×R + PLH×PLH - RL×RL) /(2×R×PLH));                 3200
          IF DA < 0 THEN DA ← 1.5708 - DA;                              3210
       FEEZ ← 6.2831853 × RN;                                           3220
       A← (SNTHZ × SIN(FFEZ));                                          3230
       B← (SNTHZ × COS(FFEZ));                                          3240
       SRA← SQRT (1- (A×A));                                            3250
       E ← ARCSIN ( B / SRA);                                           3260
       F ← (ALF - E);                                                   3270
       G ← (ALF + E);                                                   3280
       CA ← ((CSTHZ ×CA ) + (SNTHZ × SA  × COS(FEEZ)));                 3290
       ALF ← ARCCOS(CA);                                                3300
       SA ← SIN (ALF);                                                  3310
        BETA ← ARCSIN (-A / SA);                                        3320
          IF A > 0  THEN KOR ← -3.14159265359  ELSE KOR ← 3.14159265359; 3330
    IF THETA <  90    AND  F<0                  THEN BETA ← (KOR -BETA);  3340
    IF THETA <  90    AND  F > 3.1415926536 THEN BETA ← (KOR -BETA);    3350
    IF THETA >  90    AND (G>0 AND G<3.14159) THEN BETA←(KOR-BETA);     3360
       BETA ← BETA + SING × DA;                                         3370
        IF BETA < -3.14159 THEN BETA ← (6.2832 + BETA) ELSE             3380
          IF BETA > 3.14159 THEN BETA ← -(6.2832 - BETA);               3390
       BITA ← 3.14159 - ABS(BETA);                                      3400
          CB ← COS (BITA);   SB ← SIN (BITA);                           3410
         IF BETA < 0 THEN SING ← (-1) ELSE SING ← +1;                   3420
          PL ← -(LN(1 - RN)) / SGTO;                                    3430
           PLTO ← 0;                                                    3440
       BHOL ← ARCSIN(RHOL / R);                                         3450
          IF BHOL < BITA THEN GO TO NSHOL;                              3460
       PO ← SQRT((RHOL×RHOL) - (R×R × SB×SB));                          3470
       PLTH ← ((R×CB - PO) / SA);                                       3480
          IF PL < PLTH THEN GO TO NSHOL;                                3490
       PLTO ← PL + (2×PO/SA);                                           3500
NSHOL:  IF PLTO > 0 THEN PL ← PLTO;                                     3510
       PLH ← PL×SA;                                                     3520
       RL ←R ;      ZL ← Z;                                             3530
       Z ← Z  - (PL×CA);                                                3540
       R ← SQRT(( R×R) + (PLH×PLH) - (2×R×PLH×CB));                     3550
        HNU ← HNUS;                                                     3560
       N ← N+1;                                                         3570
                GO TO REHIT;                                            3580
EXPP: % END OF PAIR PRODUCTION CALCULATION                              3590
END;                                                                    3600
                GO TO NUHNU;                                            3610
PEZ:                                                                    3620
                                                                        3630
```

```
%%%%%%%%%          FIRST EVENT  COMPTON CALCULATION                    3640
                                                                        3650
CO7:     PROB ← RN3 / SGNCO;                                            3660
                                                                        3670
%%%%%%%%%          SELECT SCATTER ANGLE, CALC NEW CROSS SECTIONS       3680
                                                                        3690
     KN(HNUZ,THTAZ);                                                    3700
     CSTHZ ← COS ( THTAZ / 57.2957795131);                              3710
     SNTHZ ← SIN ( THTAZ / 57.2957795131);                              3720
         HNU ← (.511 × ALFA) / (ALFA × (1 - CSTHZ) + 1);                3730
         ALFM ← HNU / .511;                                             3740
         EE  ← HNUZ - HNU ;  R ← RZ ;   Z ← ZZ;                        3750
          NUMB ← 1;                                                     3760
   SGCO←0.70355×(((1+ALFM)/(ALFM×ALFM))×((2×(1+ALFM)/(1+2×ALFM))-       3770
            ((LN(1+2×ALFM))/ALFM)) + (LN(1+2×ALFM))/(2×ALFM)-           3780
            ((1+3×ALFM)/((1+2×ALFM)×(1+2×ALFM))));                      3790
     SGPE ← .00263717 / (HNU  * 2.92); %REV 9/1/69                      3800
   IF HNU < 1.02 THEN SGPP ← 0  ELSE SGPP ← 0.01197×(HNU - 1.02);       3810
      SGTO ← SGCO + SGPE + SGPP;                                        3820
      FEEZ ← 6.2831853 × RN;                                            3830
                                                                        3840
%%%%%%%%%          COORDINATE TRANSFORMATION                           3850
                                                                        3860
     A← (SNTHZ × SIN(FEEZ));                                            3870
     B← (SNTHZ × COS(FEEZ));                                            3880
     SRA← SQRT (1- (A×A));                                              3890
     E ← ARCSIN ( B / SRA);                                             3900
     CAZ ← -CAZ;                                                        3910
     F ← (ALF - E);                                                     3920
     G ← (ALF + E);                                                     3930
     CA ← ((CSTHZ ×CAZ) + (SNTHZ × SAZ × COS(FEEZ)));                   3940
     ALF ← ARCCOS(CA);                                                  3950
     SA ← SIN (ALF);                                                    3960
      BETA ← ARCSIN (-A / SA);                                          3970
       IF A > 0  THEN KOR ← -3.14159265359  ELSE KOR ← 3.141592653591;  3980
   IF THTAZ <  90   AND  F<0            THEN BETA ← (KOR -BETA);       3990
   IF THTAZ <  90   AND  F > 3.1415926536 THEN BETA ← (KOR -BETA);      4000
   IF THTAZ >  90   AND (G>0 AND G<3.14159) THEN BETA←(KOR-BETA);       4010
      IF BETA < 0 THEN SING ← (-1) ELSE SING ← +1;                      4020
     BITA ← 3.14159 - ABS(BETA);                                        4030
       CB ← COS (BITA);   SB ← SIN (BITA);                              4040
                                                                        4050
COMMENT  CALCULATE PATH LENGTH IN CENTER HOLE;                          4060
                                                                        4070
NUHIT:                                                                  4080
       PL ← -(LN(1 - RN)) / SGTO;                                       4090
        PLTO ← 0;                                                       4100
     BHOL ← ARCSIN(RHOL / R);                                           4110
       IF BHOL < BITA THEN GO TO NOHOL;                                 4120
     PO ← SQRT((RHOL×RHOL) - (R×R × SB×SB));                            4130
     PLTH ← ((R×CB - PO) / SA);                                         4140
       IF PL < PLTH THEN GO TO NOHOL;                                   4150
     PLTO ← PL + (2×PO/SA);                                             4160
NOHOL:  IF PLTO > 0 THEN PL ← PLTO;                                     4170
     PLH ← PL×SA;                                                       4180
       Z ← Z - (PL × CA);                                               4190
        R ← SQRT (R×R + (PLH×PLH) -(2 × R × PLH × CB));                 4200
                                                                        4210
%%%%%%%%%%         ELIMINATE ONE-INTERACTION COMPTON EVENTS            4220
                                                                        4230
     IF NUMB = 1 THEN                                                   4240
BEGIN                                                                   4250
     IF R > RMAX OR (Z < 0  OR Z > DISTO) THEN                          4260
BEGIN                                                                   4270
     ONECO ← ONECO + 1;                                                 4280
    ENCO ← ENCO + EE;                                                   4290
      GO TO SCAT1;                                                      4300
END;                                                                    4310
     MTO(RZ,ZZ,EE);                                                     4320
         KIND ← -1;                                                     4330
END                                                                     4340
ELSE   BEGIN                                                            4350
                                                                        4360
```

```
%%%%%%%%%%          IN-DETECTOR TEST                                    4370
                                                                        4380
      IF R > RMAX THEN GO TO NUHNU;                                     4390
      IF Z < 0 OR Z > DISTO THEN GO TO NUHNU;                           4400
END;                                                                    4410
      RN4 ← RN;                                                         4420
                                                                        4430
%%%%%%%%%%          TEST FOR COMPTON  (AFTER FIRST INTERACTION)        4440
                                                                        4450
      IF RN4<(SGCO / SGTO) THEN GO TO COMPTN;                           4460
                                                                        4470
%%%%%%%%%%      TEST FOR PHOTOELECTRIC  (AFTER FIRST INTERACTION)       4480
                                                                        4490
      IF RN4 < ((SGCO + SGPE)/SGTO) THEN GO TO PES;                     4500
                                                                        4510
%%%%%%%%%%      BEGIN PAIR PRODUCTION CALCULATION (AFTER FIRST INTERACT) 4520
                                                                        4530
BEGIN                                                                   4540
LABEL       ANHNUB,NAHOLB,REHITB,INDETB,WORKB,SCATAB,EXPPB,NSHOLB;      4550
          KIND ← -3;                                                    4560
      EE ← HNU - 1.022;                                                 4570
      MTO(R,Z,EE);                                                      4580
      ALFP ← 3.14159265 x RN ;                                          4590
      BTAP ← 3.14159265 x RN ;  %BTAP IS INSIDE ANGLE                   4600
      RZ ← R;      ZZ ← Z;                                              4610
          M ← 0;                                                        4620
        SAP ← SIN(ALFP);                                                4630
        SBP ← SIN (BTAP);                                               4640
        CAP ← COS(ALFP);                                                4650
        CBP ← COS(BTAP);                                                4660
      BHOLA ← ARCSIN (RHOL / RZ);                                       4670
ANHNUB:  HNU ← .511;      N←2;      PLTO←0;                             4680
      K ← 0;                                                            4690
      ALF ← ALFP;                                                       4700
      ALFM ← 1;                                                         4710
      RL ← RZ;      ZL ← ZZ;                                            4720
      PL ← -(LN(1-RN)) / .45  ;                                         4730
         IF BHOLA <ABS(BTAP)  THEN GO TO NAHOLB;                        4740
      PO ← SQRT (( RHOL×RHOL) - (RZ×RZ× SBP×SBP));                      4750
      PLTH ← (( RZ× CBP - PO) / SAP);                                   4760
         IF PL < PLTH THEN GO TO NAHOLB;                                4770
PLTO ← PL + (2× PO / SAP);                                              4780
NAHOLB: IF PLTO > 0 THEN PL ← PLTO;                                     4790
      PLH ← PL x SAP;                                                   4800
      Z ←ZZ - (PL×CAP);                                                 4810
      R ← SQRT ((RZ×RZ) + (  PLH x PLH  ) - (2×RZ× PLH  ×CBP));         4820
REHITH:                                                                 4830
   IF R > RMAX OR ( Z < 0  OR Z > DISTO )  THEN                         4840
BEGIN                                                                   4850
      IF M = 1 THEN GO TO EXPPB;                                        4860
      M ← M + 1;                                                        4870
          GO TO ANHNUB;                                                 4880
END;                                                                    4890
INDETB: IF N ≠ 2 THEN GO TO WORKB;                                      4900
```

```
      SGCO ← 0.435;                                                     4910
      SGPE ← 0.0186;  %REV 9/1/69                                       4920
      SGTO ← 0.4536;  % REV 9/1/69                                      4930
       SA ← SAP;                                                        4940
       SB ← SBP;                                                        4950
       CA ← CAP;                                                        4960
       CB ← CBP;                                                        4970
```

```
WORKB:    RN5 ← RN × SGTO;                                              4980
          IF RN5 < SGCO THEN GO TO SCATAB;                              4990
      PETO ← PETO - 1;                                                  5000
      EE← HNU;                                                          5010
      MTO(R,Z,EE);                                                      5020
         M ← M+1;                                                       5030
         IF M>1 THEN GO TO EXPPB;                                       5040
      ALFP ← 3.14159265 - ALFP ;                                        5050
      BTAP ← BTAP - 3.14159265 ;                                        5060
        CAP ← -CAP;                                                     5070
       SBP ← -SBP;                                                      5080
      CBP ← -CBP;                                                       5090
                GO TO ANHNUB;                                           5100
SCATAB:PROR ← RN5 × SGTO / SGCO;                                        5110
      NUMB ← NUMB + 1;                                                  5120
      SRHNU ← SQRT(HNU);                                                5130
      KN(HNU,THETA);                                                    5140
      CSTHZ ← COS ( THETA / 57.2957795131);                             5150
      SNTHZ ← SIN ( THETA / 57.2957795131);                             5160
         HNUS ← (.511 × ALFM) / (ALFM × (1 - CSTHZ) + 1);               5170
      ALFM ← HNUS / .511;                                               5180
      EE ← HNU - HNUS;                                                  5190
      MTO(R,Z,EE);                                                      5200
     SGCO+0.70355×(((1+ALFM)/(ALFM×ALFM))×((2×(1+ALFM)/(1+2×ALFM))-     5210
               ((LN(1+2×ALFM))/ALFM)) + (LN(1+2×ALFM))/(2×ALFM)-         5220
               ((1+3×ALFM)/((1+2×ALFM)×(1+2×ALFM))));                   5230
      SGPE ← .00263717 / (HNUS * 2.92); %REV 9/1/69                     5240
        SGTO ← SGCO + SGPE;                                             5250
      OA ← ARCOS((R×R + PLH×PLH - RL×RL) /(2×R×PLH));                   5260
         IF OA < 0 THEN OA ← 1.5708 - OA;                               5270
      FEEZ ← 6.2831853 × RN;                                            5280
      A← (SNTHZ × SIN(FEEZ));                                           5290
      B← (SNTHZ × COS(FEEZ));                                           5300
      SRA← SQRT (1- (A×A));                                             5310
      E ← ARCSIN ( B / SRA);                                            5320
      F ← (ALF - E);                                                    5330
      G ← (ALF + E);                                                    5340
      CA ← ((CSTHZ ×CA ) + (SNTHZ × SA  × COS(FEEZ)));                  5350
      ALF ← ARCOS(CA);                                                  5360
      SA ← SIN (ALF);                                                   5370
       BETA ← ARCSIN (-A / SA);                                         5380
        IF A > 0  THEN KOR ← -3.14159265359  ELSE KOR ← 3.14159265359;  5390
    IF THETA <  90   AND  F<0                THEN BETA ← (KOR -BETA);   5400
    IF THETA <  90   AND  F > 3.1415926536 THEN BETA ← (KOR -BETA);     5410
    IF THETA >  90   AND (G>0 AND G<3.14159) THEN BETA←(KOR-BETA);      5420
      BETA ← BETA + SING × OA;                                          5430
       IF BETA < -3.14159 THEN BETA ← (6.2832 + BETA) ELSE              5440
        IF BETA > 3.14159 THEN BETA ← -(6.2832 - BETA);                 5450
      BITA ← 3.14159 - ABS(BETA);                                       5460
         CB ← COS (BITA);   SB ← SIN (BITA);                            5470
       IF BETA < 0 THEN SING ← (-1) ELSE SING ← +1;                     5480
       PL ← -(LN(1 - RN)) / SGTO;                                       5490
        PLTO ← 0;                                                       5500
      BHOL ← ARCSIN(RHOL / R);                                          5510
        IF BHOL < BITA THEN GO TO NSHOLB;                               5520
      PO ← SQRT((RHOL×RHOL) - (R×R × SB×SB));                           5530
      PLTH ← ((R×CB - PO) / SA);                                        5540
        IF PL < PLTH THEN GO TO NSHOLB;                                 5550
      PLTO ← PL + (2×PO/SA);                                            5560
NSHOLB: IF PLTO > 0 THEN PL ← PLTO;                                     5570
      PLH ← PL×SA;                                                      5580
      RL ←R ;     ZL ← Z;                                               5590
      Z ← Z  - (PL×CA);                                                 5600
      R ← SQRT(( R×R) + (PLH×PLH) - (2×R×PLH×CB));                      5610
       HNU ← HNUS;                                                      5620
      N ← N+1;                                                          5630
                GO TO REHITB;                                           5640
EXPPB:% END OF PAIR PRODUCTION CALCULATION                              5650
END;                                                                    5660
                GO TO NOHNU;                                            5670
                                                                        5680
```

```
%%%%%%%%%%          RECORD PHOTOELECTRIC EVENT  (AFTER FIRST INTERACTION      5690
                                                                               5700
PES;                                                                           5710
PETO + 1;                                                                      5720
     EE + HNU;                                                                 5730
     MTO(R,Z,EE);                                                              5740
              GO TO NUHNU;                                                     5750
                                                                               5760

%%%%%%%%%%      COMPTON INTERACTION CALCULATION (AFTER FIRST INTERACTION      5770
                                                                               5780
COMPTN;                                                                        5790
     NUMB + NUMB + 1;                                                          5800
                                                                               5810
%%%%%%%%%           SELECT SCATTER ANGLE, CALC NEW CROSS SECTIONS             5820
                                                                               5830
     PROB + RN4 * SGTO / SGCO;                                                 5840
     SRHNU + SQRT(HNU);                                                        5850
     KN(HNU,THETA);                                                            5860
     CSTHZ + COS ( THETA / 57.2957795131);                                     5870
     SNTHZ + SIN ( THETA / 57.2957795131);                                     5880
    HNUS + HNU;                                                                5890
         HNU + (.511 * ALFM) / (ALFM * (1 - CSTHZ) + 1);                       5900
     EE + HNUS - HNU;                                                          5910
     MTO(R,Z,EE);                                                              5920
         ALFM + HNU / .511;                                                    5930
   SGCO+0.70355*(((1+ALFM)/(ALFM*ALFM))*((2*(1+ALFM)/(1+2*ALFM))-              5940
              ((LN(1+2*ALFM))/ALFM)) + (LN(1+2*ALFM))/(2*ALFM)-                5950
              ((1+3*ALFM)/((1+2*ALFM)*(1+2*ALFM)))));                          5960
     SGPE + .00263717 / (HNU  + 2.92); %REV 9/1/69                             5970
   IF HNU < 1.02 THEN SGPP + 0  ELSE SGPP + 0.01197*(HNU - 1.02);              5980
      SGTO + SGCO + SGPE + SGPP;                                               5990
     FEEZ + 6.2831853 * RN;                                                    6000
     PLH + PL * SA;                                                            6010
     OA + ARCCOS(( R*R + PLH*PLH - RZ*RZ) / (2 * R * PLH));                    6020
        IF OA < 0 THEN OA + 1.5708 - OA;                                       6030
                                                                               6040
%%%%%%%%%%          COORDINATE TRANSFORMATION                                 6050
                                                                               6060
     A+ (SNTHZ * SIN(FEEZ));                                                   6070
     B+ (SNTHZ * COS(FEEZ));                                                   6080
     SRA+ SQRT (1- (A*A));                                                     6090
        E + ARCSIN ( B / SRA);                                                 6100
     F + (ALF - E);                                                            6110
     G + (ALF + E);                                                            6120
     CA + ((CSTHZ *CA ) + (SNTHZ * SA  * COS(FEEZ)));                          6130
     ALF + ARCCOS(CA);                                                         6140


     SA + SIN (ALF);                                                           6150
      BETA + ARCSIN (-A / SA);                                                 6160
        IF A > 0  THEN KOR + -3.14159265359  ELSE KOR + 3.141592653591;        6170
   IF THETA <  90   AND  F<0              THEN BETA + (KOR -BETA);             6180
   IF THETA <  90   AND  F > 3.1415926536 THEN BETA + (KOR -BETA);             6190
   IF THETA >  90   AND (G>0 AND G<3.14159) THEN BETA+(KOR-BETA);              6200
     BETA + BETA + SING * OA;                                                  6210
       IF BETA < -3.14159 THEN BETA + (6.2832 + BETA) ELSE                     6220
       IF BETA > 3.14159 THEN BETA + -(6.2832 - BETA);                         6230
     BITA + 3.14159 - ABS(BETA);                                               6240
      CB + COS(BITA);      SB + SIN (BITA);                                    6250
       IF BETA < 0 THEN SING + (-1) ELSE SING + +1;                            6260
                 GO TO NUHIT;                                                  6270
                                                                               6280
```

```
%%%%%%%%%%     MONTE CARLO RUN FINISHED, LIST RESULTS, TEST TAPE  DATA      6290
                                                                            6300
TALLY;                                                                      6310
   TIMM (DMWD,1);%                                                          6320
      PEZTO + SANPE x (NUSTO - EZIT);                                       6330
      NUSTO + NUSTO + PEZTO;                                                6340
      NTOTL + NUSTO x (1/(1 - MTF1 - MFTO));                                6350
      NUSTO + NUSTO - EZIT;                                                 6360
      PASS + EZTT + NTOTL x MTF1;                                           6370
      ENCO + ENCO / ONECO;                                                  6380
  WRITE(DMWD,TFMB,HNUZ,RHOLE,RMAX,D,THIK);                                  6390
  WRITE(DMWD,TFMC,NUSTO,PASS,PEZTO,ONECO,ENCO,J,NTOTL×MFHOL,                6400
        NTOTL×(1- MFHOL - MFTO),NTOTL);                                     6410
      REWIND(MTFL);                                                         6420
        WRITE(DMWD[PAGE]);                                                  6430
        FOR L + 1 STEP 1 UNTIL 60 DO                                        6440
BEGIN                                                                       6450
      READ (MTFL,1023,AR[*]);                                               6460
      READ (MTFL,1023,AZ[*]);                                               6470
      READ (MTFL,1023,AE[*]);                                               6480
        FOR M + 0 STEP 1 UNTIL 10 DO                                        6490
      WRITE (DMWD,FMB,M,AR[M],AZ[M],AE[M]);                                 6500
END;                                                                        6510
NOMO:                                                                       6520
END.                                                                        6530
%DATA KRD                                                                   6540
  1.836130    .450      1.550      1.600      1.800      100                6550
```

INCIDENT ENERGY(MEV)= 0.320080

SOURCE TO DETECTOR DISTANCE(CM)= 1.600

RHOLE(CM)= 0.350 RMAX(CM)= 1.550

DETECTOR THICKNESS(CM)= 1.800

NUMBER INTERACTING IN DETECTOR = 42393

NUMBER PASSING THROUGH DETECTOR = 63640

NUMBER OF PHOTOELECTRIC FIRST EVENTS = 5558

NUMBER ESCAPING AFTER ONE COMPTON EVENT = 19432

AVERAGE ENERGY LOSS FOR ONE COMPTON ONLY (MEV)= 0.080211

NUMBER INTERACTING TWO OR MORE TIMES = 17403

NUMBER PASSING THROUGH HOLE = 2016

NUMBER OUTSIDE DETECTOR SOLID ANGLE = 658910

TOTAL NUMBER OF PHOTONS FROM SOURCE = 766959

	R	Z	ENERGY	
0	0.000000	0.000000	0.000000	
1	1.506575	2.472781	0.168535	
2	1.450947	2.369530	0.151545	
3	-1.000000	1.000000	1.000000	(PRINTOUT OF FIRST TEN DATA
4	0.889622	1.801160	0.132032	
5	0.670218	2.270963	0.016673	SETS OF EACH 1024-SET
6	0.682243	2.299191	0.171375	BLOCK FROM TAPE)
7	-1.000000	2.000000	1.000000	
8	1.332569	2.757221	0.132524	
9	1.261016	2.771167	0.005451	
10	1.278265	2.769155	0.064008	
0	0.532750	1.935971	0.143424	
1	-1.000000	1.000000	1.000000	
2	0.835198	1.901031	0.062175	
3	1.207504	2.303180	0.102859	
4	-1.000000	2.000000	0.000000	
5	0.510906	1.604949	0.042192	
6	0.541563	1.623989	0.016178	
7	1.248893	1.754294	0.025893	
8	-1.000000	3.000000	0.000000	
9	0.566147	2.038530	0.046911	
10	0.646104	2.594866	0.049951	
0	1.071532	3.154830	0.093248	
1	0.575866	3.176914	0.009472	
2	0.562370	3.167555	0.023944	
3	0.569935	3.214303	0.088457	
4	-1.000000	4.000000	1.000000	
5	1.172061	2.012457	0.008768	
6	1.262759	2.268572	0.116385	
7	-1.000000	2.000000	0.000000	
8	0.354040	2.098158	0.032411	

Listing of Program "DCTAL" (Reads Output Tape from "DC3")

```
%COMPILE XXXXXX/DCTAL   ALGOL          .01E600904          WALKER D M          0
%PROCESS=030;   ID=030                                                        10
%COMMENT    TAPE   TAPE IN "PD6629"  #880                                     20
%DATA.                                                                        30
BEGIN                                                                         40
                                                                              50
%%%%%%%%%%          DECLARATIONS                                              60
                                                                              70
FILE IN KRD (2,10);                                                           80
FILE OUT DMWD 15(2,15);                                                       90
FILE IN MTFL 2 "PD6629"(2,1023,1023);                                        100
REAL  HNUZ,RHOLE,RMAX,D,THIK,DLAD,DLAI,DLBI,DLBD,EEA,EFB;                    110
REAL GAUSIT,P0,P1,P2,P3,P4,P5,COUNTS;                                        120
REAL  ALOW,AUP,BLOW,BUP;                                                     130
INTEGER NUSTO,KEVCH,ADRES,LASCH,I,J,K,L;                                     140
INTEGER SA,SB;                                                               150
INTEGER AMP,BMP;                                                             160
INTEGER A1,GA1, GB1,FA1,FB1;                                                 170
SAVE INTEGER ARRAY SPECA,SPECB,SPECT[0:1022];                                180
SAVE INTEGER ARRAY EADIS,EBDIS,FADIS,FBDIS[0:60];                            190
SAVE INTEGER ARRAY NODIS[0:20];                                              200
SAVE INTEGER ARRAY GSPEC[0:1022];                                            210
SAVE INTEGER ARRAY MPAB[0:30,0:30];                                          220
SAVE REAL ARRAY ELOSS[0:60];                                                 230
SAVE REAL ARRAY AR,AZ,AE[0:1022];                                            240
LABEL  ARRIN,TALLY, TELLY,RESET;                                             250
LABEL EXIT;                                                                  260
LABEL RERUN;                                                                 270
$ CARD
$$ A 4100                                                                     0
   WRITE (FILE[OBL],15,A[*]);%                                            16400
                                                                       99999999
$ CARD LIST
LIST ED(FOR K ← 0 STEP 1 UNTIL 39 DO ELOSS[K]);                              280
LIST  ND(FOR K ← 0 STEP 1 UNTIL 19 DO NODIS[K]);                             290
LIST  LSPCA(K,FOR L ← 0 STEP 1 UNTIL 9 DO SPECA[K+L]);                       300
LIST  LSPCB(K,FOR L ← 0 STEP 1 UNTIL 9 DO SPECB[K+L]);                       310
LIST  LSPCT(K,FOR L ← 0 STEP 1 UNTIL 9 DO SPECT[K+L]);                       320
LIST LSPCG(K,FOR L ← 0 STEP 1 UNTIL 9 DO GSPEC[K+L]);                        330
LIST LMPAB[K,FOR L←0 STEP 1 UNTIL 24 DO MPAB[K-1,L]);                        340
FORMAT                                                                       350
   FMA(5R10.6,T6),                                                           360
   FMB(/,"INCIDENT ENERGY(MEV)=  ",R10.6,X10,"RHOLE(CM)= ",R7.3,X10,         370
     "RMAX(CM)=  ",R7.3,//,"SOURCE TO DETECTOR DISTANCE(CM)=  ",             380
     R7.3,X10,"DETECTOR THICKNESS(CM)=  ",R7.3),                             390
   FMC(/,"DIMENSIONS FOR DEAD LAYER BOUNDARIES(CM)=  ",4R12.3,//,            400
     "KEV PER CHANNEL FOR SPECTRA =  ",I3),                                  410
   FMD(/,"NUMBER OF PHOTONS SCATTERING TWO OR MORE TIMES = ",I8),            420
   FME("SCATTERING NUMBER DISTRIBUTION",/,10I10,/,10I10),                    430
   FMF("SPECTRUM FOR A-HALF OF DETECTOR",/),                                 440
   FMG(I5,5I10,X5,5I10),                                                     450
   FMH("SPECTRUM FOR B-HALF OF DETECTOR",/),                                 460
   FMI("SPECTRUM FOR DIODE OPERATION OF DETECTOR",/),                        470
   FMJ("DISTRIBUTION OF EVENTS VS ENERGY IN A AND B ,  50 KEV / GROUP",      480
     /,"ENERGY(MEV)",X25,"GOOD EVENTS",X42,"BAD EVENTS",/,X32,"A",X19,       490
     "B",X29,"A",X19,"B"),                                                   500
   FMK(R7.3,X20,I10,X10,I10,X20,I10,X10,I10,/,                               510
          X27,I10,X10,I10,X20,I10,X10,I10,/);                                520
FORMAT  FML(7R10.6),                                                         530
   FMS(//,"WINDOW SETTINGS IN MEV:    A =  ",2R7.3,"    B =  ",2R7.3/),      540
   FMR(/,X10,25I4),                                                          550
   FMQ(/,I5,X5,25I4),                                                        560
   FMP(/,"GOOD FIRST EVENTS IN A,B :   ",2I8,X10,                            570
      "BAD FIRST EVENTS IN A,B :  ",2I8),                                    580
   FMO(////"AVERAGE ENERGY LOSS PER SCATTER / NUMBER OF EVENTS",             590
     /10R10.6,/10R10.6,//10I10,/10I10),                                      600
   FMN(//// "        RUN TERMINATED BY PARITY BIT ERROR" ////),              610
   FMM("SPECTRUM FOR DIODE WITH RESOLUTION FWHM= ",R7.2,/);                  620
```

```
                                                                        630
%%%%%%%%%%          BEGINNING OF COMPUTATION                          640
                                                                        650
WRITE (OMWD[NO1,<" ">);                                                 660
                                                                        670
%%%%%%%%%%           READ CARD INPUT DATA                               680
                                                                        690
READ (KRD,FMA,HNUZ,RHOLE,RMAX,D,THTK,NUSTD) [EXIT];                     700
     READ ( KRD,FML,GAUSIT,P0,P1,P2,P3,P4,P5);                          710
READ (KRD,FMA,ALOW,AUP,BLOW,BUP) [EXIT];                                720
RERUN;                                                                  730
READ (KRD,FMA,DLAD,DLAT,DLBI,DLBO,KEVCH) [EXIT];                        740
BEGIN                                                                   750
                                                                        760
%%%%%%%%%%      INITILIZE ALL ARRAY ELEMENTS TO ZERO                    770
                                                                        780
     J ← L ← 0;                                                         790
     A1 ← GA1 ←GB1 ←FA1 ← FB1 ← 0;                                      800
   FOR I ← 0 STEP 1 UNTIL 1022 DO                                       810
BEGIN                                                                   820
     SPECA[I] ← SPECB[I] ← SPECT[I] ← GSPEC[I] ← 0;                     830
     AR[I] ← AZ[I] ← AE[I] ← 0;                                         840
END;                                                                    850
   FOR I ← 0 STEP 1 UNTIL   60 DO                                       860
     EADIS[I] ← EBDIS[I] ← EADTS[I]  ← EBDIS[I] ← 0;                    870
   FOR I ← 0 STEP 1 UNTIL   20 DO                                       880
     NODIS[I] ← 0;                                                      890
   FOR K ← 0 STEP 1 UNTIL 25 DO                                         900
   FOR I ← 0 STEP 1 UNTIL 25 DO                                         910
     MPAB[K,I] ← 0;                                                     920
ARRIN;                                                                  930
                                                                        940
%%%%%%%%%%        READ ONE RECORD BLOCK FROM TAPE (1024 DATA SETS)      950
                                                                        960
       READ(MTFL,1023,AR[*]) [TALLY;TELLY];                             970
       READ(MTFL,1023,AZ[*]) [TALLY;TELLY];                             980
       READ(MTFL,1023,AE[*]) [TALLY;TELLY];                             990
   FOR I ← 0 STEP 1 UNTIL 1022 DO                                       1000
                                                                        1010
%%%%%%%%%%          TEST FOR END OF A SEQUENCE                        1020
                                                                        1030
BEGIN                                                                   1040
   IF AR[I] < 0 THEN                                                    1050
BEGIN                                                                   1060
     J ← J + 1;                                                         1070
     ADRES ← EEA × 1000/KEVCH;                                          1080
     NODIS[AZ[I]] ← NODIS[AZ[I]] + 1;                                   1090
                                                                        1100
%%%%%%%%%%     (YES)  TEST FOR COINCIDENCE, (YES) RECORD DATA IN ARRAYS 1110
                                                                        1120
   IF (SA + SB) < 2 THEN                                                1130
              GO TO RESET;                                              1140
   IF EEA < ALOW OR EEB < BLOW THEN                                     1150
              GO TO RESET;                                              1160
   IF EEA > AUP OR EEB > BUP THEN                                       1170
              GO TO RESET;                                              1180
     AMP ← ADRES × .032;                                                1190
     SPECA[ADRES] ← SPECA[ADRES] + 1;                                   1200
     ADRES ← EEB × 1000/KEVCH;                                          1210
     BMP ← ADRES × .032;                                                1220
     SPECB[ADRES] ← SPECB[ADRES] + 1;                                   1230
     MPAB[AMP,BMP] ← MPAB[AMP,BMP] + 1;                                 1240
     ADRES ← (EEA + EEB)× 1000/KEVCH;                                   1250
     SPECT[ADRES] ← SPECT[ADRES] + 1;                                   1260
   IF (EEA + EEB)≥ (HNUZ - .001) THEN                                   1270
BEGIN                                                                   1280
     ADRES ← ENTIER(EEA/.050);                                          1290
     EADIS[ADRES] ← EADIS[ADRES] + 1;                                   1300
     ADRES ← ENTIER(EEB/.050);                                          1310
     EBDIS[ADRES] ← EBDIS[ADRES] + 1;                                   1320
   IF A1 = 1 THEN GA1 ← GA1 + 1                                         1330
    ELSE GB1 ← GB1 + 1;                                                 1340
END                                                                     1350
```

```
ELSE                                                                    1360
BEGIN                                                                   1370
     ADRES ← ENTIER(EEA/.050);                                          1380
     FADIS[ADRES] ← FADIS[ADRES]  + 1;                                  1390
     ADRES ← ENTIER(EEB/.050);                                          1400
     FBDIS[ADRES] ← FBDIS[ADRES] + 1;                                   1410
   IF A1 = 1 THEN FA1 ← FA1 + 1                                         1420
    ELSE FB1 ← FB1 + 1;                                                 1430
END;                                                                    1440
RESET;                                                                  1450
     SA ← SB ← EEA ← EEB ← 0;                                           1460
     L ← 0;                                                             1470
     A1 ← 0;                                                            1480
END                                                                     1490
ELSE                                                                    1500
BEGIN                                                                   1510
                                                                        1520
%%%%%%%%%%     (NO)  CATALOG SINGLE INTERACTION PER INPUT SPECIFICATIONS 1530
                                                                        1540
     L ← L + 1;                                                         1550
     ELOSS[L] ← ELOSS[L] + AE[I];                                       1560
     ELOSS [L + 20] ← ELOSS[L + 20] + 1;                                1570
   IF AR[I] > DLAO AND AR[I]< DLAI THEN                                 1580
BEGIN                                                                   1590
     EEA ← EEA + AE[I];                                                 1600
     SA ← 1;                                                            1610
   IF L = 1 THEN A1 ← 1;                                                1620
END                                                                     1630
ELSE                                                                    1640
   IF AR[I] > DLBI AND AR[I]< DLBO THEN                                 1650
BEGIN                                                                   1660
     EEB ← EEB + AE[I];                                                 1670
     SB ← 1;                                                            1680
END;                                                                    1690
END;                                                                    1700
END;                                                                    1710
               GO TO ARRIN;                                             1720
TELLY:   WRITE(DMWO,FMN);                                               1730
TALLY:                                                                  1740
                                                                        1750
%%%%%%%%%%          WRITE SUMMARY OF TABULATED DATA                   1760
                                                                        1770
          REWIND (MTFL);                                                1780
       WRITE(DMWO,FMB,HNUZ,RHOLE,RMAX,D,THIK);                          1790
       WRITE(DMWO,FMC,DLAO,DLAI,DLBI,DLBO,KEVCH);                       1800



       WRITE(DMWO,FMD,J);                                               1810
WRITE(DMWO,FMP,GA1,GB1,FA1,FB1);                                        1820
WRITE (DMWO,FMS,ALOW,AUP,BLOW,BUP);                                     1830
       WRITE(DMWO,FME,ND);                                              1840
          FOR I ← 1 STEP 1 UNTIL 20 DO                                  1850
          ELOSS[I] ← ELOSS[I] /(ELOSS[I + 20] + .001);                  1860
       WRITE(DMWO,FMD,ED);                                              1870
       WRITE(DMWO [PAGE]);                                              1880
          LASCH ←(10 + HNUZ × 1000 / KEVCH);                            1890
       WRITE(DMWO,FMF);                                                 1900
       FOR K ← 0 STEP 10 UNTIL LASCH DO                                 1910
       WRITE(DMWO,FMG,LSPCA);                                           1920
       WRITE(DMWO [PAGE]);                                              1930
       WRITE(DMWO,FMH);                                                 1940
       FOR K ← 0 STEP 10 UNTIL LASCH DO                                 1950
       WRITE(DMWO,FMG,LSPCB);                                           1960
       WRITE(DMWO [PAGE]);                                              1970
       WRITE(DMWO,FMI);                                                 1980
       FOR K ← 0 STEP 10 UNTIL LASCH DO                                 1990
       WRITE(DMWO,FMG,LSPCT);                                           2000
       IF GAUSIT > 0 THEN                                               2010
                                                                        2020
```

```
%%%%%%%%%%      APPLY ENERGY RESOLUTION TO SPECTRA
BEGIN
   FOR I ← 5 STEP 1 UNTIL LASCH DO
BEGIN
     COUNTS ← P0 × SPECT[I] +
              P1 × (SPECT[I+1] + SPECT[I-1]) +
              P2 × (SPECT[I+2] + SPECT[I-2]) +
              P3 × (SPECT[I+3] + SPECT[I-3]) +
              P4 × (SPECT[I+4] + SPECT[I-4]) +
              P5 × (SPECT[I+5] + SPECT[I-5]) ;
     GSPEC[I] ← COUNTS;
END;
       WRITE(DMWD [PAGE]);
       WRITE(DMWD,FMM,GAUSIT);
   FOR K ← 0 STEP 10 UNTIL LASCH DO
       WRITE(DMWD,FMG,LSPCG);
END;
       WRITE(DMWD [PAGE]);
       WRITE(DMWD,FMJ);
     FOR K ← 0 STEP  2 UNTIL (HNU7 × 20.1)  DO
    WRITE (DMWD,FMK,(K×.05),FADIS[K],FBDIS[K],FADIS[K],FBDIS[K],
       FADIS[K+1],FBDIS[K+1],FADIS[K+1],FBDIS[K+1]);
              WRITE (DMWD [PAGE]);
   FOR K ← 25 STEP -1 UNTIL 1 DO
       WRITE(DMWD,FMQ,LMPAR);
       WRITE ( DMWD,FMR,FOR L ← 1 STEP 1 UNTIL 25 DO L);
              WRITE(DMWD [PAGE]);
              GO TO RERUN;
EXIT;
END;
   TIMM (DMWD,1);%
END OF PROGRAM .
%DATA KRD
   .661635    .000000  2.2        1.0        4.0       12345
  3.0         .568      .207       .009       .0         .0          .0
   .000     10.0         .000    10.0
   .400      1.5        1.5       2.17       2.00
```

Sample of Output from Program "DCTAL"

```
INCIDENT ENERGY(MEV)=    0.661635  RHOLE(CM)=   0.000          RMAX(CM)=    2.200
SOURCE TO DETECTOR DISTANCE(CM)=    1.000  DETECTOR THICKNESS(CM)=    4.000
DIMENSIONS FOR DEAD LAYER BOUNDARIES(CM)= 0.100      1.300      1.400      2.170
KEV PER CHANNEL FOR SPECTRA =   2
NUMBER OF PHOTONS SCATTERING TWO OR MORE TIMES =    15791
GOOD FIRST EVENTS IN A,B :  1377     913   BAD FIRST EVENTS IN A,B :  2245     579

WINDOW SETTINGS IN MEV:   A =    0.000 10.000   B =    0.000 10.000

SCATTERING NUMBER DISTRIBUTION
        0      2178      7819      3610      1412       549       171        41
        0         0         0         0         0         0         0         0

AVERAGE ENERGY LOSS PER SCATTER / NUMBER OF EVENTS
 0.000000  0.274933  0.152184  0.109130  0.086020  0.086300  0.083061  0.081796  0.0748
 0.052162  0.000000  0.000000  0.000000  0.000000  0.000000  0.000000  0.000000  0.0000
        0     15792     15792      8319      4093      1728       631       199
        1         0         0         0         0         0         0         0
```

DISTRIBUTION OF EVENTS VS ENERGY IN A AND B , 50 KEV / GROUP

ENERGY(MEV)	GOOD EVENTS A	GOOD EVENTS B	BAD EVENTS A	BAD EVENTS B
0.000	84	7	465	607
	105	20	380	414
0.100	140	135	358	355
	341	190	305	308
0.200	380	234	254	251
	222	186	242	192
0.300	201	189	256	172
	178	222	229	192
0.400	236	320	197	147
	203	398	95	141
0.500	158	177	39	27
	33	102	3	13
0.600	8	89	1	5
	1	21	0	0

15	0	0	0	0	0	0	0	0	0	0	0	0	0	0	0
14	0	0	0	0	0	0	0	0	0	0	0	0	0	0	0
13	0	0	0	0	0	0	0	0	0	0	0	0	0	0	0
12	0	0	0	0	0	0	0	0	1	0	0	0	0	0	0
11	0	6	0	0	0	0	0	0	0	0	0	0	0	0	0
10	2	15	68	0	0	0	0	0	0	0	0	0	0	0	0
9	27	18	95	109	0	0	0	0	0	0	0	0	0	0	0
8	61	59	19	123	152	0	0	0	0	0	0	0	0	0	0
7	61	88	58	22	116	160	0	0	0	0	0	0	0	0	0
6	42	83	64	47	12	92	155	0	0	0	0	0	0	0	0
5	32	63	45	56	43	10	152	218	0	0	0	0	0	0	0
4	42	47	43	48	54	42	12	249	244	0	0	0	0	0	0
3	24	43	56	61	51	47	43	33	136	126	0	0	0	0	0
2	15	38	48	37	57	44	69	81	38	66	79	0	0	0	0
1	10	13	16	25	20	21	45	72	34	4	55	6	0	0	0
	1	2	3	4	5	6	7	8	9	10	11	12	13	14	15

SPECTRUM FOR A-HALF OF DETECTOR

0	13	25	23	23	18	22	31	24	20	25
10	17	21	22	24	20	26	25	18	24	17
20	19	20	25	18	21	16	20	16	21	13
30	32	21	12	18	19	21	20	17	19	15
40	23	28	17	17	19	16	19	20	21	25
50	12	16	20	17	22	16	21	17	19	17
60	21	20	19	25	20	24	20	26	21	20
70	20	17	22	19	24	24	17	27	21	16
80	22	26	21	24	22	10	21	24	18	33
90	19	25	23	51	39	27	34	48	27	25
100	30	35	36	28	35	27	24	33	27	17
110	19	28	18	26	23	26	22	16	28	28
120	19	25	18	18	29	19	25	24	23	13
130	12	14	24	21	28	27	19	19	21	17
140	10	14	22	16	18	19	11	18	14	22
150	9	20	20	25	24	25	19	18	17	16
160	27	20	16	18	11	17	18	17	15	19
170	13	17	22	13	21	12	14	13	20	22
180	13	12	17	22	16	14	16	19	16	16
190	14	17	14	17	16	13	15	21	20	18
200	15	15	17	27	17	13	21	17	23	15
210	19	12	24	17	25	13	17	12	16	14
220	21	15	18	15	13	15	16	10	10	14
230	15	8	12	11	12	9	4	16	8	13
240	10	10	15	11	11	14	13	15	18	13
250	6	9	10	7	10	7	1	18	11	9
260	7	10	6	13	6	10	3	17	4	4
270	7	10	5	6	3	3	3	1	2	4
280	3	1	1	5	1	0	3	1	1	0
290	2	1	2	0	1	0	0	1	1	0
300	0	0	0	0	1	0	1	0	1	1
310	1	0	1	2	0	1	0	0	0	0
320	0	0	0	0	0	0	0	0	0	0
330	0	1	0	0	0	0	0	0	0	0
340	0	0	0	0	0	0	0	0	0	0

SPECTRUM FOR B-HALF OF DETECTOR

0	13	28	32	29	28	22	27	22	19	20
10	27	25	22	34	18	16	31	31	24	13
20	27	25	29	21	23	12	20	31	23	26
30	11	23	21	16	20	16	13	12	17	14
40	11	14	14	20	16	18	11	18	19	20
50	14	16	15	14	6	25	12	21	24	17
60	26	18	15	20	25	15	28	28	21	14
70	24	26	24	20	22	13	23	19	17	24
80	23	19	24	18	25	18	19	17	27	27
90	13	22	23	19	17	16	13	20	17	22
100	20	19	19	15	17	19	25	14	14	23
110	27	22	20	26	23	17	22	23	19	14
120	24	18	14	17	12	17	13	15	19	19
130	12	12	23	17	17	14	18	12	16	10
140	15	9	12	11	14	16	14	22	21	15
150	15	11	22	14	11	13	19	22	10	15
160	14	14	17	10	15	10	14	9	10	16
170	13	17	14	17	17	17	12	17	19	20
180	19	20	12	13	16	18	13	15	15	15
190	11	13	19	12	10	18	26	28	14	21
200	16	9	15	15	18	16	14	20	19	12
210	18	17	26	20	14	24	20	17	22	14
220	27	20	19	25	21	30	15	24	24	30
230	38	30	27	34	48	33	33	33	33	16
240	12	12	16	13	9	8	11	5	7	12
250	14	17	12	7	12	8	13	8	6	8
260	4	10	11	7	11	6	6	8	13	4
270	3	2	4	5	4	7	6	5	1	8
280	4	6	7	4	6	6	7	4	4	3
290	9	6	2	4	5	4	3	5	4	0
300	3	8	2	4	3	4	7	5	4	7
310	2	2	0	3	7	4	3	3	4	3
320	5	2	3	4	2	3	2	5	5	4
330	1	1	0	0	0	0	0	0	0	0
340	0	0	0	0	0	0	0	0	0	0

SPECTRUM FOR DIODF OPERATION OF DETECTOR

0	0	0	1	1	0	0	1	0	0	0
10	0	0	1	2	1	1	1	1	1	1
20	1	1	1	2	0	1	1	3	1	2
30	2	0	2	1	5	1	1	3	3	1
40	0	4	2	2	0	2	0	4	3	0
50	1	1	3	1	2	3	2	3	2	1
60	1	7	3	4	2	2	4	1	2	6
70	2	5	4	3	2	5	5	4	2	4
80	4	4	1	4	2	7	3	14	9	6
90	7	7	7	12	1	7	9	8	4	7
100	10	8	9	5	7	8	6	7	6	6
110	11	8	8	9	6	8	5	8	10	7
120	5	8	8	11	3	5	11	11	10	14
130	5	7	10	3	3	11	10	14	5	8
140	5	12	8	10	10	11	7	7	7	20
150	13	10	16	8	9	10	6	15	9	13
160	14	6	12	9	7	7	11	11	10	11
170	7	9	15	12	12	10	15	17	10	16
180	16	13	10	10	11	13	15	19	9	10
190	14	14	18	14	13	19	15	13	15	8
200	10	17	16	18	16	20	24	19	19	22
210	19	18	17	17	17	21	18	19	22	17
220	11	22	17	24	21	23	16	16	19	17
230	21	16	16	13	20	16	16	24	13	17
240	24	15	28	18	25	19	17	13	16	17
250	16	19	12	10	20	14	14	25	16	12
260	20	13	17	15	22	16	11	6	13	14
270	7	3	12	8	10	11	11	6	2	7
280	8	3	7	3	4	5	6	3	6	4
290	3	2	1	1	2	3	5	4	2	3
300	3	4	5	4	6	9	5	4	8	4
310	3	1	3	6	8	5	3	4	6	5
320	3	2	7	6	8	3	3	7	9	7
330	9	2288	0	0	0	0	0	0	0	0
340	0	0	0	0	0	0	0	0	0	0

SPECTRUM FOR DIODF WITH RESOLUTION FWHM= 3.00

0	0	0	0	0	0	0	1	0	0	0
10	1	0	1	2	1	0	1	2	1	1
20	0	1	1	1	0	2	1	2	3	2
30	1	1	1	2	3	1	1	2	3	1
40	1	3	2	2	1	3	2	3	3	1
50	1	1	2	2	2	2	3	3	2	1
60	2	5	5	4	2	2	5	2	3	4
70	3	4	4	3	3	5	5	4	3	4
80	4	3	2	3	3	5	6	11	9	7
90	4	7	8	3	5	6	8	7	6	7
100	6	9	8	6	7	7	7	8	6	7
110	6	9	8	8	7	7	6	7	9	7
120	6	7	9	8	9	7	10	11	11	11
130	7	7	8	9	5	9	11	11	8	7
140	7	10	9	10	10	10	8	7	10	16
150	14	12	13	10	9	8	9	12	11	12
160	12	9	10	9	9	8	10	11	10	10
170	8	10	13	13	12	12	14	15	13	15
180	15	13	11	10	11	13	15	16	11	11
190	13	15	16	15	15	17	15	14	13	10
200	11	15	17	17	17	20	22	20	20	21
210	10	18	17	17	18	19	19	19	20	17
220	15	19	19	22	22	19	18	17	18	18
230	19	17	15	15	18	21	18	20	16	18
240	21	20	23	22	22	17	17	15	16	17
250	17	17	13	13	17	15	16	21	18	15
260	17	15	16	16	18	16	11	9	12	12
270	8	6	9	9	10	11	10	6	4	6
280	7	5	5	4	4	5	5	5	6	5
290	3	2	1	1	2	3	4	4	3	3
300	3	4	5	5	6	7	6	7	7	5
310	3	2	3	5	7	5	5	6	6	5
320	3	3	6	7	7	5	6	7	8	28
330	480	1302	474	21	0	0	0	0	0	0
340	0	0	0	0	0	0	0	0	0	0

APPENDIX II

SUPPLEMENTAL INFORMATION ON THE EXPERIMENTAL PROGRAM

The Instrumentation

The specific instrumentation used for the sum-coincidence and two-parameter experiments is listed in Table 19, and a photograph of all instrumentation is given in Figure 44. This information is provided so that any portion of the research described in this thesis may be reexamined at any future time.

Operation of the Sum-Coincidence System

Several factors are observed to be of importance for effective sum-coincidence operation of the electronics system. The linear signals into the sum amplifier must not only be carefully balanced for zero setting and gain, but the signals must have very nearly the same waveshape. If the waveshapes are dissimilar, the waveform of the sum signal will vary according to the fractional component of each input signal, and error may be introduced into the pulse height analysis. For leading-edge triggering of the single channel analyzers, the risetime of the pulses from each amplifier must also be matched to preserve the coincidence overlap.

System timing is observed to be very critical for assuring that each true coincidence is registered and yet that system resolution and counting rate are not degraded. It was necessary to measure the signal transit time, triggering level, and pulse rise and fall times for each

Table 19. Instruments Used in the Sum-Coincidence Spectrometer System

Instrument	Manufacturer	Model No.	Serial No.
Detector	Emory University	SCS #3	----
Preamp "A"	Canberra	1408 A/B	68941
Preamp "B"	Tennelec	TC-135	2
Amplifier "A"	Ortec	485	328
Amplifier "B"	Ortec	485	379
SCA "A"	Canberra	1435	58290
SCA "B"	Canberra	1435	58289
Coincidence Gate	Nuclear Chicago	27351	51
Gate & Delay Generator	Ortec	416	412
Sum Amplifier	Ortec	433	137
Delay Amplifier	Ortec	427	323
Multichannel Analyzer	Nuclear Data	ND2200	6416
HV Supply (dual)	Ortec	428	341
Nim Bin Supply	Tennelec	TB-1	68
Nim Bin Supply	Hamner	NH84A	706012 2AS
Teletype	Teletype Corp.	33 TU	----
Pulser	Tennelec	TC800	43
Oscilloscope	Tektronik	555	9110
	Two-Parameter Equipment		
Pulse Height Anal. "A"	TMC	210B	ARC 26
Pulse Height Anal. "B"	TMC	210B	ARC 27
Program Unit	TMC	243	ARC 28
Multichannel Analyzer	TMC	CN1024	
Display Control	TMC	240	
Data Output Unit	TMC	220C	
Display Scope	Tektronik	503	

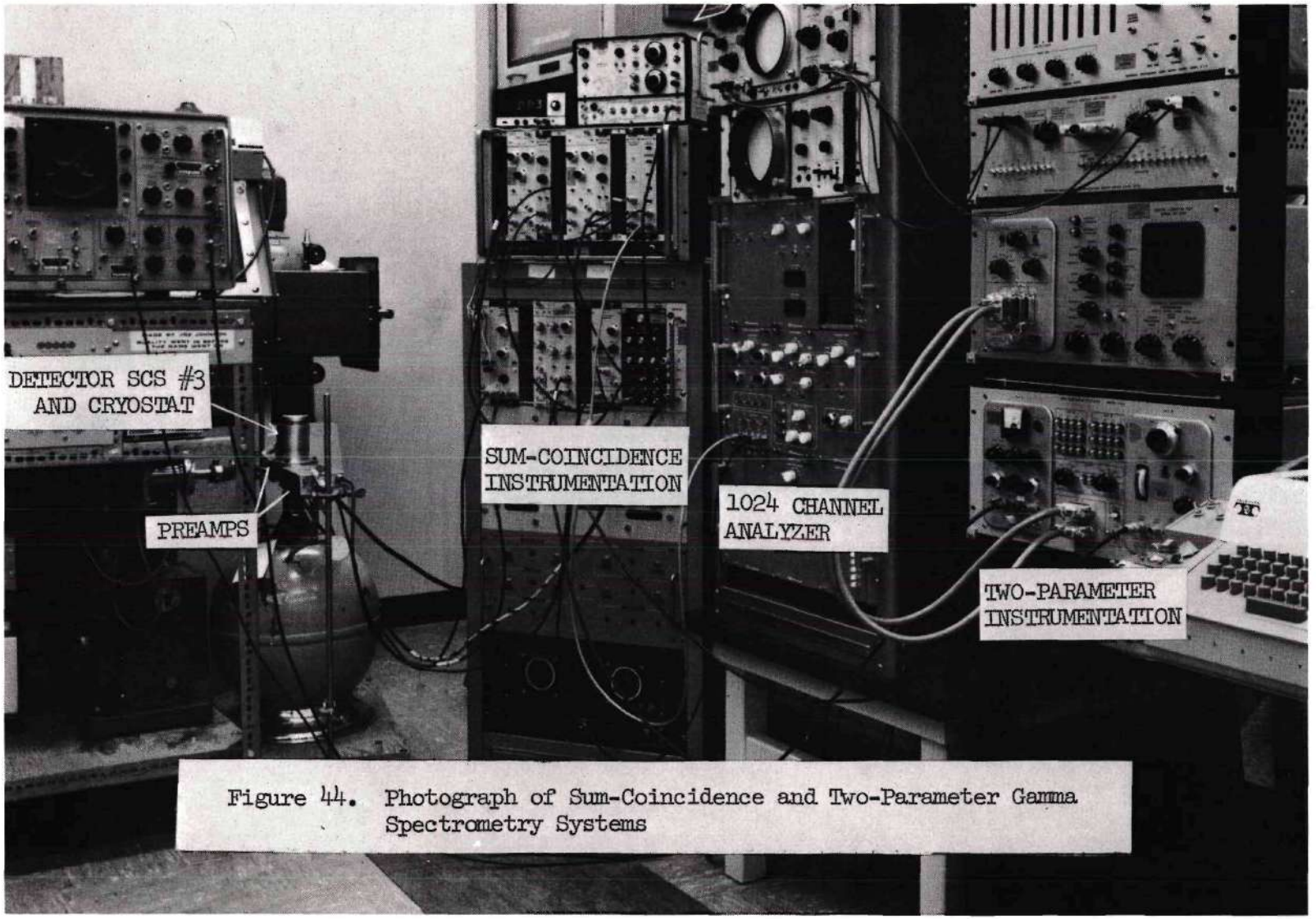

Figure 44. Photograph of Sum-Coincidence and Two-Parameter Gamma Spectrometry Systems

electronic module in order to "fine tune" the system for stable sum-coincidence performance with minimum FWHM resolution.

Initial measurements of resolution of the separate detector sections versus bias voltage, counting rate, and wave shaping time constants were made using Hewlett-Packard 5582-A and Canberra 1417 spectroscopy amplifiers. Detector bias voltages of 800 volts, with leakage currents of approximately one to three nanoamperes, were selected as giving suitable charge collection time in the detectors, while at the same time remaining within the ten nanoampere leakage current limit of the preamplifiers. The pulse shaping studies showed that time constants of greater than about three microseconds did not appreciably improve the system resolution.

Because of the pulse shape problem mentioned earlier, the use of identical Ortec 485 general purpose amplifiers was observed to give better sum-coincidence system performance than did use of the two higher quality spectroscopy amplifiers. The lack of fine-gain control on the Ortec 485 amplifiers was overcome by precise balancing of the "A" and "B" signals with the fine balance control on the summing amplifier. For sum-coincidence work, the Ortec 485 amplifiers were operated in the unipolar pulse mode with an output pulse having a maximum at 2.3 microseconds and a pulse duration of approximately 7.0 microseconds.

Both leading-edge and crossover timing from the amplifier output pulse by the single channel analyzers were evaluated. For crossover timing, a bipolar amplifier output pulse with zero crossing at 3.3 microseconds was used. Timing jitter between "A" and "B" signals from the SCA modules was observed to be less for leading-edge timing, therefore this

timing method was selected. The rise time control on the SCA was increased until a stable, single output pulse was obtained for each pulse from the amplifier. This risetime adjustment corresponded to a 3.5 microsecond minimum delay time in the SCA. The 1.0 microsecond wide output pulses from the "A" and "B" SCA modules were matched for maximum time overlap by using the adjustable 1000 nanosecond time delay of the SCA. The total pulse transit and delay time for the linear and logic signals up to the linear gate was approximately 4.5 microseconds and the gate signal pulse width was an additional 5.3 microseconds. The gate pulse was timed to open the gate about 250 nanoseconds before the arrival of the linear signal to prevent the leading edge of the pulse from being cut off by time jitter of the output pulse from the coincidence unit. Gate pulse widths of greater than 6 microseconds caused a deterioration of resolution for sum-coincidence operation of the system.

Calibration of the energy discriminator settings for the SCA's was accomplished by first setting the pulser signal to coincide with detector output for a known energy component. The waveforms of the amplifier and the SCA output pulses for the calibrated pulser signal input were then displayed on the dual beam oscilloscope, with the SCA output triggering both beams. As the discriminator level was adjusted through the pulser energy level, both oscilloscope traces disappeared, thus associating a known energy with a dial setting on the SCA. The calibration procedure was repeated each time the gain of either amplifier was adjusted.

For comparing actual and computed performance of the SCS system, it is essential that every coincident event be recorded without fail by

the experimental system, since the computer model cannot account for events lost in the electronics system. Proper operation of the coincidence circuitry was checked by displaying the coincidence module output on one oscilloscope beam and the sum of the outputs from the "A" and "B" SCA modules on the other beam. When triggering the oscilloscope on the coincidence output, the presence of overlapping "A" and "B" signals only indicated true coincidences were being observed. When triggering on overlapping SCA pulses only, the presence of the coincidence pulse trace with no "baseline" traces indicated that each coincident pulse pair into the coincidence module was producing an output pulse. Stable performance could be achieved by adjusting the pulse delay time in the SCA units and the permissible overlap time in the coincidence module.

Typical spectra recorded with detector SCS #3 are given in Figures 45 through 48. Both sum-only and sum-coincidence spectra are given for four isotopes: chromium-51, cesium-137, cobalt-60, and yttrium-88. The effect of lower-level energy discriminator settings for the sum-coincidence mode may be seen from the plots.

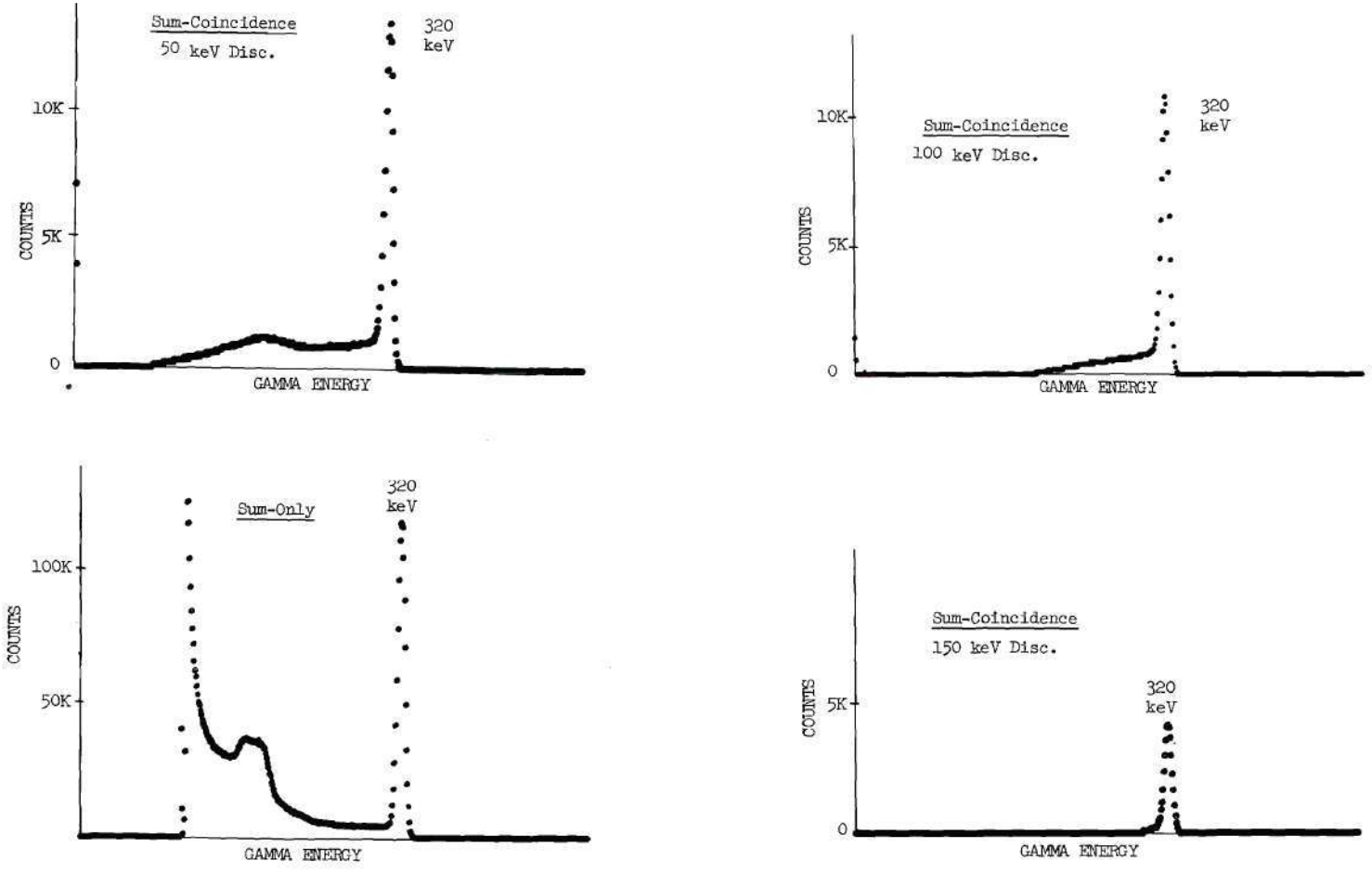

Figure 45. Sum-Coincidence and Sum-Only Energy Spectra for ^{51}Cr as Taken with Detector SCS #3 (4000 second live-time count)

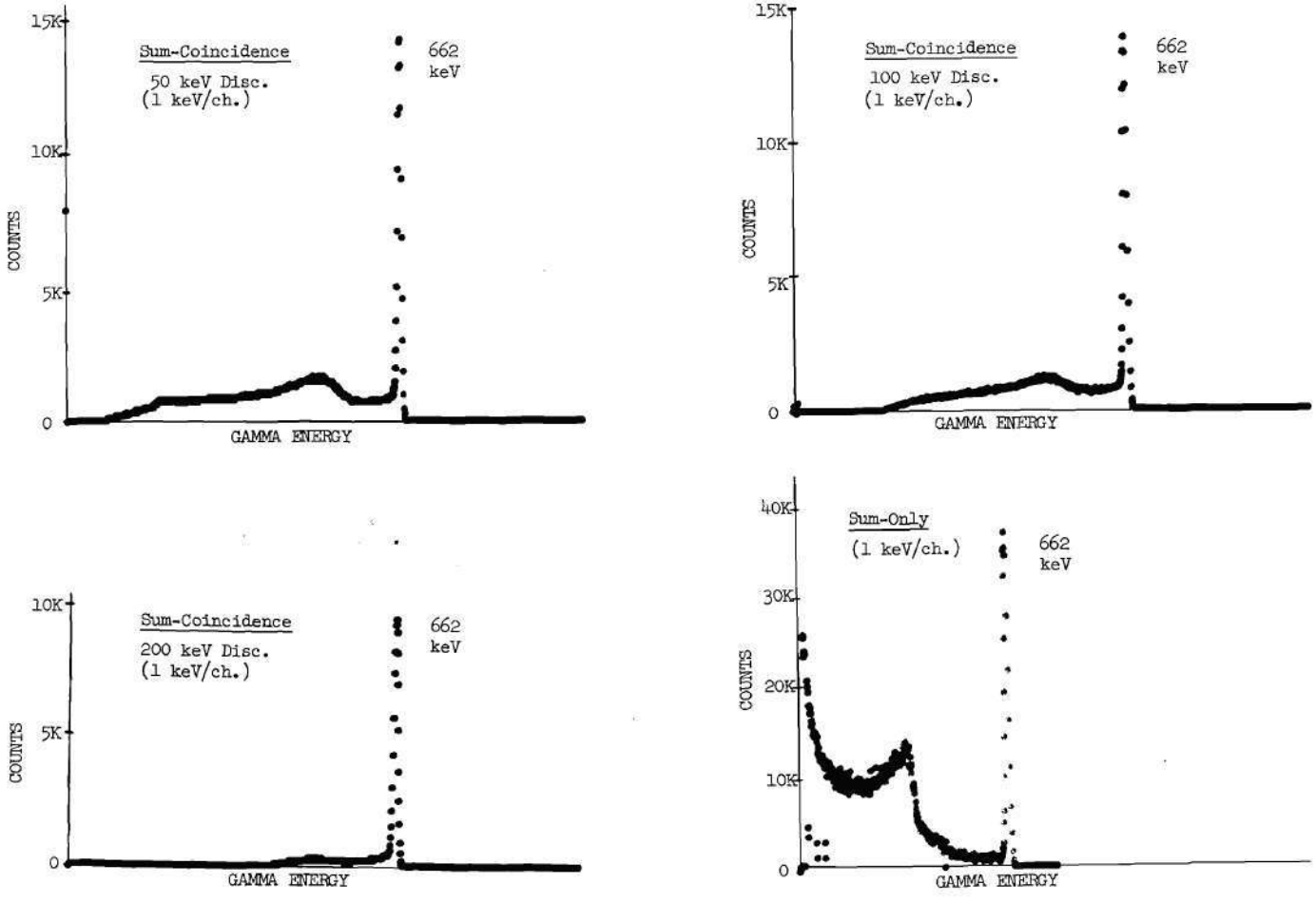

Figure 46. Sum-Coincidence and Sum-Only Energy Spectra for ^{137}Cs as Taken with Detector SCS #3 (8000 second live-time count)

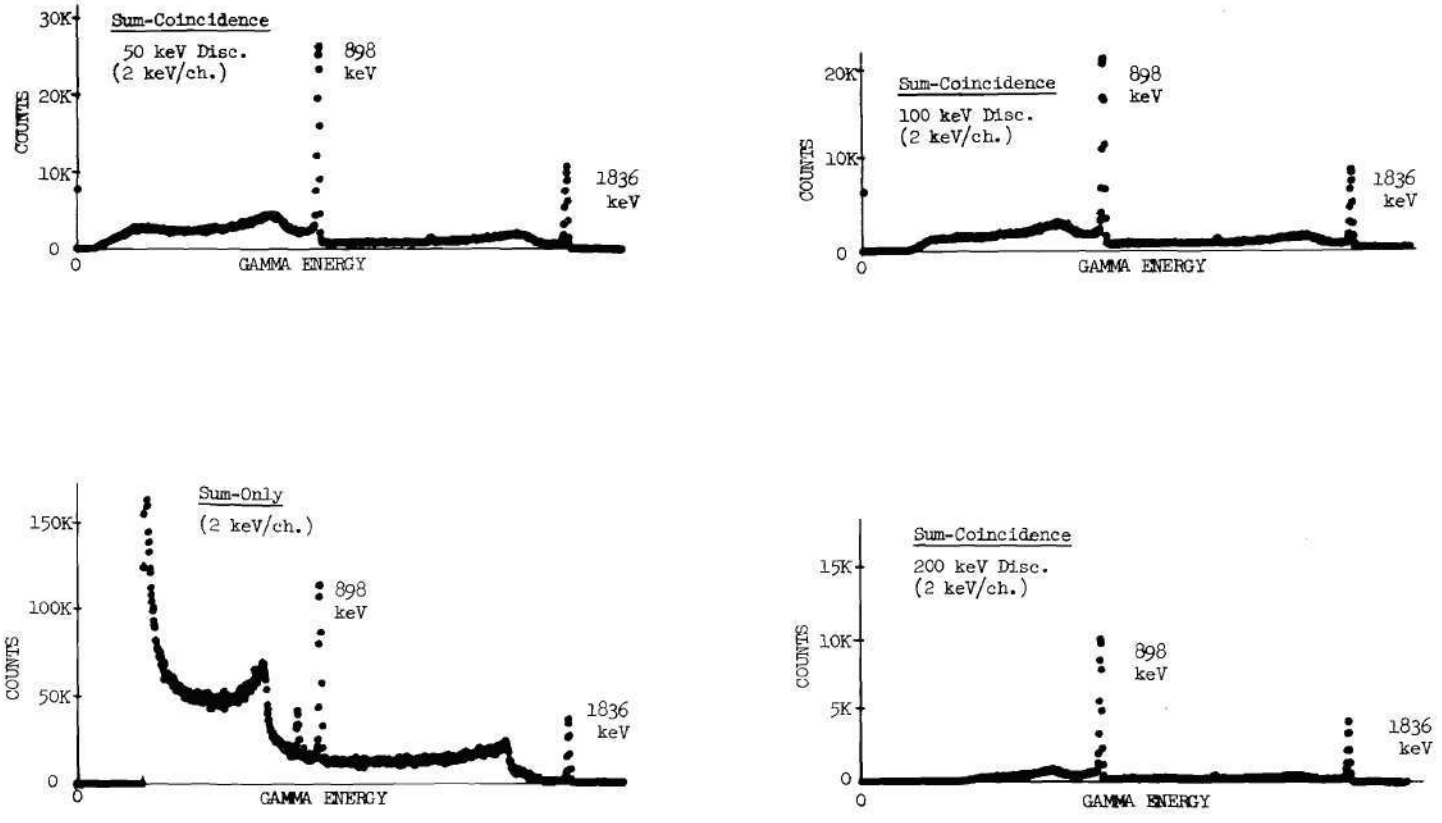

Figure 47. Sum-Coincidence and Sum-Only Energy Spectra for ^{60}Co as Taken with Detector SCS #3 (8000 second live-time count)

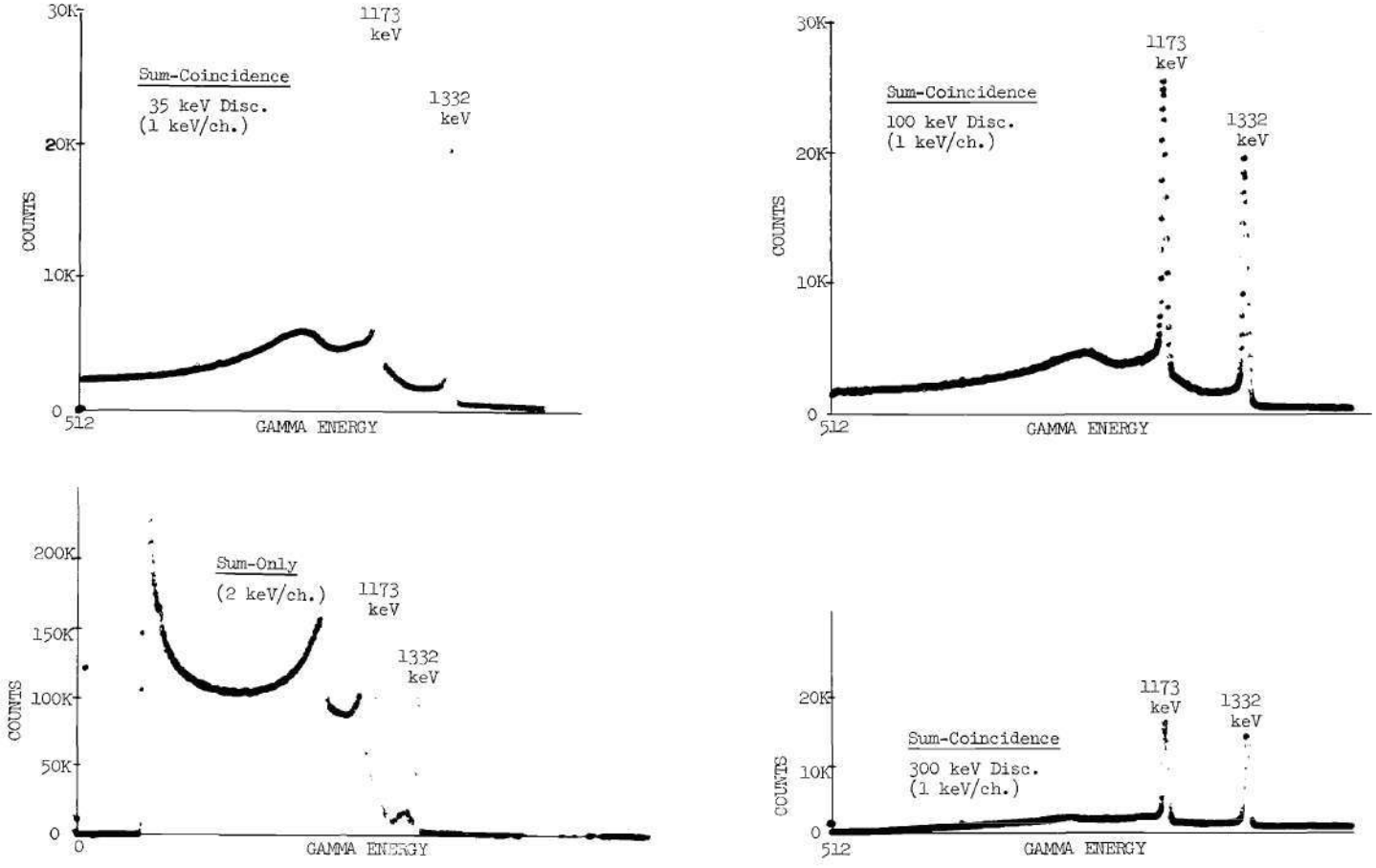

Figure 48. Sum-Coincidence and Sum-Only Energy Spectra for ^{88}Y as Taken with Detector SCS #3 (8000 second live-time count)

BIBLIOGRAPHY*

1. G. T. Ewan and A. J. Tavendale, Can. J. Phys., 43, 2286 (1964).

2. J. M. Hollander, Nucl. Instr. and Meth., 43, 65 (1966).

3. D. C. Camp, USAEC Contractor Report UCRL 50156 (1967).

4. A. J. Haverfield, F. M. Bernthal, and J. M. Hollander, Nucl. Phys., 94, A337 (1967).

5. P. V. Rao, Nucl. Instr. and Meth., 45, 22 (1966).

6. J. Block and D. A. Shirley, Phys. Rev., 143, 911 (1966).

7. E. Matthias, D. A. Shirley, J. S. Evans, and R. A. Newman, Phys. Rev., 140, B264 (1965).

8. J. J. Huntzicker, E. Matthias, S. S. Rosenblum, and D. A. Shirley, USAEC Contractor Report UCRL 11828 (1964).

9. S. Nilsson, IAEA Proc. Panel Vienna, 163 (1966).

10. Ann Ng, R. E. Wood, J. M. Palms, P. V. Rao, and R. W. Fink, Phys. Rev., 176, 1329 (1968).

11. J. R. DeVoe (ed.), Modern Trends in Activation Analysis, NBS Special Publication 312 (1969).

12. Nuclear Activation Techniques in the Life Sciences, Proceedings of the Symposium on Nuclear Activation Techniques in the Life Sciences, Amsterdam, May 8-12, 1967, IAEA, Vienna (1967).

13. S. Buhler and L. Marcus, Nucl. Instr. and Meth., 50, 170 (1967).

14. G. J. Lutz, R. J. Boreni, R. S. Maddock, and W. W. Meinke, Activation Analysis: A Bibliography, NBS Technical Note 467 (1968).

15. J. W. M. DuMond, Rev. Sci. Instr., 18, 626 (1947).

16. K. Siegbahn, in Alpha-, Beta-, and Gamma-Ray Spectroscopy, K. Siegbahn, ed., North Holland Publishing Company, Amsterdam, 1965.

---

*The abbreviations used herein follow the form used in the IEEE Transactions on Nuclear Science, NS-15 (1968).

BIBLIOGRAPHY (Continued)

17. S. C. Curran, in Alpha-, Beta-, and Gamma-Ray Spectroscopy, K. Siegbahn, ed., North Holland Publishing Company, Amsterdam, 1965.

18. P. J. Cambelton, Int. J. Appl. Rad. & Isotopes, 19, 219 (1968).

19. H. Genz, J. P. Renier, and R. W. Fink, USAEC Report ORO-3346-48 (1969).

20. J. B. Birks, The Theory and Practice of Scintillation Counting, Pergamon Press, New York, 1964.

21. J. H. Neiler and P. R. Bell, in Alpha-, Beta-, and Gamma-Ray Spectroscopy, K. Siegbahn, ed., North Holland Publishing Company, Amsterdam, 1965.

22. S. C. Curran and W. R. Baker, Rev. Sci. Instr., 19, 116 (1948).

23. W. J. Price, Nuclear Radiation Detection (2nd ed.), McGraw-Hill Book Company, Inc., New York, 1966.

24. P. J. Van Heerden, The Crystal Counter, a New Instrument in Nuclear Physics (Ph.D. Thesis), Noord-Hollandsche Uitgevers-Mij, Amsterdam (1945).

25. K. G. McKay, Phys. Rev., 76, 1537 (1949).

26. F. J. Walter, J. W. T. Dabbs, L. D. Roberts, and H. W. Wright, USAEC Contractor Report CF 58-11-99 (1958).

27. D. W. Freck and J. Wakefield, Nature, 4816, 669 (1962).

28. See, for example, the April 6, 1970 inventory list of Nuclear Diodes, Inc., Prarie View, Illinois.

29. G. Bertolini, in Semiconductor Detectors, G. Bertoline and A. Coche, eds., North Holland Publishing Co., Amsterdam, 1968.

30. K. L. Swinth, L. D. Philipp, and N. C. Hoitink, IEEE Trans. Nuc. Sci., NS-15, 486 (1968).

31. F. S. Goulding, Nucl. Inst. and Meth., 43, 1 (1966).

32. G. Bertolini and A. Coche (eds.), Semiconductor Detectors, North Holland Publishing Company, Amsterdam, 1968.

33. G. Dearnaley and D. C. Northrup, Semiconductor Counters for Nuclear Radiations (2nd. ed.), E. & R. N. Spon, London, 1966.

BIBLIOGRAPHY (Continued)

34. A. Coche and P. Siffert, in Semiconductor Detectors, G. Bertolini and A. Coche, eds., North Holland Publishing Company, Amsterdam, 1968.

35. J. L. Moll, Physics of Semiconductors, McGraw-Hill Book Company, Inc., New York, 1964.

36. E. M. Pell, J. Appl. Phys., 31, 291 (1960).

37. J. W. Mayer, N. A. Bailey, and H. L. Dunlap, from Proceedings of the Conference on Nuclear Electronics, held in Belgrade, May 1961, IAEA, Vienna (1961).

38. W. Shockley, Czech. J. Phys., 11, B81 (1961).

39. G. Restelli and A. Rota, in Semiconductor Detectors, G. Bertolini and A. Coche, eds., North Holland Publishing Company, Amsterdam, 1968.

40. R. D. Evans, The Atomic Nucleus, McGraw-Hill Book Company, Inc., New York, 1955.

41. R. R. Roy and R. D. Reed, Interaction of Photons and Leptons with Matter, Academic Press, New York, 1968.

42. C. M. Davisson, in Alpha-, Beta-, and Gamma-Ray Spectrometry, K. Siegbahn, ed., North Holland Publishing Company, Amsterdam, 1965.

43. P. B. Moon, Proc. Royal Society (London), 63, A1189 (1950).

44. E. Storm and H. I. Israel, LA-3753, June 1967.

45. W. J. Velgele, E. Briggs, B. Bracewell, and M. Donaldson, USAEC Contractor Report KN-798-69-2(R)(1969).

46. R. D. Cooper and G. L. Brownell, Nuc. Instr. and Meth., 51, 72 (1967).

47. J. A. Cooper, N. A. Wogman, and R. W. Perkins, IEEE Trans. Nucl. Sci, NS-15, 407 (1968).

48. V. J. Orphan and N. C. Rasmussen, Nucl. Instr. and Meth., 48, 282 (1967).

49. D. C. Camp, in Semiconductor Nuclear Particle Detectors and Circuits, National Academy of Science Publication 1593, Washington, 1969.

BIBLIOGRAPHY (Continued)

50. R. L. Auble, D. B. Beery, G. Berzins, L. M. Beyer, R. C. Etherton, W. H. Kelly, and Wm. C. McHarris, Nucl. Instr. and Meth., 51, 61 (1967).

51. J. Kantele and P. Suominen, Nucl. Instr. and Meth., 41, 41 (1966).

52. W. Michaelis and H. Kupfer, Nucl. Instr. and Meth., 56, 181 (1967).

53. R. Hofstadter and J. A. McIntyre, Phys. Rev., 78, 619 (1950).

54. M. Wahlgren, J. Wing, and J. Hines, Proceedings of the 1965 International Conference on "Modern Trends in Activation Analysis," Texas A & M University, College Station (1965).

55. J. A. Cooper, USAEC Contractor Report BNWL-SA-2940 (1970).

56. C. R. Gruhn, J. V. Kane, W. H. Kelly, T. Kuo, and G. Berzins, Nucl. Instr. and Meth., 54, 268 (1967).

57. I. Hayashi, H. E. Kern, J. W. Ridgers, and G. H. Wheatley, IEEE Trans. Nucl. Sci., NS-13, 214 (1966).

58. J. Kantele and P. Suominen, Nucl. Instr. and Meth., 56, 351 (1967).

59. W. H. Kraner and R. L. Chase, IEEE Trans. Nucl. Sci., NS-15, 381 (1968).

60. A. R. Sayres and J. A. Baicker, IEEE Trans. Nucl. Sci., NS-15, 393 (1968).

61. J. M. Palms, R. E. Wood, and O. H. Puckett, IEEE Trans. Nucl. Sci., NS-15, 397 (1968).

62. C. Broude, O. Hausser, H. Malm, J. F. Sharpey-Schafer, and T. K. Alexander, Nucl. Instr. and Meth., 69, 29 (1969).

63. H. Hick and R. Pepelnik, Nucl. Instr. and Meth., 68, 240 (1969).

64. C. D. Zerby and H. S. Moran, USAEC Contractor Report ORNL-3169 (1961). Modified for semiconductor detectors: E. S. Fry, J. M. Palms, and R. B. Day, USAEC Contractor Report LA-3456 (1966).

65. K. M. Wainio and G. F. Knoll, Nucl. Instr. and Meth., 44, 213 (1966).

66. N. V. deCastro Faria and R. J. A. Levesque, Nucl. Instr. and Meth., 46, 325 (1967).

BIBLIOGRAPHY (Concluded)

67. W. J. Snow, USAEC Contractor Report ANL-7314 (1966).

68. G. Bertolini, M. Cocchi, and A. Rota, preprint on paper presented at the International Symposium on Nuclear Electronics, September 10, 1968.

69. Fourteen papers on this subject make up the first chapter of Semiconductor Nuclear-Particle Detectors and Circuits, National Academy of Sciences Publication 1593, Washington (1969).

70. P. Moon and D. E. Spencer, Field Theory for Engineers, D. Van Nostrand Company, Princeton, 1961.

71. L. Katz and A. S. Penfold, Rev. Mod. Phys., 24, 28 (1952).

72. D. C. Camp, USAEC Contractor Report UCRL-71825 (1969).

73. R. H. Pratt, Phys. Rev., 117, 1017 (1960).

74. R. H. Pratt, R. D. Levee, R. L. Pexton, and W. Aron, Phys. Rev., 134, A898 (1964).

75. D. M. Walker and J. D. Clement, NASA Report NASA-CR-75309 (1966).

76. W. Heitler, The Quantum Theory of Radiation, O. U. P., London, 1944.

77. P. V. C. Hough, Phys. Rev., 73, 226 (1948).

78. H. A. Bethe and W. Heitler, Proc. Royal Soc. (London), 146, A83 (1934).

79. J. Rama Rao, V. Lakshminarayana, A. Su, and S. Jnanananda, Proc. Phys. Soc. (London), 81, 949 (1963).

80. E. Seidman, Burroughs Corporation Report PTS-062 (1964).

81. H. Kahn, USAEC Report AECU-3259 (1956).

82. D. H. Lehmer, Annals. Comp. Lab. Harvard Univ., 26, 141 (1951).

83. H. E. Carr, unpublished report, 1968.

84. B. Jansson, Random Number Generators, Victor Pettersons Bokindustri Aktiebolag, Stockholm, 1966.

85. L. J. Gannon and L. A. Schmittroth, USAEC Contractor Report IDO-16921 (1963).

VITA

David Marshall Walker was born in Newton, North Carolina on August 12, 1937. He attended school through the seventh grade at Carolina Beach, North Carolina, and graduated from Monroe High School, Monroe, North Carolina in 1955. During his undergraduate years in electrical engineering at Georgia Tech, he spent 22 months at Oak Ridge, Tennessee as an engineering co-op student in a nuclear instrument development group. Upon receiving his Bachelor of Electrical Engineering degree from Georgia Tech in 1960, he became a research engineer on the SNAP (Systems for Nuclear Auxiliary Power) reactor program at Atomics International in Canoga Park, California. This work involved the development of thermoelectric powered electromagnetic liquid metal pumps and later the direction and participation in the nuclear radiation effects studies for the SNAP electronic systems. During this time period he was a graduate student in physics at UCLA.

He returned to Georgia Tech in 1963 as a graduate student in physics and became a graduate research assistant with the Nuclear Sciences Division of the Engineering Experiment Station in 1964. Upon receiving the M.S. Degree in Physics in 1966, he became a Research Physicist with the Nuclear Sciences Division and a Ph.D. student in the School of Nuclear Engineering. His work at the Georgia Tech Nuclear Research Center has involved theoretical and experimental studies of the interaction of radiation in solids as applied to practical problems of radiation effects and advanced radiation detector systems. Presently his

efforts and interests are directed toward the application of nuclear technology to areas such as nuclear-bioengineering and nuclear-electronic semiconductor devices and processing.

He married the former Mary Aline Terry of Monroe, North Carolina in June of 1960. They have three sons, Terry, Donald, and Michael, and their present home is in Doraville, Georgia.